THESIS

A NEW HURRICANE IMPACT LEVEL RANKING SYSTEM USING ARTIFICIAL NEURAL NETWORKS

Submitted by

Stephanie F. Pilkington

Department of Civil and Environmental Engineering

In partial fulfillment of the requirements

For the Degree of Master of Science

Colorado State University

Fort Collins, Colorado

Spring 2015

Master's Committee:

Advisor: Hussam Mahmoud

John van de Lindt
Russ Schumacher

Copyright by Stephanie F. Pilkington 2015

All Rights Reserved

ABSTRACT

A NEW HURRICANE IMPACT LEVEL RANKING SYSTEM USING ARTIFICIAL NEURAL NETWORKS

Tropical cyclones are intense storm systems that form over warm water but have the potential to bring multiple related hazards ashore. While significant advancements have been made for forecasting of such extreme weather, the estimation for the resulting damage and impact to society is significantly complex and requires substantial improvements. This is primarily due to the intricate interaction of multiple variables contributing to the socio-economic damage on multiple scales. Subsequently, this makes communicating the risk, location vulnerability, and the resulting impact of such an event inherently difficult.

To date, the Saffir-Simpson Scale, based off of wind speed, is the main ranking system used in the United States to describe an oncoming tropical cyclone event. There are models currently in use to predict loss by using more parameters than just wind speed. However, they are not actively used as a means to concisely categorize these events. This is likely due to the scrutiny the model would be placed under for possibly outputting an incorrect damage total. These models use parameters such as; wind speed, wind driven rain, and building stock to determine losses.

The relationships between meteorological and locational parameters (population, infrastructure, and geography) are well recognized, which is why many models attempt to account for so many variables. With the help of machine learning, in the form of artificial neural networks, these intuitive connections could be recreated. Neural networks form patterns for

nonlinear problems much as the human brain would, based off of historical data. By using 66 historical hurricane events, this research will attempt to establish these connections through machine learning.

In order to link these variables to a concise output, the proposed Impact Level Ranking System will be introduced. This categorization system will use levels, or thresholds, of economic damage to group historical events in order to provide a comparative level for a new tropical cyclone event within the United States. Discussed herein, are the effects of multiple parameters contributing to the impact of hurricane events, the use and application of artificial neural networks, the development of six possible neural network models for hurricane impact prediction, the importance of each parameter to the neural network process, the determination of the type of neural network problem, and finally the proposed Impact Level Ranking System Model and its potential applications.

ACKNOWLEDGEMENTS

I would like to express my sincerest gratitude to my advisor, Dr. Hussam Mahmoud, for his continued support, encouragement, and motivation during my research. I will forever appreciate his generosity in providing me with the opportunity to pursue this research idea, while allowing me the creative and intellectual freedom. I would also like to express my thanks to my additional committee members, Dr. John van de Lindt and Dr. Russ Schumacher, for their support and interest in the progression of this research.

I would like to also personally thank my family for their unwavering support and reassurance in this endeavor. I am truly fortunate to have such inspirational parents who will continually back me in the pursuance of my passion and to have a brother in my life that is always willing to lend a hand. Without these individuals, I would not be where I am today.

TABLE OF CONTENTS

LIST OF TABLES

LIST OF FIGURES

CHAPTER 1

INTRODUCTION

1.1 Statement of the Problem

There is a long history of attempts being made to create a concise forecasting system, which would encompass all the variables involved during a natural hazard event. The focus of the problem stems from the communication gap that exists between the atmospheric scientists, structural engineers, and the general public. Specifically for hurricanes, the general public often misuses the Saffir-Simpson Scale and the sole reliance on this category ranking system, which mainly serves to illustrate meteorological severity, has become problematic when communicating the possible overall effects of an oncoming storm. For example, hurricane Andrew, in the early 1990s was a Category 5 hurricane and while it does rank in the list of most costly hurricanes, both Hurricane Katrina and Sandy surpassed it as Category 3 and 1, respectively.

The Saffir-Simpson Scale itself has previously been adjusted to incorporate more meteorological parameters in addition to just wind. At one point it also included storm surge due to the general concept that stronger winds and a lower central pressure would indicate higher storm surge. However, even this addition was eventually dropped as a result of categorization issues where a tropical cyclone would fall within the wind speed range for one category but the storm surge for another. Additionally, the meteorological parameters alone do not translate to the resulting risk without some assessment of the location of landfall. Noteworthy, the detailed explanations given by TV meteorologists, using various tools and models are not as popular as the category ranking by the Saffir-Simpson Scale, which is what individuals remember most.

Atmospheric scientists are aiming to perfect forecasting methods, while engineers are working towards more reliable and sustainable infrastructure an sociologists are examining the effects of varying locational demographics, yet there is very little overlap. Combining these fields, by using their relevant variables during a hurricane event, into one succinct system with familiar rankings could be a step towards addressing this problem. As a result of bridging the gap between multiple subject areas, the understanding of risk and vulnerability could improve through the development of a new ranking system as a mean to paint a more accurate picture of the possible impact to the general public.

1.2 Objectives and Scope of Research

This research serves to create a system that could be further used along with the Saffir-Simpson scale as a means of communicating hurricane risk in a concise manner. Following a hurricane event, society tends to focus on the outcome in terms of economic damage and loss of life. Given this main assumption, this thesis will aim to link the multiple variables involved in a landfalling hurricane event to the resulting economic damage. Instead of determining a damage estimate, the proposed system will use more of a range of economic damage or grouping approach as a means of comparison for the general public as proposed in Table 1-1. This approach will account for the possible range of error that comes with financial forecasting as well as provide the public with a general sense of damage in reference to historical hurricane events.

Table 1-1 Proposed Impact Level Ranking System

Impact Level	Economic Damage Amount (based on 2012 USD)	Example Event
0	< $25 million	2012 Tropical Storm Beryl
1	≥ $25 million, < $100 million	2007 Hurricane Humberto
2	≥ $100 million, < $1 billion	2008 Tropical Storm Fay
3	≥ $1 billion, < $10 billion	2008 Hurricane Gustav
4	≥ $10 billion, < $50 billion	2011 Hurricane Irene
5	≥ $50 billion	2005 Hurricane Katrina

This proposed system divides storm events into damage Impact Levels 0 through 5, chosen to better mirror current ranking systems for ease of understanding, i.e. the Enhanced Fujita Scale of EF-0 to EF-5 and the Saffir-Simpson scale from a Tropical Storm to Category 5 Hurricane ranking. An Impact Level of zero indicates minimal, or possibly zero, reportable damage. Minimal damage qualifies as below the $25,000,000 threshold established by the Property Claims Service. If a storm does not exceed this threshold, the damage amount is typically not reported by the National Hurricane Center. The highest Impact Level of 5 is an extremely damaging and expensive event costing more than $50 billion (2012 USD). Only two events in all the reference historical data qualify as Impact Level 5 events: Hurricane Katrina 2005 and Hurricane Sandy 2012. The Impact Levels, following Level 0, were determined based on typically discussed threshold values that society would reference as well as "evenly" distributing the used events so that Impact Level 5 had the rarest occurring events followed by Level 4, leaving Levels 3, 2, and 1 as relatively more common rankings.

Due to the high level of complexity and non-linearity associated with this problem, artificial neural networks (ANNs or simply "neural networks") will be used for estimating an event's impact level. The use of ANNs is beneficial since research has established that ANNs are useful in capturing significant nonlinear characteristics, if present. Neural networks will be able to establish connections by learning the historical data just as experts in this field have and

produce the results in a concise manner. In order to accomplish this objective, the following tasks and subtasks are to be accomplished:

- Task 1: Conduct Comprehensive Literature Review
- Task 2: Collect Historical Data
  - Extract meteorological parameters, landfall location(s), reported economic damage, and deaths from Tropical Cyclone Reports published by the National Hurricane Center
  - Download and use the most recent U.S. Census population data
  - Extract tropical storm wind radii for time of landfall(s) from archived NHC Public Advisories (as far back as possible)
  - Merge population data with wind radii to determine the population affected within the overlapped area
  - Adjust data to a comparable standard
- Task 3: Build Multiple Model Networks
  - Determine options for data arrangement
  - Position data into matrix form (varying for the input and a singular target matrix)
  - Use neural network pattern recognition to build multiple initial networks
- Task 4: Discuss the Developed Models Network and the Corresponding Results
  - Evaluate each model's network performance for comparison
  - Conduct trial runs for specified hurricanes with known results
  - Rebuild networks and extract resulting neuron weights and biases for evaluation of input variable importance
  - Assess results for best model network

- Task 5: Enhance Selected Model Networks
  - Adjust number of hidden neurons with data separation and training algorithm held constant
  - Adjust data separation with the number of hidden neurons and training algorithm held constant
  - Assess various training algorithms with the number of hidden neurons and data separation held constant
- Task 6: Interpret the Results to Build Final Model
  - Evaluate the effect of increasing the number of hidden neurons
  - Evaluate the effect of changing the separation of data
  - Compare the results produced by each training algorithm
  - Attempt to combine all results to produce lowest possible error
- Task 7: Conduct Evaluation of Final Model
  - Assess implications of the lowest possible error reached
  - Conduct additional trial runs with the same specified storms from Task 4
- Task 8: Discuss Usability, Possible Applications, and Societal Benefits of the Resulting Final Model Network

The proposed Impact Level Ranking System will be further discussed within the first half of this thesis, following the literature review. The evaluation of the use of neural networks will follow as well as the implications of the results. The neural network models will not only be evaluated for the best possible approach, but also for the implication of results. These results also include evaluation of the importance of the multiple variables used as they pertain to the

resulting economic damage. The thesis will conclude with proposing a final model network and its possible future applications to help communicate the risk of an oncoming hurricane event.

CHAPTER 2

BACKGROUND AND LITERATURE REVIEW

2.1 Natural Disasters' Impact on Society

Worldwide, natural hazards lead to destruction, economic damage, mass displacements of population, and in some cases, loss of life. These events can be both climatological, covering situations ranging from extreme temperatures to tropical cyclones, and geological, covering landslides to movement of tectonic plates. All of these events are highly location-dependent based on proximity to fault lines, coastal areas, and specific atmospheric conditions. Eastern Asia is an example of a location subject to tropical cyclone conditions and tectonic plate activity. This locale (including Japan and the Philippians) along with India have the most natural hazard events in the world (Bryant, 2005). Conversely, tornadoes are most prominent in Tornado Alley in the United States and rarely occur in other locations. In fact, according to Bryant (2005) tornadoes in the U.S. are the most commonly occurring event in the world as shown in Table 2-1. However, this does not make them the costliest (Table 2-2) or deadliest (Table 2-3) those titles belong to earthquakes and flooding, respectively.

Table 2-1 Frequency of Hazards in the 20th Century (Bryant, 2005)

Hazard Type	# of Events
Tornadoes (US)*	9476
Flood	2389
Tropical Cyclone	1337
Tsunami	986
Earthquake	899
Wind (other)	793
Drought	782
Landslide	448
Wild Fire	269
Extreme Temperature	259
Temperate Winter Storm	240
Volcano	168
Tornadoes (non-US)	84
Famine	77
Storm Surge	18

* Tornadoes in the US are for F2-F5 tornadoes 1950-1995

Table 2-2 Cost of Natural Hazards from 1900 – 2001 (Bryant, 2005)

Hazard Type	Cost
Earthquake	$248,624,900,000.00
Flood	$206,639,800,000.00
Tropical Storm	$80,077,700,000.00
Wind Storm	$43,890,000,000.00
Wild Fire	$20,212,800,000.00
Drought	$16,800,000,000.00
Cold Wave	$9,555,000,000.00
Heat Wave	$5,450,000,000.00
Total	$631,250,200,000.00

Table 2-3 Deaths Resulting from Natural Hazards in the 20th Century (Bryant, 2005)

Hazard Type	Associated Deaths
Floods	6,851,740
Earthquakes	1,816,119
Tropical Cyclones	1,147,877
Volcano	96,770
Landslides, avalanches, mud flows	60,501
Extra-Tropical Storms	36,681
Heat Wave	14,732
Tsunami	10,754
Cold Wave	6,807
Tornado	7,917
Fires	2,503
Total	10,052,401

Even though most media coverage encompasses hurricane and tornado deaths, the biggest killer in the U.S. is heat/drought followed by cold weather as shown in Figure 2-1 (Borden & Cutter, 2008). According to the U.S. Federal Emergency Management Agency (FEMA), most disaster declarations in the U.S. are categorized under severe weather, flooding, and fire (Figure 2-2). Tropical Cyclones account for roughly 47% of all billion-dollar events, which account for 80% of U.S. losses from combined severe weather and climate events (Smith & Katz, 2013). While severe weather and tornadoes may occur more often, these events are often small in size and happen in lower population areas of the country where communities are more spread out, putting fewer people and infrastructure in harms way.

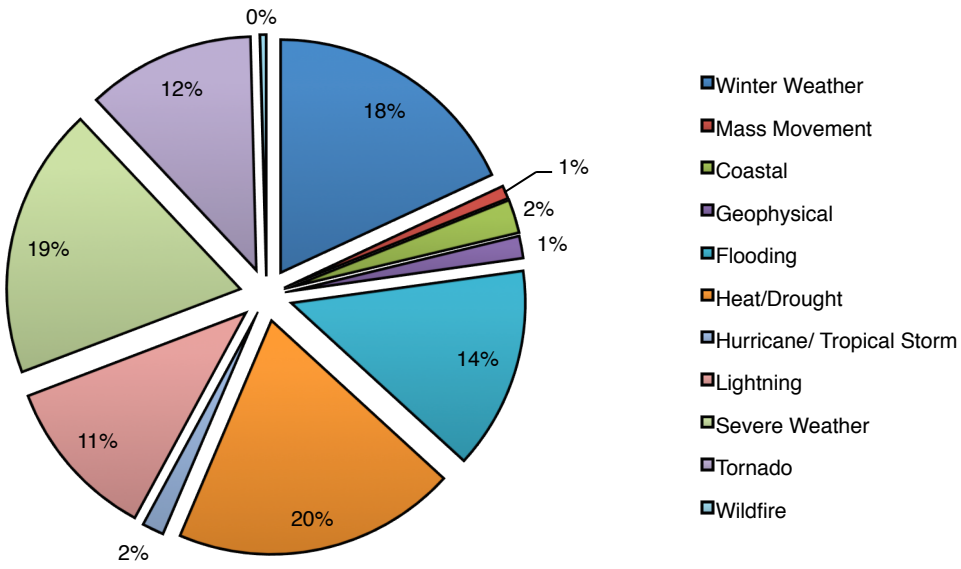

Figure 2-1 Deaths by natural hazard type in the U.S; after: **(**Borden & Cutter, 2008)

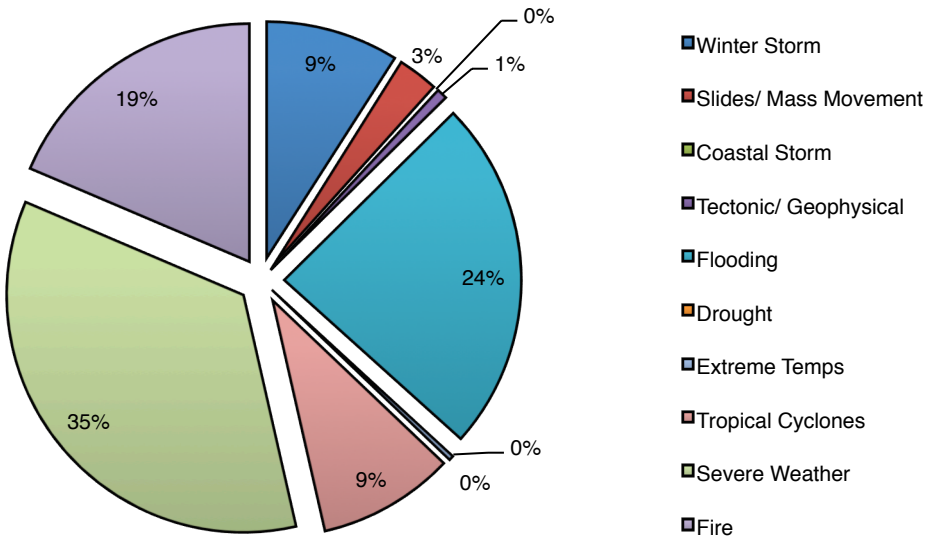

Figure 2-2 Disaster declarations by type; data from (FEMA, n.d.)

Tropical cyclones, which will be the focus of this research, are among the costliest and deadliest natural disaster events worldwide. In the U.S. only 9% of FEMA disaster declarations are for tropical cyclones (hurricanes and tropical storms) even though these storms are some of the highest in terms of economic damage to occur in the U.S. It is a common societal perception that hurricanes are increasing in intensity, resulting in increased destruction. When the U.S. hurricane data is normalized there is actually no significant trend supporting increased intensity/damage from 1900-2005 (Pielke Jr. et al., 2008). Normalizing the data involves accounting for inflation and population and societal changes - essentially hypothesizing what would happen if a storm from the early 1900s hit today. The cause for increase in economic damage from hurricanes is more of a result of increase in population along the coastline in addition to an increase in wealth (i.e. people have more "stuff" today). The Galveston hurricane of 1900 resulted in $30 million in damage at the time, but could be adjusted to $72-78 billion in

2005 USD. Without any adjustment, the Galveston Hurricane is still the deadliest hurricane in U.S. history with 8,000 lives lost (National Hurricane Center, 2012).

A study by Nirupama (2013) indicated that there is actually no unique manner to rank hurricanes (tropical cyclones) within the U.S.. This means that of the different criteria used for ranking, no one hurricane, from 1960 through 2012, appeared within the top in all of the categories. This is shown in Figure 2-3, which covers popular hurricane events and their respective ranking in 9 of the 10 categories (number of coastal counties affected is excluded). Hurricane Sandy (Category 1), which hit New York/New Jersey in 2012, has surpassed Hurricane Andrew (a Category 5) in economic damage, and is now second to Hurricane Katrina (Category 3 at landfall). In this same ranking system, Sandy also came in second to Katrina with respect to deaths with 253 and 1,833, respectively. Hurricane Charley (2004) was a Category 4 with a storm surge of 2 meters and Hurricane Katrina was a Category 3 with a storm surge of 8.7 meters (National Oceanic and Atmospheric Administration, 2009). Katrina currently ranks as the costliest hurricane in U.S. History, while Charley does not reach the top ten.

Figure 2-3 demonstrates the discrepancies between the various meteorological parameters and the resulting impact, suggesting a more complex relationship between the two. In using the Saffir-Simpson Scale, there is no direct way to link the severity of an oncoming storm to the resulting impact. The high level of exposure and economic damage along with the insufficient connection between parameters is what makes tropical cyclones an ideal natural hazard for this research.

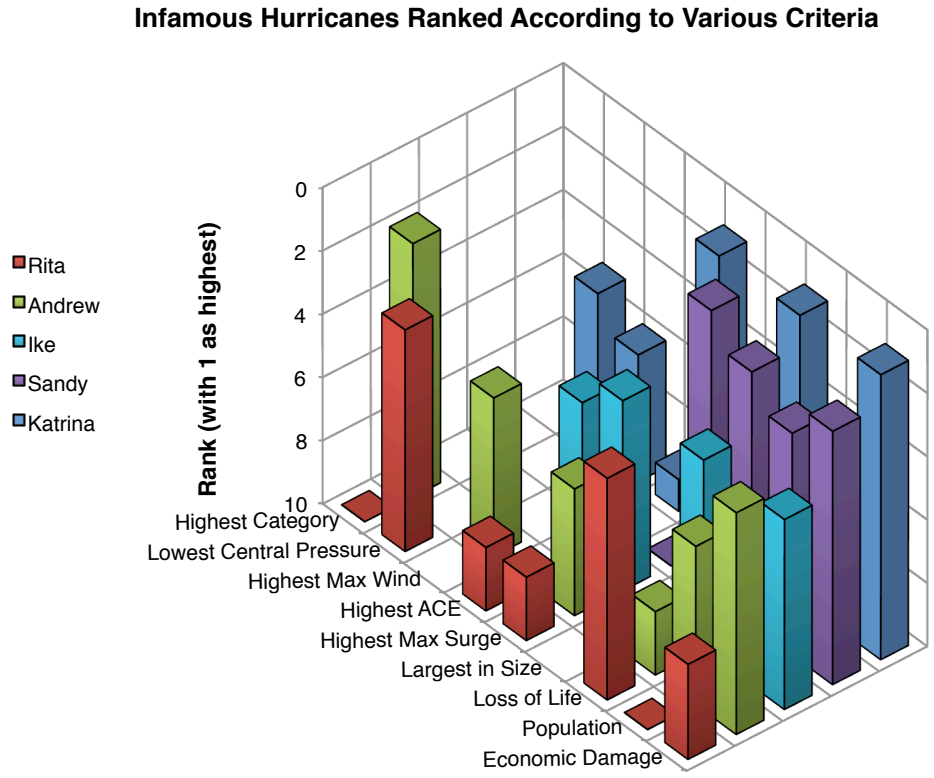

Figure 2-3 Ranking of various infamous hurricanes extrapolated from Nirupama (2013)

2.2 Parameters of Hurricane Impact Prediction

2.2.1 Meteorology

2.2.1.1 Hurricane Basics

Hurricanes (term for tropical cyclones that form in the northern Atlantic and eastern Pacific oceans) are essentially low-pressure systems with no fronts, which form over warm tropical oceans that have high humidity and very light winds. The high humidity helps to build the thunderstorm clusters, similarly to how thunderstorms form on hot humid days across the United States, by allowing the water vapor in the air to condense and form the clouds to build thunderstorms. This condensation releases latent heat, which is converted to wind energy to drive

the storm. The light winds in the tropics produce very low wind shear, which allows the hurricane to maintain its structure. The ocean temperature must typically be around 27^{o}C or higher and extend for a depth of approximately 50 meters from the ocean surface. The warm water provides the energy needed to feed the hurricane. As the system builds, the strong winds and lowering pressure cause the ocean water to mix, which is why the ocean must maintain the high temperature at greater depths. These conditions typically occur in the North Atlantic and North Pacific from June through November, resulting in the standard hurricane season (Ahrens, 2008).

Once these systems form, there are various stages of classification starting with a tropical depression (maximum sustained winds of 33 knots or less), with the system then becoming a tropical storm (maximum sustained winds of 34 to 63 knots), and lastly reaching hurricane status (maximum sustained winds of 64 knots or higher). Hurricanes are then named and given a category ranking based on the Saffir-Simpson Scale as summarized in Table 2-4:

Table 2-4 Saffir-Simpson Hurricane Wind Scale as used by the National Hurricane Center (updated to only incorporate sustained wind speed).

Category	Sustained Winds	Types of Damage
1	64- 82 kt	**Some Damage:** Possible roof and shingle damage. Snapped tree branches and shallow rooted trees could be uproots, likely leading to power outages.
2	83- 95 kt	**Extensive Damage:** Possible major roof damage to well-constructed homes. Uprooted trees leading to blocked roads and near total power loss is to be expected.
3	96- 112 kt	**Devastating Damage:** Major roof damage or possible removal of roof decking could occur on even well-built framed homes. Electricity and water unavailable for several days.
4	113- 136 kt	**Catastrophic Damage:** Well-built homes could lose most of the roof structure with damage to exterior walls. Possibly power outages for weeks to months leading to an uninhabitable area.
5	> 137 kt	**Catastrophic Damage:** Large amount of well-constructed homes will be destroyed (roof failure and wall collapse). Power outages will last weeks to months leading to an uninhabitable area.

On average, hurricanes are approximately 500 km in diameter (Ahrens, 2008) with and eye approximately ten kilometers in diameter (Willoughby, Rappaport, & Marks, 2007). The eye is the clear area at the center of the hurricane with an adjacent eyewall consisting of intense thunderstorms. The whole storm system essentially rotates around the eye center in a counter-clockwise or cyclonic motion in the northern hemisphere. The center of the storm is also where the lowest pressure is, with the eyewall consisting of the heaviest precipitation and strongest winds. A hurricane is essentially an organized system of thunderstorms. In the below cross-section, Figure 2-4, it can be seen that the hurricane consists of rings of rain bands circling around the low-pressure center.

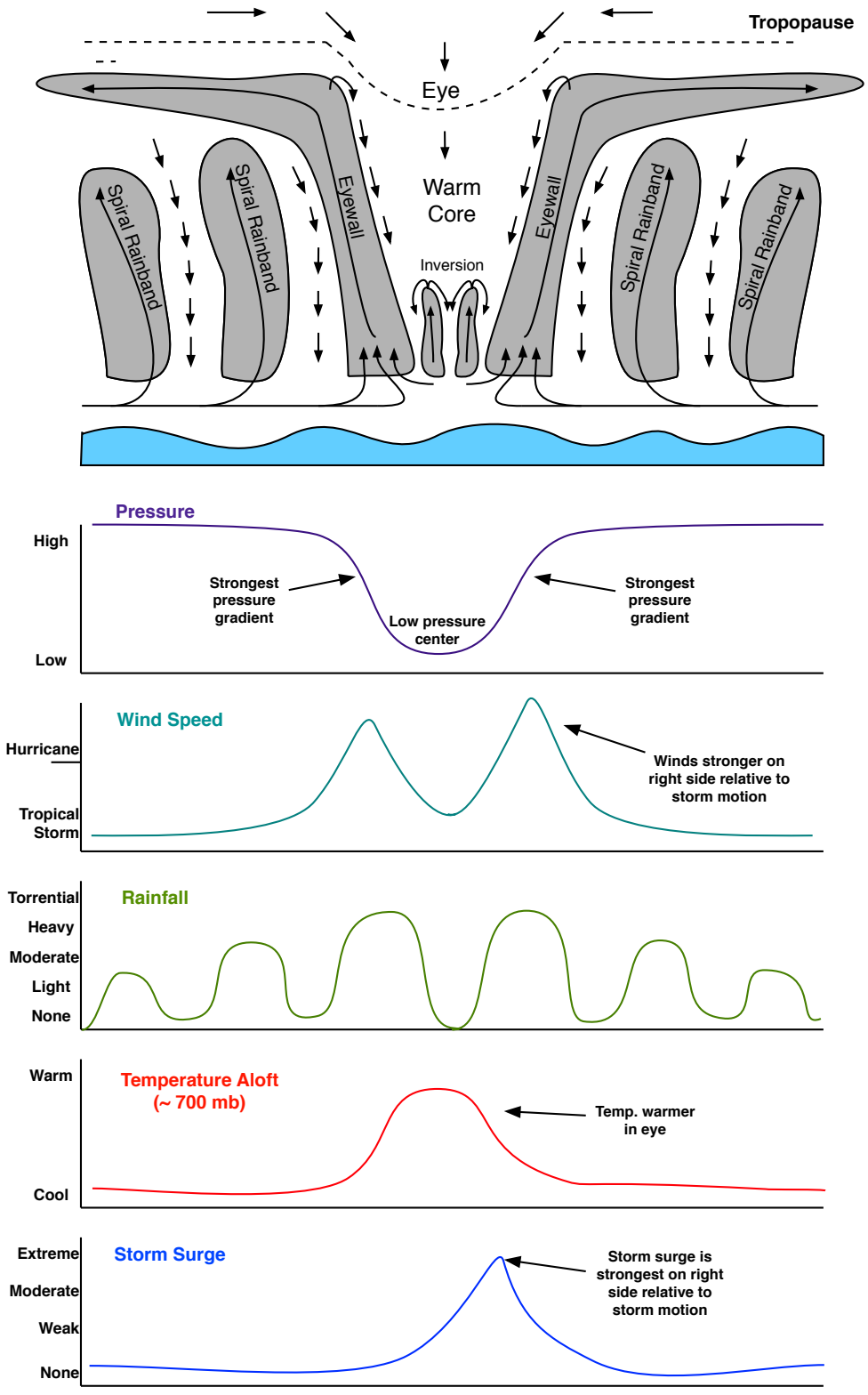

Figure 2-4 Cross-sectional depiction of a hurricane along with the location of significant meteorological attributes; after: (Rauber, Walsh, & Charlevoix, 2008)

2.2.1.2 Wind, Storm Surge, and Precipitation

As can be seen in Figure 2-4, the meteorological parameters of a hurricane vary in relation to location within the storm itself. The strongest winds are typically on the right side of the eyewall as the storm approaches. These stronger winds are a resultant of the incorporation of the wind associated with the storm movement (translational winds). Due to the way the storm rotates in the northern hemisphere, the translation speed is added to the wind speed on the right and subtracted on the left as shown in Figure 2-5 (Rauber et al., 2008). On the left hand side, the translational winds (V_T) are subtracted from the rotational winds (V_R) resulting in 75 knots (or 86.25 mph) wind speed. On the right hand side, V_T is added to V_R resulting in 125 knots (or 143.75 mph) wind speed.

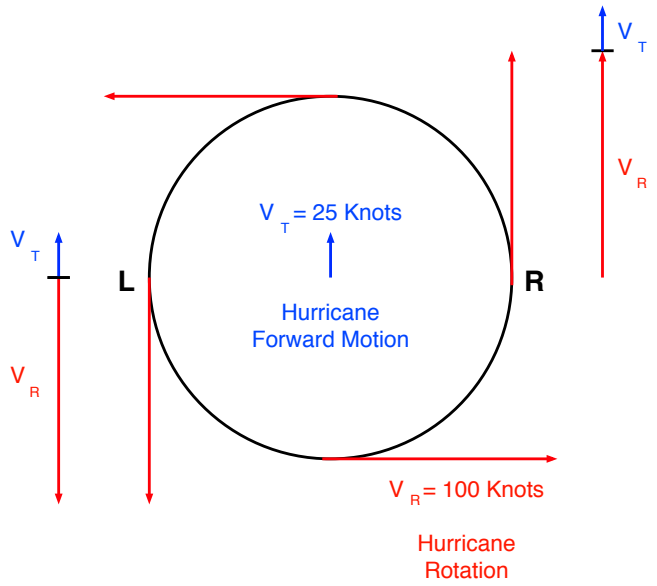

Figure 2-5 Illustration of how hurricane motion, or translational speed, affects the overall winds associated with the hurricane rotation; after: (Rauber et al., 2008)

Storm surge is the abnormal rise in ocean surface level caused by the storm's central low pressure and strong winds. The low pressure causes the ocean water to rise, similar to air being removed from a straw and water rising upwards (Rauber et al., 2008). Due to the wind structure

discussed above, the strongest storm surge occurs on the right side of the hurricane relative to its approach. The stronger winds on the right side result in ocean water being pushed in the direction of motion and consequently piling on the right side, whereas the water on the left is being removed. Storm surge can also be enhanced by other factors such as high tide, which occurred when Hurricane Sandy made landfall in New Jersey. As Rauber et al. (2008) indicated, the shoreline at the landfall location as well as waves can also create a more dangerous situation with concern to storm surge and will be further discussed later in more detail.

Along with flooding due to storm surge, heavy precipitation is also associated with hurricanes. Precipitation falls within the rainbands and thunderstorms of a hurricane with the heaviest precipitation within the eyewall. The amount of rain that falls in one location is also tied to the storm's translation speed. A slow moving hurricane can linger over an area and produces 76 to 102 cm of rain in two days resulting in severe inland flooding (Rauber et al., 2008). Inland flooding due to Hurricane Mitch in 1998 was tied to over 18,000 deaths (Rauber et al., 2008). The combination of storm surge and inland flooding can cause more extensive and widespread damage than wind.

2.2.2 Infrastructure

2.2.2.1 Buildings

During a hurricane event, infrastructures (mainly structures) are subjected to extreme loading demands and are expected to withstand the combined assault of severe winds and intense flooding. The vulnerability of structures in a hurricane event encompasses both the exterior components as well as the interior assets. The exterior is mainly affected by wind, whereas the interior is mainly affected by flooding due to storm surge and heavy rains (including wind-driven rain).

Wind interacts with a standard low-rise building as shown in Figure 2-6 below. The windward side feels a positive pressure exerted on it, while the leeward side experiences a negative pressure force. In other words, there is a "suction-like" force being exerted on the leeward wall. The roof and sidewalls have a similar negative pressure on most, possibly all, of the respective surface areas. This is how it appears that houses are leaning in certain diagrams and pictures relating hurricane winds. If windborne debris puncture the building the wind interaction with the building will change to what is shown in Figure 2-7. This results in the development of internal pressure that will combine with the external pressure to increase damage to a structure (Yau, Lin, & Vanmarcke, 2011). Hurricane preparedness measures therefore include boarding up the windows of a house, since these are one of the weakest points when it comes to wind-borne debris susceptibly.

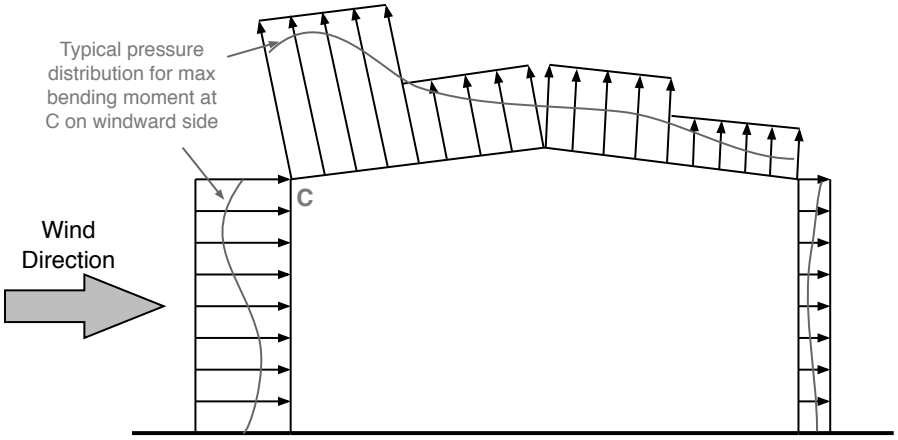

Figure 2-6 Instantaneous and simplified external pressure distribution on a low-rise building along with the static load distribution for a bending moment in association with the applied wind load (top corner C); after: (Holmes & Syme, 1994)

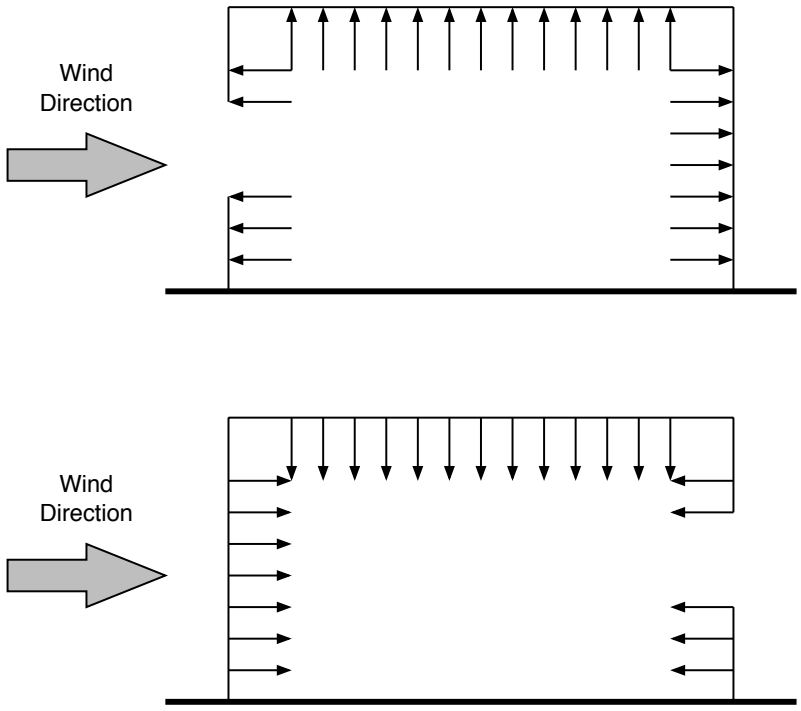

Figure 2-7 Internal pressure of building with a large/dominant opening and how this differs with location of the opening relative to wind direction

Even though windows and doors are most vulnerable to windborne debris, the damage, and possible loss, of a roof, can also drastically change the internal pressure. In damage surveys done after severe wind events resulting from hurricanes and tornados, one of the main building components inspected for damage is the roof and its connections. The failure of a roof can include failure of multiple roof-wall connections and possibly the complete loss of a roof (Stenabaugh & Kopp, 2012). According to Stenabaugh and Kopp (2012), failure of a connection occurs when the uplift force becomes greater than the roof's dead load or the connection's capacity. The flight of a roof, however, depends on many other factors including the wind speed and direction, as well as the aerodynamic coefficients (Stenabaugh & Kopp, 2012). These are the factors that determine how the roof (or its panels) moves once it begins to be airborne. Stenabaugh and Kopp (2012) concluded that as more than one roof to wall connections fails, a

temporary gap can form creating a change in the internal pressure as previously discussed and could lead to the roof taking flight. It was also mentioned how the combination and change in wind direction should also be taken into account. Failure of any part of a building is not as simple as a direct correlation to a sustained wind speed; many factors can go into the destruction of a building even just on the windward side.

In a study done by Christian Unanwa (2000) the relative resistivity indices (RRIs) used in determining building damage would decrease in higher story building. This would seem logical since wind speed increases with height and are not impeded as much by friction in higher heights (Unanwa & McDonald, 2000). Unanwa used these RRIs to determine the degree of damage to a specific building by using damage bands which would bound the extreme degrees of damage that a certain building class would sustain in a severe wind event. Building classes are commonly used in wind damage prediction, but can be broad in spectrum, the goal of these damage bands was to provide a more accurate damage estimation to a building or groups of buildings (Unanwa & McDonald, 2000). The use of RRIs also touches of the effects other buildings have on each other. The RRI for a building is determined using many factors, one of which being the building's surrounding infrastructure (Unanwa & McDonald, 2000). Also, for a group or cluster of buildings the RRI would be averaged over the group (Unanwa & McDonald, 2000). The factors used in creating these damage bands illustrate the importance other features, such as the surrounding environment, in addition to construction type and height.

In another study Yau (2011) evaluated the integration of similar various factors in wind damage to residential structures. This integrated model approach accounts for both the change in wind direction and speed as a storm passes as well as the effects of damage from buildings clustered together, similar to a residential neighborhood. As a hurricane moves along its track,

the wind direction will change at a given location. It is theorized that the more wind directional shift involved, the more susceptible the structure is to wind-induced damage due to increasing the windward exposure areas. These areas are also more exposed to windborne debris, similarly increasing the potential for structural damage (Yau et al., 2011).

The other component of Yau's research theorized that residential structures clustered together affect each other. This was supported by an example run of a 65 m/s and 45^{o} angle wind field over a cluster of homes (4x4) identical in structure (Figure 2-8 illustrates this layout). The result showed that the homes at the corner where the winds first hit are less damaged than the homes downwind in the cluster. The increased damage in the homes downwind is more obvious in the increased percent of window and door damage. This could likely indicate that the debris from the first structures impacted the houses down wind. Once one home was damaged it created a chain like event of continuing damage downwind (Yau et al., 2011). What this discretely touches on is how population density directly correlates to an infrastructure density issue. A denser infrastructure can lead to an increase in overall damage likely because of the obvious: there is more to be damaged. The other possibility of an increase in damage is what Yau (2011) highlighted that a building's surroundings affect how it responds to extreme wind circumstances, correlating that high infrastructure density leads to higher damage for identical storms.

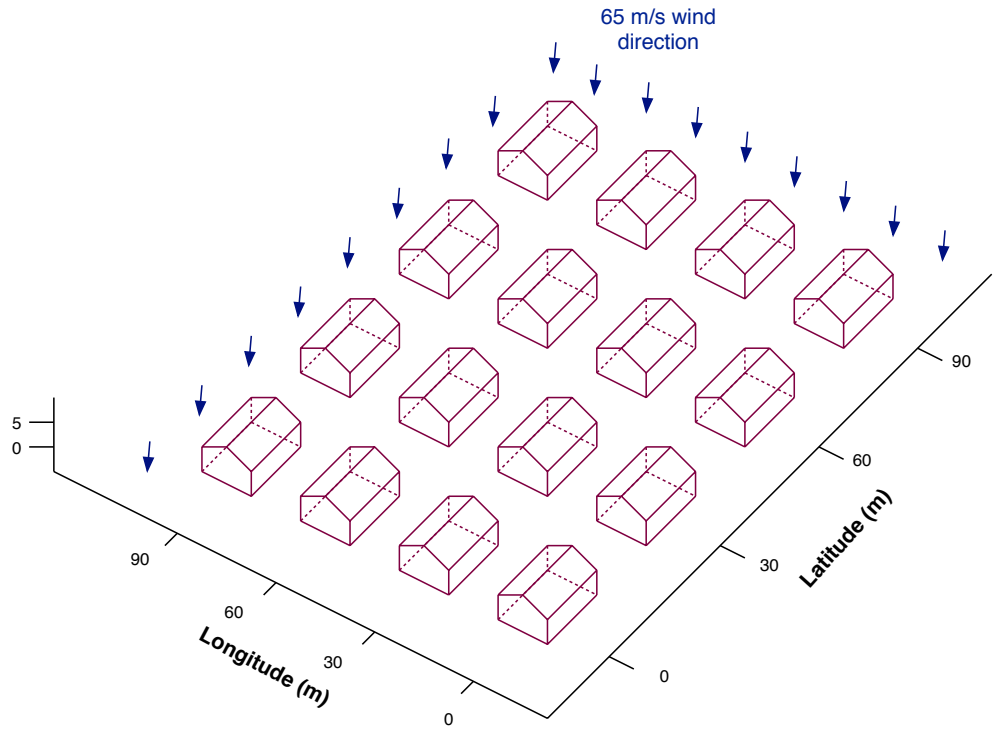

Figure 2-8 Neighborhood layout for; after: Yau et. al. (2011)

The building quality is also an important factor in how a structure will respond to extreme winds as mentioned in a FEMA and URS report on observations and recommendations made by FEMA's Mitigation Assessment Team (MAT) (Herseth & Ashley, 2013). In addition to high infrastructure density leading to high damage, most high population areas also have buildings greater than 3 stories, which can have a lower resistivity to extreme winds than the typical home. In correlation to building heights, most findings and recommendations made by FEMA tie to construction quality; year built, roof types, and construction faults and errors (Herseth & Ashley, 2013). The construction quality and year built are large factors in how a building will perform under a severe event. The 95-cooridor from Washington D.C. to Boston is very old with many buildings in those areas date back to the 1700s and might not be fully compliant with current codes and standards. Older structures not up to recent building codes are

typically more vulnerable to extreme weather events. Essentially, more populated, older locations will experience more damage for a set wind speed than smaller towns with new construction.

The FEMA MATs also evaluated damage due to storm surge and flooding since these factors are commonly known to be the more damaging and deadly factors of a hurricane. Storm surge is arguably the larger contributor to overall economic damage associated with a hurricane. An analysis of combined loss from wind and storm surge for a hurricane, highlighted that storm surge has a more significant impact on homes nearer to the coast than wind, in fact their resulting cost ratios show that storm surge serves as the main factor in damage with approximately 85 – 97% of the total damage (Dao, Li, van de Lindt, & Bjarnadottir, 2013). While the effects of storm surge can reach as far inland as 1 km, simply raising the house by 1.5 to 2 meters can result in the storm surge damage dropping off almost completely (Li, van de Lindt, Dao, Bjarnadottir, & Ahuja, 2012). Either raising the house or moving the house back from the shoreline to a higher ground level elevation can result in lowering the damage due to storm surge.

The rise of ocean water can result in inundation (exacerbated by rainfall, scour, and erosion) and provide transport for waterborne debris, which are a main contributor to structural damage. However, flooding in general, including storm surge, causes mainly nonstructural damage. Damage to the floor and interior items such as electronics and furniture are also assessed for damage in terms of cost to repair or replace (Li et al., 2012). Once storm surge (flooding), passes over the floor, most of the contents are considered ruined. Some components are considered fine after drying out (mainly the floor), but others (mainly electronics) are not repairable. Interior items can be costly to replace and are typically insured, and therefore accounted for in resulting damage estimates.

2.2.2.2 Utilities

The effects hurricanes have on public utilities are more common and widespread than the effects to structures. Power outages and interruption of water treatment and distribution are the main issues. Power outages are affected on "grid levels" and water treatment and storm water management are handled at city and county level, so instead of affecting one family, a disruption to these services can impact hundreds to millions of people at once.

Possibly the most common occurrence and most costly result of a hurricane is power disruption. On average, major storms cost electric utilities $270 million per year (2003 USD) in damages (Peters, DiGioia, A M, Hendrickson, & Apt, 2007). This can cost consumers approximately $2.5 billion a year (Peters et al., 2007). Power outages can be caused by down power lines from wind and heavy rain, flooded underground conduits, and structural failures. Electric transmission lines are currently designed to account for climatic loads, security loads, construction and maintenance loads, and code loads. However, when the load exerted on transmission lines exceeds what is designated in these standards, such as extreme wind and heavy rain, a structural failure will result (Peters et al., 2007). Approximately 27% of reported significant disturbances in power were due to structural failure from 1984-2000 (Peters et al., 2007).

In an assessment of power failures in Louisiana and Mississippi after Hurricane Katrina, the causes were: flooding-related power outage, destroyed central offices (CO), engine fuel starvation, and partial switch damage (Kwasinski, Weaver, Chapman, & Krein, 2009). It appears that the most common cause for power outages was fuel starvation. Once a blackout occurs, batteries usually support the load until a generator set kicks on to provide power (Kwasinski et al., 2009). The generators run on diesel fuel and require replenishment while being used until the

problem that caused the outage is fixed. After a hurricane event, complications occur due to difficulty reaching these generators as a result of damaged roadways, debris, and possible public unrest; therefore the generators continue to operate until the fuel runs out. The next most common contributor to power outages was the destruction of central offices mainly due to storm surge (Kwasinski et al., 2009). For wireless communication systems, many indoor base stations were situated on the ground, below sea level, when these systems should have been raised to an above sea level elevation for protection (Kwasinski et al., 2009). Katrina was an extreme event, however, it highlighted the vulnerability of power systems during hurricane events.

Power loss can precede complications with water utilities (an arguably more critical infrastructure system). Power loss of a water/wastewater treatment plant can subsequently impact the surrounding population with a water shortage. Since the World Health Organization (WHO) recommends a total of 20 liters a day per person for drinking and sanitary purposes, the loss of access to water can become a critical issue immediately following a hurricane (Blake, Walker, & Walker, 2011). In addition to power loss, disruption in water treatment can also be tied to damage to the treatment facility due to wind or floodwater, shifting and fracturing of water pipelines, infrastructure becoming submerged by floodwater, flooding and corrosion of electrical components, and debris. This impact can become worse for weak and old infrastructure (Blake et al., 2011). After the storm has passed, supplying clean water to residents can also emerge as difficult due to the resulting chaos, debris, and floodwater obstructed infrastructure (Blake et al., 2011; Chisolm & Matthews, 2012). Similarly, chaos and obstruction prompt difficulty reaching treatment facilities in order to perform repairs.

Hurricane Katrina is a popular case study for how a hurricane can affect water utilities due to the negative effects induced on 1,220 drinking water systems and 200 sewage treatment

plants in Louisiana, Mississippi, and Alabama (Chan & Revkin, 2005). The state of these water systems left 2.4 million people without safe drinking water in Louisiana and Mississippi (National Resources Defense Council (NRDC), 2005). Similar to the damage causes discussed above, most of the damage to water systems from Hurricane Katrina was a result of floodwaters. Many treatment plants were essentially submerged due to flooding and therefore unable to operate; this included the largest drinking water plant in New Orleans (Copeland, 2005). These same extreme floodwaters led to fractures, breaks, and separation of various underground water pipes due to soil subsidence (Chisolm & Matthews, 2012). Another cause of pipe separation is a result of floodwaters moving structures, which severs the connection to associated service pipelines (Chisolm & Matthews, 2012). These systems were also subjected to clogging from waterborne debris while the mechanical and electrical systems (pump stations) were flooded and corroded by saltwater (Chisolm & Matthews, 2012). In order to recover and rebuild these systems the floodwaters must first be removed (dewatering) then the repairs and rebuilding can begin. For Hurricane Katrina, it took more than a year to fully restore the water/wastewater infrastructure while still finding ways to supply residents and workers with potable water (Blake et al., 2011).

2.2.2.3 Transportation

As can be inferred from the overlap in utility use, many of these infrastructure systems are interconnected. Transportation is another critical system previously mentioned in relation to blocking recovery efforts for other forms of infrastructure. The main risk for a transportation system, be it roads, bridges, or subway systems, is flooding. Even in non-hurricane events, floodwaters can manage to undercut a road and create a river in a matter of minutes. In New York City (NYC), Hurricane Sandy produced enough storm surge and heavy rain to flood

subway stations and bring public transit, which most people utilize in NYC, to a complete halt. These effects can leave people stranded and prevent relief efforts from making it to locations that are in need of supplies, power, and water.

Bridges spanning over waterways are especially vulnerable to the impacts of hurricanes due to their obvious exposure to flood waters, storm surge, and debris. One of the most common causes of bridge damage is scour. Scour occurs due to floodwaters, storm surge, and waves attacking the riprap at the bridges approach and ultimately shifting the soils below it, undermining the structural integrity (Lwin, Yen, & Shen, 2014; Stearns & Padgett, 2012). Waves and rising floodwaters can also cause damage to bridge decks. The waves and rising water create uplift force acting on the underside of the deck and when this force exceeds the weight of the deck itself, the decks can move laterally or "hop" in the direction of the wave propagations (Lwin et al., 2014). Hurricane Ike made landfall in Texas in 2008 bringing a peak storm surge exceeding 4 meters causing damage or destruction to 26 bridge structures along the coast (Stearns & Padgett, 2012). Hurricane Katrina brought a storm surge in excess of 8.5 meters resulting in the damage of 44 bridges, the most distinguished being the US-90 bridge that crosses the St. Louis Bay (Stearns & Padgett, 2012).

Another impact to transportation that would be more prevalent in the "95-cooridor", and brought to attention by Hurricane Sandy in 2012, is the lack of usability of public transportation services. Hurricane Sandy caused extreme flooding (4 meter storm surge in Battery Park (Kaufman, Qing, Levenson, & Hanson, 2012)) damage in New York City and New Jersey resulting in the flooding of New York City's traffic tunnels and subways. The Metropolitan Transportation Authority (MTA) states that approximately 10 million people rely on the regions subways, busses, commuter rails (to surrounding boroughs, New Jersey, etc.), tunnels, and

bridges. Floodwaters entered the Battery and East River (connecting Manhattan with Brooklyn and Queens) subway tunnels as well as the PATH stations in Hoboken, Jersey City, and World Trade Center tunnel. MTA chairman, Joe Lhota, stated that the damage sustained during Sandy was the worst the MTA has ever experienced (Kaufman et al., 2012). Most of these floodwaters had to be pumped out by MTA workers with special equipment due to power outages. In addition, the areas flooded with saltwater had special consideration since the salt water corrodes as well as conducts electricity and could short out the equipment (potential fire hazard) (Kaufman et al., 2012). This coupled with flooded tunnels and compromised bridges that surround the island of Manhattan, caused an incredibly dismal traffic situation leaving many forced to find alternate routes only to be unable to move and left stranded.

The vulnerability and destruction of a community's transportation system is another parameter that attributes to economic damage associated with a hurricane event. Aside from down trees and indirect causes, transportation damage is generally a result of floodwaters (mainly storm surge) and can drive up the economic damage total as well as impact of infrastructure areas requiring extensive recovery efforts. Transportation, along with utilities and built structures, are the main parameters affected by the meteorological components of a hurricane and therefore directly linked to the resulting economic damage total.

2.2.3 Geographical and Societal

2.2.3.1 Location Specific Geography

Similar to infrastructure, the effects of geography are highly dependent on location. While, infrastructure is the focus for damage, geographical parameters can contribute to how the meteorological parameters affect infrastructure. The geography of the U.S. coastline varies in both natural and man-made features. Nature has an interesting way of having systems that restore

balance and provide protection. Many natural features along the coast, for the most part, protect the main shore and inland. These features are primarily south of the Mason-Dixon line and consist of wetlands and barrier islands. Man-made features can actually worsen the impacts by disrupting the natural processes (i.e. urbanization). The highly populated 95-corridor is an example where concrete overtakes soil. Other features, such as bay areas, also have a unique interaction with hurricanes depending on certain characteristics. Essentially, landfall location characteristics can become a factor in the resulting outcome of a hurricane event.

It is a generally accepted concept that wetlands can reduce the effects of storm surge and waves due to friction (Ferreira, 2011; Wamsley, Cialone, Smith, Atkinson, & Rosati, 2010). There are, of course, additional factors that contribute to this including storm intensity, track, and the surrounding topographic and bathymetric features (Wamsley et al., 2010). Larger and more intense hurricanes, with substantial storm surges, can overcome wetlands and still devastate main inland areas. Slower and more persistent hurricanes have also been found to overcome these natural barriers, since wetlands generally slow the surge propagation and wind due to friction (Ferreira, 2011; Wamsley et al., 2010). In 1985, Farber estimated that the loss of a one mile strip wetlands along the Louisiana coast could result in a discounted loss from hurricane damage of $1.1-$3.7 million in 1980 dollars (Farber, 1987).

Louisiana and Mississippi showcase geography of multiple natural protection features, i.e. wetlands and barrier islands (see Figure 2-9(a) for reference). Barrier islands (also found as the Outer Banks, North Carolina) serve as a means of "absorbing" storm impact and protecting the mainland where most of the population and infrastructure resides. However, Hurricanes Camille and Katrina showed that high storm surges can overtop the islands and impact the mainland (Morton, 2007). Another common landfall location, Corpus Christi, TX, has not only wetlands

and barrier islands, but a bay area as well (see Figure 2-9(b) for reference). In a study by Ferreira (2011), "values showed that, for areas inside Nueces Bay, the storm surge could vary up to four times depending on the parameter selection, for areas inside Corpus Christi Bay, the storm surge varied around three times and behind the barrier island the storm surge high variation was less than three times" (Ferreira, 2011). This indicates that further in, behind the barrier island, and inside the bay is more protected from storm surge. However, bays can be a blessing or a curse to the inland population depending on the hurricane intensity, track, spatial and temporal scales, as well as the bay geometry and depth. The hurricane track is a large component in determining how a bay area or channel will be affected. As was the concern with Manhattan for Hurricane Sandy, if the storm track is just right, then the winds can act as a driving force to move the storm surge into the bay, or in this case the Hudson into Manhattan (see Figure 2-9(c) for reference). In a study of the Chesapeake Bay after Hurricane Isabel in 2003 (Zhong, Li, & Zhang, 2010), it was found that strong winds moving into the Bay area resulted in larger storm surges with winds moving outward causing a depression within the bay (see Figure 2-9(d) for reference). However, due to the size and geometry of the Chesapeake Bay–the upper, middle, and mouth of the bay could all experience a different affect (i.e. a depression in the upper Bay could align with a surge in the lower/mouth Bay). It was also determined, that slow moving storms could allow the surge to build up within the Bay. A shallow bay can also cause amplification of the storm surge (Chen, Wang, & Tawes, 2008). Most storm surge models in use account for these features as well as the friction characteristics of wetlands and other vegetation.

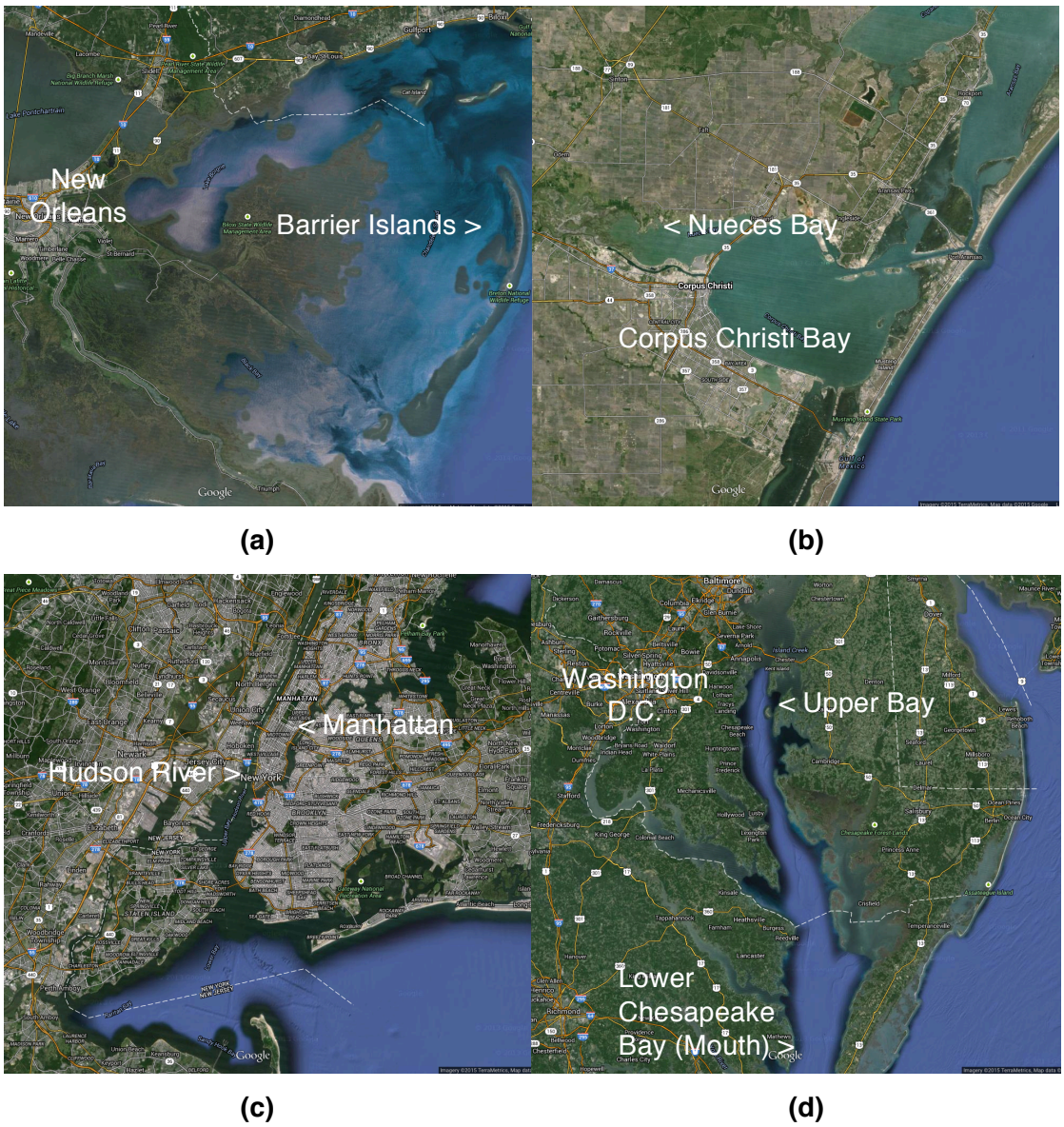

Figure 2-9 Satellite views of (a) Louisiana coastline near New Orleans, (b) Corpus Christi Bay, TX, (c) New York City, and (d) Chesapeake Bay near Maryland and Virginia (Google Map Data, 2015)

These natural features can be affected and altered as urbanization increases. New Orleans, LA, is a popular example of this. Rivers, such as the Mississippi, will wander and change paths as time progresses. Levees along the Mississippi River were constructed in attempt to protect the people living in New Orleans from flooding. As a consequence of building the levees in an attempt to control the Mississippi, sediment was prevented from being deposited, which

eventually aided in the sinking of New Orleans to below sea level. The prevention of sediment deposits along with subsurface mining can result in accelerated soil compaction (Syvitski et al., 2009). Lack of sediment deposits coupled with hurricane impacts can also deteriorate the same barrier islands that protect the coast (Morton, 2007).

In general, urbanization can increase flooding within the area. In areas where the ground (soil) is able to naturally absorb rainfall faster than the average rainfall rate for that area, most water will reach the stream channels in its basin – instead the water either absorbs into the soil, is evaporated off of vegetation, or percolates into the groundwater system (Booth, 1991). Soil and areas with lush vegetation can absorb precipitation into the ground and reduce flooding. There are situations where the rainfall rate exceeds absorption rate, and in these cases water moves toward open channels (Booth, 1991). In highly urbanized areas, there are more impervious surfaces where water cannot penetrate through the surface and instigates faster flow due to reduced friction and absorption. Urbanized areas have stormwater systems consisting of pipes and drainage basins to help manage the extra runoff created by roads, parking, lots, and other construction. In a heavy precipitation event, the water will rush to these systems and potentially overwhelm it, resulting in enhanced flooding. Along the coastline, heavily populated and highly urbanized areas are more vulnerable to inland flooding from a hurricane than its more rural counter parts.

Where a hurricane makes landfall is vital in understanding its potential for damaging effects. From the above discussion, it could be inferred that a much less intense hurricane would impact a highly urbanized area more than a rural coastal area. While nature appears to have some built in defenses, man has also managed to weaken those defenses and impact the locality's vulnerability. Most of the negative factors in relation to geography and hurricanes seem to be a

direct result of man-made structures and urbanization and seem to worsen in older, heavily populated locale.

2.2.3.2 Demographics

In 1990, 28% of the United States' population lived in coastal counties. In 2003, to the coastal population was at 53% with more than 150 million Americans living near the coast (Crossett, Culliton, Wiley, & Goodspeed, 2004). Since most of the US coastlines are vulnerable to hurricanes, this in turn puts the majority of the population at risk. Population is one of the most vital factors in determining the potential impact a hurricane can inflict. The demographics of coastal population can have a direct effect on the resulting damage as well as those who are able to evacuate. In addition, highly populated areas bring a mess of problems including increased infrastructure and socio-economic discrepancies. While hurricane damage is becoming more expensive and more media attention is showing the true hazards of coastal living, more people are still moving to coastal areas.

Generally, the increase in population indicates an increase in homes and other infrastructure, leading to an inflation of damage. The converse of this has also been looked into, while increase in population is linked to increased hurricane impacts, the activeness of a hurricane season can also affect an area's population and building quality. The years 1970-1989 consisted of relatively low hurricane activity for South Florida; as a result the population increased significantly. However, the homes built to accommodate that increase were found to experience more intense damage from later hurricanes than homes constructed from 1930-1934 and 1946-1955 (Tansel & Sizirici, 2011). The periods of 1930-1934 and 1946-1955 follow significant hurricane events; the 1926 Great Miami Hurricane and the Southeast Florida Hurricane in 1945 and Hurricane King in 1950, respectively. Consequently, more attention was

given to the quality of the construction to mitigate the impact of such events. A population decrease also occurred in 1993, immediately following Hurricane Andrew (1992) (Tansel & Sizirici, 2011). In recent years, Florida has obtained more year-round residents instead of seasonal ones, many of which are retired or work in tourism (Cutter & Emrich, 2006). Overall, Florida is similar to the rest of the US coastline in experiencing an overall increase in population, resulting adverse impact changes, through the years.

It is not just the quantity of people that live in a hurricane vulnerable zone that contributes to its outcome; it is also a characteristic of population demographics. A large percentage of the world's population lives near the coast, but the U.S. possesses a lower death toll and higher economic damage from coastal hazards due to being a more developed country (Nicholls & Small, 2002). This implies that higher income areas are more likely to afford safer housing as well as being more capable to react in a hazardous situation (Cutter, Boruff, & Shirley, 2003; Simmons & Sutter, 2005). Higher income areas are also linked to increase in damage costs by the increase in median home values (Hall & Ashley, 2008). In coastal cities, the higher income areas are right on the shore as it is "prime real estate" and the income brackets decrease out from the shoreline (Cutter & Emrich, 2006). According to the 2010 U.S. Census, New York City has the highest population and eight of the top ten highest income states are coastal locations (plus one for District of Columbia) (U.S. Department of Commerce, 2013). Therefore, the coast not only boasts the highest population, but the highest incomes as well, attributing to higher economic damage.

The combination of socioeconomic status and demographics data were used at the University of South Carolina (Cutter et al., 2003) in order to create the Social Vulnerability Index (SoVI). The SoVI relates the two main components of location vulnerability: physical

vulnerability (i.e. hurricane prone area), and the various characteristics of a population that determine how people are able to cope and recover from natural hazards (Cutter & Emrich, 2006). The SoVI was designed based off of the (modified) Hazards of Place Model shown in Figure 2-10 (Cutter, 1996). The main factors of social vulnerability that are widely accepted include age, race, gender, and socioeconomic status. The SoVI uses 11 factors (variables), in an additive model in order to produce a SoVI score for each U.S. county. These 11 factors account for 76.4 percent of the variance among U.S. counties. The SoVI county scores range from -9.6 (lowest) to 49.51 (highest) with a mean score of 1.54 and a standard deviation of 3.38. Corresponding to the demographics discussed, Manhattan Borough (New York City) was found to be the most vulnerable county in the U.S. Excluding that, the most vulnerable areas of the country appear to be in the southern half where there are more ethnic inequalities and higher population growth. The low vulnerability areas are less populated and generally homogeneous in nature (i.e. mainly white, suburban, and well-educated). These areas are New England, eastern side of the Appalachian Mountains from Virginia to North Carolina, and the Great Lakes Region with Yellowstone National Park County topping the list. The results of the SoVI make it clear that variables such as unemployment, access to resources, homelessness, non-English speaking immigrants, wealth, race, built environment, etc. play a key role in how prepared and susceptible a location is to a natural hazard.

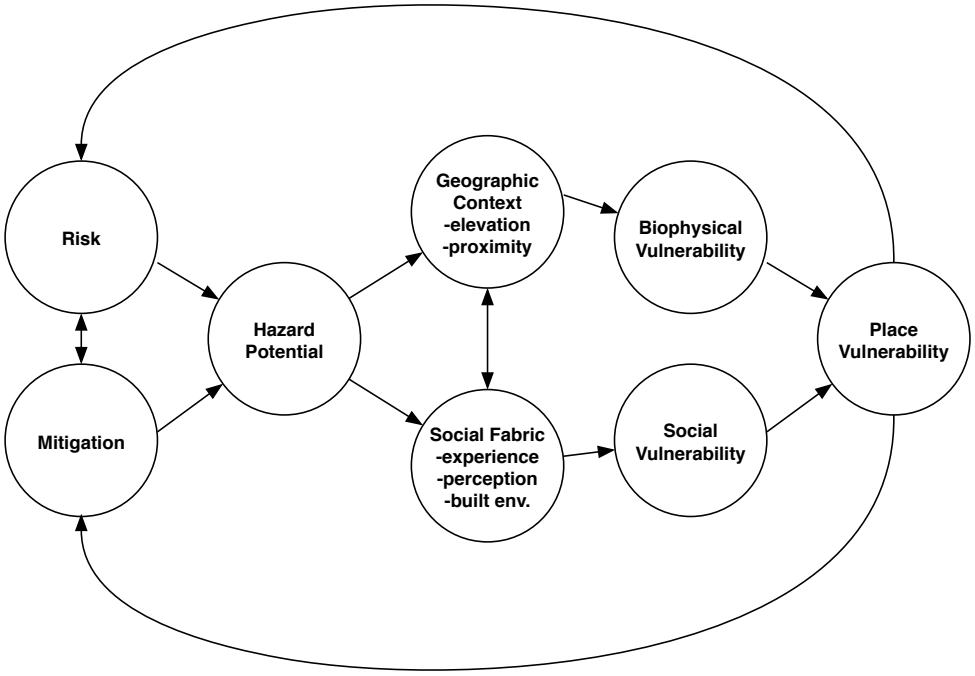

Figure 2-10 Hazards-of-Place Model of Vulnerability; after: (Cutter, 1996)

Cutter, Boruff, and Shirley (2003) did not find any statistically significant results when comparing the SoVI to presidential declared natural disasters, however incorporating SoVI into disaster modeling has gained attention in recent years. In a study done by Burton (Burton, 2010), the SoVI was used with FEMA hurricane damage assessments in specific areas where the factors had an impact. Damage that was less extensive was mainly focused on hurricane winds and storm surge and societal aspects did not make a significant contribution until "extensive" damage was reached. However, overall the meteorological impacts (storm surge) played a larger role than the societal factors did. That being said, the social vulnerability factors that appeared to stand out more had to do with urban population, race, agriculture, and poverty level. Urban populations have more "housing stock" contributing to higher damage numbers. Simply put: more houses, more damage.

2.2.3.3 Societal Perception

The main basis behind this thesis relies on the lack of understanding of risk during a hurricane or even a severe weather event. This is a continuing struggle in the field of natural disasters both on the engineering and meteorology side. How can engineers and scientists correctly communicate the apparent risks for a natural hazard so that the general population understands the risk? If there is a misinterpretation or a misperception of risk by the public, the responsibility to correct this problem should fall on those trying to communicate the message. On the other side of the argument, if citizens are accounting for different factors when deciding to evacuate, why aren't engineers, scientists, and emergency managers, when evaluating evacuation orders, considering those same factors?

Many studies are done within various disciplines to help determine how people decide to evacuate during a hurricane, mainly based on perceived risk. Individuals must recognize the risk at hand as being imminent or they will not act (evacuate) (Sorensen, 2000). If the risk is underestimated, this could put more lives at risk. The level of risk perceived, therefore, directly correlates to the level of precautions taken by the individual (Stein, Dueñas-Osorio, & Subramanian, 2010). However, the risk perceived does not necessarily correlate to the evacuation orders given (Stein et al., 2010). Evacuation orders are mainly determined based on storm surge since this poses the greatest risk to lives (Henk et al., 2007). A study done for Harris County, Texas following Hurricane Ike in 2008 found that 62% of shadow evacuees (those who were not under evacuation order but evacuated anyways) had accurate perceptions of the potential hazards and were therefore correct in evacuating (Stein et al., 2010). The areas not likely to suffer from storm surge flooding can still experience extreme winds and inland flooding due to rain. These shadow evacuees seem to have intuitively grasped this concept. Dow and

Cutter (2000) determined that those who are well aware of hurricane hazards no longer wait for the official government warning when deciding to evacuate (Dow & Cutter, 2000).

The other possibility with individuals determining risk independently could result in those in evacuation zones deciding not to evacuate. In a study done by Stein (2010), it was determined that the awareness of an evacuation order only had a modest effect on how people determined to evacuate (Stein et al., 2010). Dow and Cutter (1998) did another study on the "crying wolf" phenomenon for South Carolina for Hurricane Bertha, which was followed by Hurricane Fran two months later. Hurricane Bertha actually had minimal effects but evacuation orders were issued anyways. It was found that only 3% evacuated for Hurricane Bertha, but not for Hurricane Fran (Dow & Cutter, 1998). "Crying wolf" is not an unusual perspective people have when listening to the news and government officials. In an article by Nicole Dash (2007), she states, "if warnings were heard and ultimately believed, then evacuation would be the end result" (Dash & Gladwin, 2007). The emphasis on this would be "believing" the warnings. Unfortunately, there are more instances where people choose not to evacuate when they should (Dash & Gladwin, 2007). Renn et. al. (1992) argued that a "social amplification of risk" could be used by integrating both the social and technical concepts of an event in order to create a broad spectrum approach to risk (Renn, Burns, Kasperson, Kasperson, & Slovic, 1992).

The information message given to the public should comprise of various characteristics including; track, intensity, landfall location, and infrastructure vulnerability (Baker, 1991). It appears, in various studies, that some people already account for this when determining to evacuate, while others choose to not evacuate possibly from experience, disbelief in officials, and a misconception of risk. People need information to be given in a more solid conception in order to understand the very real possible dangers (Dash & Gladwin, 2007). The warnings given

should be clear, concise, and specific in order for people to appreciate the risks involved and evacuate (Mileti & Beck, 1975). The National Hurricane Center and The Weather Channel both attempt to cover the hazards associated with a storm event. The advisories issued should be a straightforward and simple assessment of the storm risk, specific to all the conditions and hazards incorporated in it; geography, wind, storm surge, rain, and infrastructure. These are items considered by the emergency managers, scientists, engineers, and (although they might not be aware) some of the public.

2.3 Existing Approaches for Hurricane Impact Prediction

2.3.1 FEMA HAZUS

Among the few models used for various natural hazard damage predictions, the HAZUS-MH (HAZardous U.S. MultiHazard) model is arguably the most popular tool as well as the only damage prediction model widely used for the entire United States. However, its level of accuracy in terms of predicting losses has been a subject of debate among researchers. Released in 2004 by FEMA, HAZUS-MH is government funded loss estimation software. The original HAZUS, was first released in 1997 as a loss estimation tool for earthquake scenarios. Since then, FEMA, along with a selected group of experts and contractors, have developed a flood and hurricane model. The multi-hazard version was created in order to integrate data sets and classification systems common in all three models. Federal agencies, academic institutions, and private companies use HAZUS-MH in order to illustrate various scenarios and to estimate damage and loss corresponding to certain natural hazard events (Schneider & Schauer, 2006).

The Earthquake Model was the first model released in 1997 and was revised three times thereafter. This model is possibly the trademark of FEMA HAZUS and includes the use of a structural building classification system, potable water network analysis capability, analysis of multiple fault segments, USGS probabilistic ground shaking maps, user specified damage and loss functions, and more. The last of the 3 revisions, HAZUS99-SR2, incorporated an "advanced engineering building module (AEBM)" in order to estimate specific building damage and loss. This allows more advanced users to model building specific response to an earthquake event and evaluate mitigation strategies (Schneider & Schauer, 2006).

The Flood Model began development in 1997 in a similar method to the Earthquake Model and was the next to be released. This model includes the use of floodplain data and building classes while accounting for debris, shelters, agriculture, and utilities. The classes of buildings and essential facilities were determined using FEMA and US Army Corps of Engineers (USACE) damage data. Since flooding is a somewhat a predictable event, the model also took into account flood warnings and effects due to certain flow velocities. Released before the Flood Model, the Flood Information Tool (FIT) users could enter certain data in order to estimate the extent and depth of a flood so that the Flood Model could then be used to estimate the resulting damage and loss. The data used for this model is entered and sorted by the users in order to create a network of all the data for the U.S. (Schneider & Schauer, 2006).

The Hurricane Model was subsequently developed similarly to the Flood Model. The main variation from the Flood Model was taking into account the wind field and track of a hurricane or tropical storm system. Also, in deference from the other models, the Hurricane Model loss estimates are based on historical data of financial losses and storm intensity (Schneider & Schauer, 2006). There are five main components, discussed by Vickery (2006), of

the Hurricane Model: the hurricane hazard model, wind load model, terrain model, physical damage model, and loss model. The first three models, which can be thought of as the environmental components or the causes, are run first and then used in the last two models (the effects of the first three) in order to determine a damage and loss estimate for a given hurricane event (Vickery, Lin, Skerlj, Twisdale, Lawrence A, & Huang, 2006; Vickery, Skerlj, et al., 2006).

The first of these model components, the hurricane hazard model, assesses meteorological hazards that contribute to the overall impact of a hurricane or tropical storm event. This includes the wind field and storm track/motion, as well as the rainfall rate for an event. For land falling hurricanes the wind speed and central pressure (lowest pressure) is assessed at landfall (Vickery, Lin, et al., 2006). The wind speed is typically highest near the center of the storm, but not exactly within the eye where the pressure is lowest. The rainfall within a hurricane is also highest near the eye wall where the strongest rain bands are within the system. The rainfall rates for each event are used mainly to determine the amount of water that could infiltrate a building through cracks and cause damage or possibly weaken the structure. Both the wind and rainfall rates are therefore tied to the storm motion, as discussed in Section 2.2.1.

The wind load model component to the HAZUS-MH Hurricane model accounts for both the wind load acting on a building and the effects of windborne debris, which are dependent on the wind field and velocity modeled in the hurricane hazards model. Windborne debris can play a significant role in the resulting damage due to wind as was illustrated in Section 2.2.2.1. Within the wind load model, the wind loads are determined based on pressure differences and account for the change in wind speed and duration as the hurricane moves (Vickery, Lin, et al., 2006). In addition, as outlined by Vickery (2006), the windborne debris impact speed, angle, and orientation when the object strikes the building is computed by modeling the different building

components and the predicted trajectory of the object. Roof gravel is a debris that is specifically modeled here due to the ease in which it can be lifted off a building making it a common projectile debris, but before it can be modeled the flow field is required in order to lift and transport the gravel (Vickery, Lin, et al., 2006). The model then uses the probability of window damage (most vulnerable part of a structure for debris puncture) from the wind load characteristics calculated in order to determine the physical damage component (Vickery, Lin, et al., 2006; Vickery, Skerlj, et al., 2006).

The next model component of the HAZUS-MH Hurricane Model is the terrain model. The main relevance of the terrain model is to account for how the surface affects the wind speed. The driving factor behind this deals with the fact that in smooth terrain, such as coastal areas, the wind speed is greater because nothing is obstructing it or slowing it down due to friction as it would in a forest or metropolitan city. In the event of a hurricane, the winds will be much stronger right at the coast, over sand, which has a very low roughness, than as the wind field crosses into the city, which has a high roughness. Therefore this is a revision to the hurricane hazard model in terms of wind, which correlates to the wind load model. The terrain model, wind load model, and hurricane hazard model all take into account how the atmospheric variables relate to the surrounding environmental as a hurricane makes landfall. The results of these modeled components tie into the physical damage model and loss model by assessing how it relates to building damage and other losses.

The physical damage model assesses building failure in response to hurricane variables. “Physical damage” in this model mainly referrers to only exterior building damage. Mainly cladding and components, roofs, windows, walls, and joints are analyzed, which is consistent with the structural features discussed in damage assessment reports. The model uses standard

geometric representation of buildings with various use and stories. The wind field for a modeled hurricane is then used to model load and resistance. If a door, window, or wall fails due to wind loads or debris, the model then adjusts for the effect on the internal pressure. This could result in additional failures causing the internal pressure to approach peak external pressure. Multiple simulations are done for a given storm event, and rainfall infiltration is accounted for in order to determine a damage state for the structure. Within HAZUS a damage state for each structure class has been developed and used within the model (Vickery, Skerlj, et al., 2006).

From the determined damage state, the economic loss due to a hurricane or tropical storm is estimated. The economic loss for a given modeled event accounts for the building itself, the contents/inventory, and the costs resulting from the inability to use the building (Vickery, Skerlj, et al., 2006). The costs of the building and its major components are computed first, then, based off of the damage to those components, the ability to repair or replace such components is computed. These are the explicit and implicit costs, respectively. The implicit costs also serve as a way to relate the exterior damage to the interior damage where rainwater infiltration becomes a factor, leading directly into assessing the contents/inventory losses. Based on the determined damage to the exterior and interior of the building, the model can estimate the time needed to repair and/or replace the building and its components, which leads to the cost associated with the inability to use the building while work is being done (Vickery, Skerlj, et al., 2006). This can be more significant for a business and/or rental communities due to loss of revenue and rental income. Using a similar method that was established early on with the Earthquake Model in HAZUS-MH, the damage and loss estimate is finally calculated for the modeled storm (Vickery, Skerlj, et al., 2006).

2.3.2 Florida Public Hurricane Loss Model

To help budget and prepare for hurricane events specifically in Florida, a commonly hurricane-prone state, the Florida Office of Insurance Regulation (OIR) assembled a team of experts to create another loss prediction model: the Florida Public Hurricane Loss Model (FPHLM) (Pinelli et al., 2011). The FPHLM is used to compute the average annual losses (AALs) and the probable maximum losses (PMLs) for a given region of Florida. The model also has the capability to run hypothetical storm events or compute the outcome of a currently occurring storm event (Pinelli et al., 2011). A detailed description of the model and its components can be found online at http://www.cis.fiu.edu/hurricaneloss/.

The FPHLM uses detailed analyses in meteorology, engineering, and insurance to create the wind hazard, vulnerability, and insured lost cost components. The model is mainly used for residential structures, since those are more prominent, but it can also be used for commercial and high-rise buildings. The meteorological hazards stem directly from the hurricane's characteristics to include; track, wind field, and terrain for effects of terrain roughness on the hurricane's wind speed. The relation of hurricane force winds to different structure types is used to estimate damage and associated costs in order to then determine specific hurricane vulnerable parts of Florida. This leads into the actuarial component, which will generate a probabilistic loss for certain zip codes, counties, or the entire state. This is also what gives the expected loss for a specific event (hypothetical or occurring).

The meteorological component is mainly used to relate to the resulting damage to the actuarial component. The damage determination is what links the hurricane characteristics to the resulting cost, similar to the FEMA HAZUS-MH Model. According to the Saffir-Simpson scale,

the wind speed is directly related to the storm intensity. In this model, wind is the main meteorological factor used in determining structural damage.

To begin analyzing wind induced damage on structures; the building type must first be determined. By using infrastructure databases for the state of Florida, the FPHLM team determined the building stock for Florida by county. The most common structural systems in Florida turned out to be one to two stories, composed of timber or masonry, a shingle or tile roof, and a roof of gable or hip shape (Pinelli et al., 2011). This covers 77% to 89% of the structures in Florida and the remaining building types are analyzed by a generic model (Pinelli et al., 2011). Each building type is analyzed by its components; walls, roof, connections, windows, and doors (including garage). Roofs tend to be a main damage indicator and are an assessment tool in determining wind strength. As with the FEMA HAZUS model, the FPHLM analyzes both wind induced pressure, wind debris, and wind driven rain. By using a "probabilistic component-based Monte-Carlo simulation", the FPHLM calculates the modeled exterior damage to the structure (Pinelli et al., 2011). The other component deals with any resultant interior damage, which could be tied to wind driven rain infiltration and/or wind induced pressure due to a puncture in the structure such that it is no longer enclosed. The resultant interior damage also includes utility damage and is modeled similar to the exterior damage using a Monte Carlo simulation (Pinelli et al., 2011).

The actuarial model component ties the resulting damage to cost. This damage cost includes the exterior damage, interior damage, and additional living expenses. The additional living expenses include the cost associated with being unable to occupy the damaged building, similar to the FEMA HAZUS-MH Model. The "ground-up" loss is computed by using the median result of a damage interval modeled for a specified wind speed (Hamid, Pinelli, Chen, &

Gurley, 2011). Deductible limits are then applied in order to calculate the net deductible loss, which is multiplied by the damage ratio for a given event in order to get the expect loss (Hamid et al., 2011). The AAL is calculated by using a probability weight of the expected loss, which was averaged over all possible damages for a given wind speed, and adjusted for inflation (Hamid et al., 2011). This is just for one building or property and can be used for a whole zip code simply by adding the AAL for all structures (and their respective type characteristics) in the desired area and so on for multiple counties. The AAL is then used to determine policy information. This approach can be used for hypothetical events in order to determine a resultant net loss.

Hamid et. al. (2011) ran 30 hypothetical hurricane events in order to determine which would be the most destructive and costly. A variation in category, landfall location, and track were used in order to produce a range of results. As would be expected, the highest damage occurred in highly populated and typically vulnerable cities. The intriguing discovery made in this study is the effect of the track on damage. As Hamid et. al. (2011) discusses, a hurricane moving over heavily populated central Florida is more destructive and costly than one that would make landfall at the southern tip and move westward. Even though Miami is heavily populated, a westward bound hurricane would go over the everglades after Miami, which is less populated and are naturally able to absorb heavy rain. An example hurricane that made landfall in Tampa and moved eastward into the Orlando area would cause more damage, emphasizing the importance of storm track and its geographic location within Florida, and similarly, anywhere else (Hamid et al., 2011).

The components used for this model are typical of various studies and similar to the FEMA HAZUS-MH Model discussed previously. As with HAZUS-MH, the typically modeled

hurricane characteristic is wind and its related conditions such as debris and driving rain. However, storm surge does not seem to be included in this model. There also does not appear to be much in relation to rainfall rate or amounts associated with a tropical system. This indicates the majority of damage due to flooding is not accounted for except for rain that is driven into a building through cracks and connections by rain.

The Florida Public Hurricane Loss model works as a mechanism for the state of Florida to retrieve annual averages and probable maximums of the loss (cost) due to hurricane events for different counties and zip codes. The FPHLM is mainly used for budgetary purposes by the state to verify claims as well as by insurance companies. The FPHLM also has the beneficial use for determining the effectiveness of various mitigation strategies, including how to allocate resources.

2.4 Artificial Neural Networks

2.4.1 General Overview

An Artificial Neural Network (hereon referred to as ANN or "neural network") is a numerical model originally created to replicate how the human brain learns. In other words, an ANN is a form of artificial intelligence (AI). A human being learns from experience by recognizing patterns. The brain makes connections based on "inputs" and what the consequences to those inputs are. With enough data, the brain determines the result to be a related outcome to that input/action. As an example, it is commonly known that students learn the most from "doing" or from failure. This is because by actually doing something the brain is strengthening connections and creating pathways to retain correlating information. Similarly, by failing, the

brain will retrace its original path in order to strengthen the correct one. These so-called "paths" are the connections between brain cells, or "neurons", of the action (input) and the consequence (output). The ANN attempts to mirror this structure of the human nervous system. The brain has approximately one billions neurons, while some of the most complex ANNs only have thousands of neurons (Sarle, 1994). In simpler computing programs, the amount of neurons is much less (usually tens). Even with far less neurons than the human brain, the computed results can still reach significant statistical correlation indicating that the ANN has formed an effective "path" just as the human brain would have if the data is properly trained.

In an ANN the computer can run through data over and over again, learning from mistakes, and establishing a pattern between the input neurons and output neurons (Hecht-Nielsen, 1988). Handwriting and speech recognition are just a couple examples of common uses of neurocomputing. In general, the main three ANN applications are: AI models, adaptive signal processors (i.e. for robots), and data analysis (Sarle, 1994). For data analysis, which is what will be discussed herein, the application of ANNs appear to "learn" in a similar fashion to statistical models (Sarle, 1994; White, 1989). The ANN will essentially find statistical correlations between the provided input and output data so that, in use, it can interpolate the closest corresponding output for the given input. Since statistical models are notoriously accurate, this implies that ANNs could be as well.

The use of ANNs for analysis and pattern recognition is what drives the various applications of ANNs. These network models provide the ability to establish forecasts and predictions using historical data (similar to a person using experience). Like many other subject areas, this is the appeal for using ANNs to predict the impact from a hurricane event. There are varied, independent, factors that are instinctively taken into account by forecasters when a

hurricane is about to make landfall but there is no way to quantify them. Forecasters, and others in this field of study, are able to assess these threats (outcomes) based on experience (i.e. historical data). The review of how ANNs operate and the various applications, discussed herein, will reveal the possibility of applying this type of computing algorithms to the field of hurricane impact prediction.

2.4.2 Using Artificial Neural Networks

2.4.2.1 Theory and Structure

The ANN is centered on the concept of neurological connections. A typical ANN is structured with the idea of "layers": the input layer, hidden layer, and output layer. When used, the data flows from the input layer through to the output layer via neuron connections. A simple linear regression model links the input to the output directly, with no hidden layers. One network could have multiple hidden layers depending on the complexity of the problem. As can be seen in Figure 2-11 below, each layer can subsequently contain multiple neurons. The input layer contains the independent variables (input neurons) and the output layer contains the predicted values (output neurons) value (Sarle, 1994). The input, hidden, and output neurons typically all connect between layers, i.e. each input will connect with each hidden neuron, which connects with each output. It is possible to structure a network where not all the neurons connect, i.e. one input neuron might only connect with a percentage of the hidden neurons, etc. How the neurons relate is classically either linear ("linear transfer" in MATLAB) or logistic ("log-sigmoid" in MATLAB), instituting not only where the neurons connect but in what respect as well. The connections and relationships are established during training so that, when in use, inputs provided will generate a relevant output.

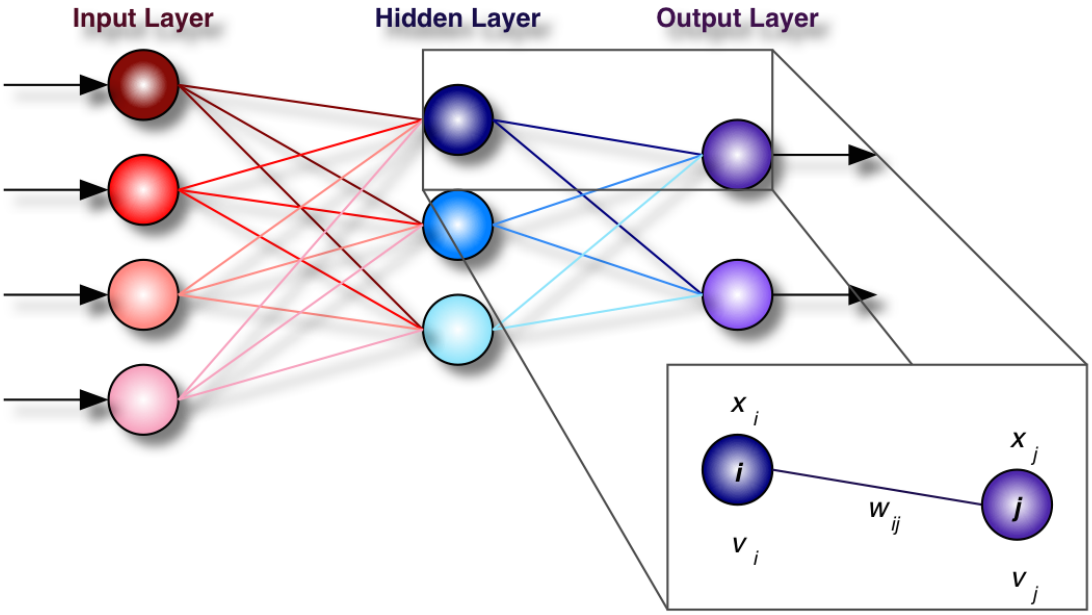

Figure 2-11 Basic neural network structure and neuron relationship

There are two main ways to train a network; supervised and unsupervised training. A supervised training approach provides known inputs and outputs ("targets") and will run multiple iterations in pursuance of a pattern between the given data. Unsupervised training involves the network learning as it goes, in other words the outputs are not initially known and the pattern develops as inputs are given and the network runs (Svozil, Kvasnieka, & Pospichal, 1997). Supervised training, commonly used for multilayer feedforward networks, is what will be used in this study and therefore discussed herein. The term "feedforward" implies that the data strictly moves from the input to hidden to output layer, instead of the possibility of backtracking through various segments of the system before producing a final output. During training, these systems use backpropagation as a learning tool, which propagates the error backwards so the data can successfully flow forwards. Multilayer feedforward networks trained with backpropagation are the most popular ANNs.

In building this type of ANN, the network must first be trained with a set of known input and output data. This can be data from past events/experiences, where the outcome is known. This will be the basis to predict the outcome for future similar events. The data should then be divided into training data, testing data, and validation data (as a starting point, this division is typically 70%, 15%, and 15%, respectively). When training, the ANN attempts to make connections between the input layer and the hidden layer(s), and then the hidden layer(s) and output layer using weights and biases on the connections between each of the neurons. The training data first establishes a pattern then the testing and validation data serves as data used to minimize the error. Each input, x_i, can range from one to any number of user determined amounts, *m*. This is the same for each output, Y_j, however, most of the time there are less outputs than inputs ($n < m$). The notation Y_j can be considered the known or desired target value, while y_j indicates the approximated value by the network. The learning tool (here backpropagation) adjusts the weights, W_{ij}, in order to resolve the approximated y_j closer to the provided target value, Y_j. This W_{ij} factor is described as the connection from the *i*th to the *j*ith neuron (see Figure 2-11). For a simple feedforward network with basic backpropagation logic, the following is assumed:

$$s_i = \sum_{j=1}^{i-1} W_{ij} x_i \tag{2.1}$$

where; s_i can be thought of as the "potential of the *i*th neuron" or the "voltage to exciting a neuron" (Svozil et al., 1997; Werbos, 1990) and $m < i \leq N+n$

$$x_i = f(s_i) \tag{2.2}$$

where; $f(s_i)$ is the "transfer function" and $m < i \leq N+n$

$$Y_j = x_{i+N} \tag{2.3}$$

where; $1 \leq i \leq n$ and N is a constant that is no less than m and the value of $N + n$ determines the total number of neurons in the network. The relationship between neurons, i.e. the transfer function or sigmoidal function, *f(s)*, can be thought of as:

$$f(s) = \frac{1}{1+e^{-s}} \tag{2.4}$$

For more complex networks (with hidden layers), the threshold (possibly the bias) value for the *i*th neuron, v_i, is added into Equation (2.1).

$$s_i = v_i + \sum_{j=1}^{i-1} W_{ij} x_i \tag{2.5}$$

In order to increase the accuracy of the network, backpropagation alters the threshold, v_i, and weights, W_{ij}, to minimize the mean square error between the approximated/computed output value, y_j, and the target output, Y_j. This is done by minimizing the objective function, E:

$$E = \sum_{j=1}^{n} \frac{1}{2} [y_j - Y_j]^2 \tag{2.6}$$

In backpropagation, the derivatives of the objective function are calculated for the output layer then the hidden layer(s) and finally the input layer. Hence, the output error propagates backwards towards the input layer in furtherance of correcting the correlations between neurons.

Multilayer feedforward networks with backpropagation are commonly used for pattern recognition problems. In training these networks, the program builds and strengthens connections between neurons by establishing statistical patterns between input and output. The allocated testing (and possibly validation) data are used to "test" the pattern it has created by the above procedure. Some programming tools, such as MATLAB, have simplified this process of creating an ANN. The learning tools are inherent and the user simply has to provide the data and

construct the network form (determine the number of hidden neurons, etc.) based off of the problem constraints. The program then progresses through the learning process and produces a usable network for prediction, forecasting, and pattern recognition.

2.4.2.2 Application

Once an ANN is trained and constructed, it can then be used to illustrate statistical relationships for practical purposes in pattern recognition, prediction modeling, and forecasting. As was previously stated, common uses consist of handwriting recognition and speech recognition. This is also one way a computer or website could "know" to suggest certain items or other sites, etc., to the user. ANNs have been developed for use in various fields, from business and finance to water resources to medicine. These have used the above concepts and applied them to serve as prediction and forecasting tools.

In the business and finance industry, forecasting the finance and stock market is a vital trade for a company. The ability to forecast future stock prices lends a financial company the capability to increase profit earnings, which is essentially vital to sustain and subsequently grow a company. Most stock market models consist of a linear relationship when the factors are not necessarily linear and can be arbitrary (Lu Dang Khoa, Sakakibara, & Nishikawa, 2006). Since profit gain is the major goal for stock market forecasting, one network model integrated a Directional Profit (DP) adjustment factor, $f_{DP}(p)$ and a Discounted Least Squared (DLS) function, w(p), to the object function denoted as $f_{TDP}(p)$ (Yao & Tan, 2000) as shown in Equation (2.7). Once the object function is found, it can be used to determine the error, $E_{TDP,}$ as shown in Equation (2.8) as a function of the approximated/computed output value, y_j, and the target output, Y_j and the to the object function, $f_{TDP}(p)$

$$f_{TDP}(p) = f_{DP}(p) \times w(p) \tag{2.7}$$

$$E_{TDP} = \sum_{i=1}^{n} \frac{1}{2} f_{TDP}(p)\left[y_j - Y_j\right]^2 \tag{2.8}$$

The DP adjustment factor, $f_{DP}(p)$, is a function of changes and directions of network price target values for a user specified threshold. The DLS adjustment factor, w(p), adjusts for the contribution of the overall error, p (Lu Dang Khoa et al., 2006). This puts the focus on profit and time allowing for periodic adjustments conforming to the complexity of stock price forecasting.

The inputs for this model included somewhat obvious factors such as, inflation, gas prices, and the Gross Domestic Product (GDP). More technical inputs were also used including the strength index, daily high, and daily low, etc (Lu Dang Khoa et al., 2006). The feedforward network used for this model resulted in a low mean square error (MSE) and a supporting statistically significant precision (Lu Dang Khoa et al., 2006). Even for a problem as complex as stock price forecasting, adjustments to the basic ANN structure resulted in a usable forecasting tool.

In a field more relevant to civil engineering, hydrologic and rainfall runoff modeling are other popular applications of ANNs. Most of these networks are multilayer with backpropagation training (Dawson & Wilby, 2001). Typically ANNs designed to model hydrologic flow compute either the discharge or model stage from a rainfall event. The variance occurs in the inputs and the method of approach, which depend on the hydrologic model classification. In general, ANNs for hydrologic modeling are considered parametric functions that relate meteorological variables to runoff using transfer functions (Dawson & Wilby, 2001). The models can be either lumped, where the catchment basin is treated as a single unit, or distributed with the use of a catchment system containing subsystems (Dawson & Wilby, 2001). The inputs can be as simple as past rainfall records to more complex. More complex and incorporative models could account for

seasonal variations, which incorporates the relative rainfall and discharge perturbations, and time step segments (Shamseldin, 1997). The designer defined input data and method can have an effect on the outputs and accuracy of the model for certain event characteristics, which results in some models becoming more useful than others in specific situations (Shamseldin, 1997). Even with that, the ANNs for hydrologic modeling seem to produce relevant enough results in comparison with other types of hydrologic modeling.

The use of neural networks in medicine appears to be the most widely used application of ANNs, so much so that MATLAB even has an example batch of patient data in order to hypothetically diagnose cancer. The prominent medical fields using these models seem to be clinical and diagnostic medicine. This application dates back to 1989 with the first use of ANNs to diagnose the risk level of chest pains (Baxt, 1995). Another study was later conducted at a cardiac ward with 365 patients where 120 of the 365 had a myocardial infarction. In using this data to train a network, the model produced the highest sensitivity and specificity for this field at the time (Baxt, 1995). This was then tested in real time with 320 patients and resulted in higher sensitivity and specificity than the physician diagnosis. Other medical applications involve using data from images, such as chest radiographs and mammograms, and waveform analysis from ECGs. The ECG data also relates anterior chest pains with myocardial infarctions, where as image data can analyze mammographic data, lung nodules, and malignant lesions for cancer. These models were also highly reliable with the image analysis determination out performing the radiologist's diagnosis (Baxt, 1995). The use of ANNs in the medical field serves as evidence to the possible accuracy of learning programs and has promoted the use and expansion into other fields.

ANNs are applicable to many more problems including credit card fraud protection, airline seating allocation, loan approval, real estate analysis, missile guidance and detonation, and continuous-casting control during steel production (Widrow, Rumelhart, & Lehr, 1994). Those applications are only the multilayer nonlinear problems, as are the above examples. Most applications of ANNs use a nonlinear system, since the priority benefit of using ANNs is to relate complicated data. Linear ANNs would be similar to best-fit analysis. The ANN type is dependent on the type of problem the designer is trying to solve and leads to a versatile application of ANNs while still proving an accurate modeling tool. The use of such a modeling tool has yet to be applied to the area of natural hazards impact prediction.

2.5 Summary

Hurricanes are one of the costliest natural disasters to occur in the U.S. with the ability to affect over half of the current population. These events are large atmospheric systems formed in warm, humid, climates, which create intense winds, heavy rainfall, and a rise in ocean level that can impact society by resulting in economic damage and loss of life. These results can vary in severity based on numerous factors from wind speed to storm surge to infrastructure to geography. These factors can then have differing values and scales of intensity, which would produce differing results. Wind speed becomes more of a hazard at higher values and in areas of dense infrastructure that result in increased debris, which puncture holes in structures, increasing internal pressures, and therefore increasing damage. Even though wind carries a destructive power, storm surge actually contributes more to the overall cost of damage due to its even more powerful nature along with the increased value of properties along the coast. Flooding, in general, is more likely to cause significant damage than wind; this includes heavy precipitation, which

can linger over a long period of time. Flooding and storm surge effects are also the main cause for destruction and disruption of utilities and transportation services. All of these factors are subsequently affected by the geography of the landfall location in which they strike. Urbanized areas are prone to worsened flooding conditions while areas with wetlands and barrier islands are more protected from harmful floodwaters. In addition, urbanized areas also have more people, and therefore more infrastructure, in harms way along with poorer communities, which tend to be less resilient to such disasters. All of these factors, and the related variations, have a contribution to the overall resulting impact of a hurricane event.

There are current models in use that combine some of these parameter in order to determine the resulting damage. The most commonly used loss estimation model is HAZUS-MH. This model serves well to estimate the resulting loss (cost) of a specific hurricane, earthquake, or flood event by using multiple hazard factors to subsequently incorporate into a damage model, which then translates to a loss model. Florida has its own similar model, which is mainly used for insurance and mitigation purposes. HAZUS-MH uses more meteorological variables than the FPHLM does; however, the FPHLM uses a more comprehensive building inventory. While these models are well served as loss estimation tools for insurance, budgetary, and mitigation purposes, neither of these are used as a means to communicate risk and vulnerability to the general public, which is still mainly reliant on the Saffir-Simpson Scale (based solely on wind speed).

Most experts working in the field of natural hazards understand these parameter variances that previous and current models have tried to capture. Neural networks are a form of artificial intelligence that can attempt to recreate these connections by learning from the same historical events that experts are basing their knowledge on. Within this research, neural networks will be fed historical data based on these varying parameters and subsequently attempt to match them

with the corresponding results provided. The neural network will accomplish this through multiple iterations of the data where the predicted result will be compared to the actual result in order to determine the error of the prediction. Backpropagation will then be used to adjust the contribution of each parameter, as it pertains to the result, until that error, is minimized. This approach will serve as another possible predictive model with the purpose of providing the predictive results in a clear and concise manner to communicate the risk of a hurricane event to the public in a way that more accurately describes the situation at hand by using multiple parameters, as most individuals do anyways. The use of such a system could also reduce instances where shadow evacuees should have actually been told to evacuate and "crying wolf" instances. This will be accomplished by using a ranking system that provides levels of expected damage, as compared to historical hurricane events, based on the various parameters previously discussed in this chapter. The product will be the proposed Impact Level Ranking System.

CHAPTER 3

PUBLICATIONS

3.1 Hurricane Impact Prediction: A Multivariable Approach Using Neural Networks

Hurricanes are complex meteorological events that impact society in different ways based on variations of multiple contributing factors. The resulting economic damage from one of these storms is a product of variations in the landfall location and population affected as well as wind speed, pressure, storm surge, and precipitation. However, the category ranking, Saffir-Simpson Scale, solely by wind speed is what the general public focuses on, but the correlation between this one parameter and the resulting damage is weak. Within this study, a new Impact Level Ranking System based on economic damage will be introduced and used as the outcome attributed to variations in these multiple hurricane parameters. Since the link between multiple parameters and one such outcome of a hurricane is a complex and non-linear problem, six neural network variations will be assessed for the best way to present such data to an artificial intelligence program. The resulting percent errors are low enough to consider each model viable, but those, which perform better through training and trial simulations, have a lower number of inputs. The ability to establish such complex connections, paves the way for a new method of forecasting hurricane events using the most applicable, and easily available, variables.

3.1.1 Introduction

Tropical Cyclones account for roughly 47% of all billion-dollar events, which amounts for 80% of The United States (U.S.) losses from combined severe weather and climate events

(Smith & Katz, 2013). With most of the U.S. population living near the coastline, tropical cyclones (hurricanes) are high-risk events. Hurricanes bring multiple meteorological factors, such as extreme winds, storm surge, and heavy precipitation, ashore, which can cause extensive damage. However, these meteorological factors are not the only contributors to the resulting damage since possible landfall locations vary in population (urbanization), infrastructure, and geography. These additional factors can either enhance or minimize the resulting impacts but are not typically well communicated or understood by the general public. Increased infrastructure can exacerbate damage by increasing debris and minimizing precipitation absorption leading to further damage downwind and increased flooding hazards, respectively. Additionally, areas with channels or bays can either direct storm surge into a populated area or serve as a protection mechanism depending on where the storm makes landfall relative to geographical features. These factors along with the range of intensity of meteorological factors can affect the actual risk of on oncoming event.

Experts have observed the above-mentioned factors and their effects over time. Existing damage models account for most of the contributing factors but usually focus on the possible damage to residential structure, likely due to the insurance focus in most models. Both states and insurance companies are interested in the degree of anticipated damage for certain hurricane events. These various models are designed for the benefit of state offices by providing damage estimates in order to process claims correctly and for insurers to provide representative insurance quotes (Hamid et al., 2011; Pinelli et al., 2011; Vickery, Lin, et al., 2006). Due to the specific focus of these models and their use, some damage contributors are neglected such as precipitation or storm surge. The use of all meteorological, population, and infrastructure factors

leads to a more encompassing impact assessment for a tropical cyclone making landfall along the U.S. coastline.

By using neural networks, a machine learning process, these connections could be recreated to produce a simplified and concise evaluation of risk. Neural networks learn based off of provided historical data in order to later match new events to a resulting outcome. The use of backpropagation by evaluating the error between the network's predicted outcome and the actual target outcome until the result is minimized is how these neural networks learn. This is similar to how the human brain learns by establishing connections between inputs and other neurons until finally a result or outcome is determined. Since experience is the biggest teacher in this field, this approach will be initially evaluated herein for the collaboration of all these variables to produce a simplified level of economic damage.

3.1.2 Data Collection

In order to create a comprehensive neural network pattern recognition model for hurricane impact prediction, the data must cover meteorological factors as well as location characteristics. For the models created herein, the variables assessed and used for neural network training are wind speed, tropical storm force wind radii, pressure, storm surge, rainfall accumulation, population, and landfall location(s). These variables were assimilated from historical reports and complied with corresponding storm impacts (economic damage). Multiple models were created from this data in order to explore possible ways of presenting the data to be trained.

The data used to train the networks were mainly referenced from the Tropical Cyclone Reports (TCRs) put together by the National Hurricane Center (NHC) for public reference (National Oceanic and Atmospheric Administration (NOAA) & National Hurricane Center

(NHC), 2014a). The TCRs not only contain the wind speed, maximum rainfall, maximum storm surge, and minimum pressure at the landfall location, these also report the estimated (and some later corrected) damage and death toll (both direct and indirect) from each storm. Since remnants of a storm are not considered in the TCR damage tally, the models inherently account for events of tropical storm ranking or higher that make landfall along the United States coastline. These TCRs trace back to the 1995 Hurricane Season, resulting in 77 events dating back from the 2012 Hurricane Season.

Typically, in one of the first tables incorporated in each TCR for the "best track", the landfall latitudes and longitudes will be given along with the maximum wind speed and minimum pressure at those locations. Sustained wind speeds were given in knots and converted to miles per hour for model use. Minimum pressure at landfall was kept in milibars. Since it is possible for a storm to make landfall at one or more position along the U.S. coast, most of the created models allow for the possibility of having four distinct landfall locations. A landfall location is determined by where the center of the storm, or eye, crosses the coastline and is entered as latitude and longitude degrees (all positive numbers since the locations are all within the same small quadrant). Some of these positions are directly next to each other, noted by the minuscule changes in these latitude-longitude coordinates. An example of this would be a hurricane that makes landfall on the small islands directly off shore of Louisiana and then the storm continuing on track to the continental shoreline of Louisiana. Due to the extremely close proximity of these locations, only one was used as a landfall position within the model. Typically, the meteorological statistics do not change between the two locations (i.e. wind speed and pressure).

The storm surge and precipitation data were extracted from a subsequent table for "surface observations" in the TCRs. In these tables "storm surge" is defined as the "water height above normal astronomical tide" and is reported in feet and entered into the models as such. The precipitation was reported as the total rainfall in inches, so those units were also used for the models. This data was less obvious to correlate. For a storm with a single landfall location, the maximum storm surge and precipitation were simply used. However, if there was more than one landfall location, an educated deduction was made for the maximum amounts relative to each landfall location, i.e. the use of precipitation maps and the knowledge that the storm surge is largest to the right of center, was applied. Also, precipitation does not vary as consistently as storm surge does and can occur further away from landfall. Since the actual storm advisories indicate that "some locations" could receive a maximum of X amount of rain, the precipitation used was the maximum independent of location. In some cases, the storm surge and precipitation data listed in the TCR were indicated to be incomplete or estimated; these values were not used for the most part, unless it was the only applicable data point. However, "unofficial" data was still used as the NHC does some quality control prior to publishing these reports. There are some storms or just landfall locations that do not have any corresponding data for storm surge or precipitation either due to no reported data or lack of significant U.S. landfall.

The population affected by a tropical cyclone event is not directly stated in any historical files; therefore, it had to be extrapolated using data shapefiles from the U.S. Census and NHC in QGIS mapping software. The U.S. Census currently has the 2010 population shapefiles available, which contain county population data (U.S. Census Bureau, 2014). The NHC keeps historical shapefiles of wind radii for past storm events tracking back to 2008 (National Oceanic and Atmospheric Administration (NOAA) & National Hurricane Center (NHC), 2014b). The wind

radii shapefiles for storms that occurred previous to 2008 had to be manually created based off of the known wind radius upon landfall from the NHC historical data (advisories) dating back to the 1998 Hurricane Season (National Oceanic and Atmospheric Administration (NOAA) & National Hurricane Center (NHC), 2012). Therefore, the wind radius, in miles, is known for each tropical cyclone event. According to the NHC, a wind radius would be larger on the right side of the storm, and were represented as such in the shapefiles. The limited availability of this data determined the cut off point for the total number of historical hurricane events for this study.

The radius of maximum winds is defined as "the distance in miles from the storm's center to the circle of maximum winds around the center" (National Hurricane Center (NHC), 2014). The wind radii shapefiles for tropical storm strength winds were used and overlapped with the U.S. Census data in QGIS in order to extract the population data from the counties that fell within the tropical storm force wind radius. Tropical storm force winds were used as a measure for outlining areas that could be subsequently connected to the resulting impact along with the possibility for damage caused by the system as it becomes post tropical. An example of this is shown in Figure 3-1(b), where the shaded area represents the overlap in the tropical storm force wind radii and U.S. counties. This created a new shapefile where the total population within the shaded area could be determined. It is worth noting that since tropical storm force winds were used, any areas that might have been affected by post tropical remnants are unlikely to be represented in this data.

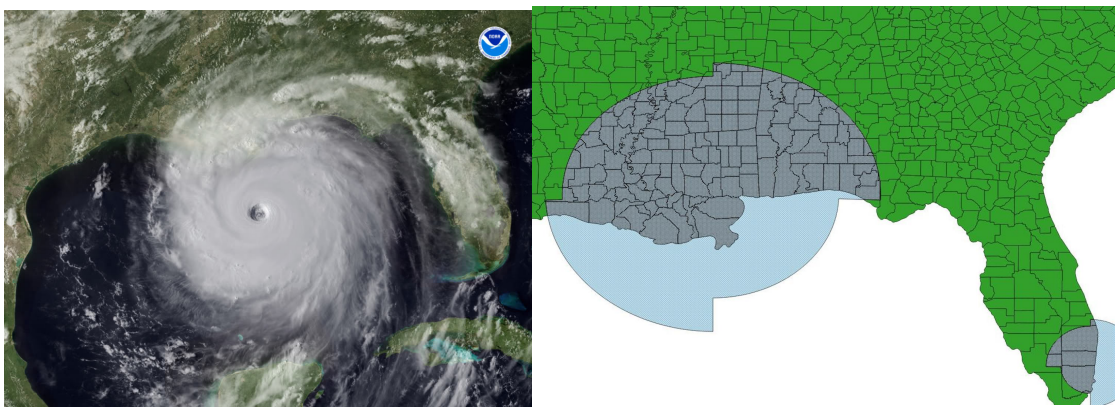

(a) (b)

Figure 3-1 Areal extent of Hurricane Katrina 2005;
(a) NOAA Satellite image (National Oceanic and Atmospheric Administration (NOAA), 2005) and (b) Radius of tropical storm force winds for both landfall location and the resulting affected counties.

This retrieved population was then scaled based on U.S. Census population in 2010 for the state of landfall and the population for the relevant year (RY) of landfall, by Equation (3.1). This number was then rounded to the nearest 100,000 in order to provide a more general number for model training and account for possible errors in using QGIS and population conversion.

$$\frac{Population_{RY}}{Population_{2010}} = \frac{State\ Population_{RY}}{State\ Population_{2010}} \tag{3.1}$$

The wind radii and extrapolated population are not as exact as the meteorological and location parameters that were simply read out of the TCRs. However, given the forecasting nature of tropical cyclones, this data would typically be reported as an educated estimate. In addition, when the media reports a population estimate of those to be affected by a major storm, the number would likely be inflated. These parameters are intended to mainly communicate a comparative amount of people and infrastructure in the path of the storm and being off by a few tens of thousands would unlikely make a large contribution to the overall amount.

The resulting deaths, both direct and indirect, and economic damage estimates were given in the TCRs under "Casualty and Damage Statistics". Doubling the insurance claims, in order to account for both insured and uninsured damage, and then adding the National Flood Insurance Program data is how the NHC determines and reports an estimate for economic damage. These estimates appear to remain substantially close to the actual resulting damage and in some cases NHC has gone back and altered the total. The damage totals were reported in current year (CY) dollars in the TCRs, therefore the TCR economic damage was converted to 2012 dollars, for consistency within the model, using Equation (3.2). This conversion referenced construction price indices (PI) provided by the U.S. Census (U.S. Census Bureau, 2010).

$$\frac{Damage_{2012}}{Damage_{CY}} = \frac{PI_{2012}}{PI_{CY}} \tag{3.2}$$

This consistency of historical data being in 2012 dollars indicates that the Impact Level Ranking System and output from the model will be in consideration of 2012 dollars as well. In order to check how this would affect certain historical events and where they fall within a respective Impact Level, the storm events from 2012 back to 1998 were ranked by both TCR estimates and the resulting 2012 adjustment. The Impact Levels for the events mainly remained the same even though some events switched rank in the overall order of most economic damage. This indicates that, while the ranking list might shift with relative economic adjustment, storm economic damage will still fall within the correct Impact Level ranking. These conversions are vital in ensuring cohesion among the historical data and are conducive to more suitable neural networks.

3.1.3 Data Communication

All the details discussed within Section 2.2 illustrate the importance of considering all the meteorological and location characteristics involved in a landfalling hurricane event. The public relies heavily on the use of the Saffir-Simpson Scale during an impending hurricane event; however while the Saffir-Simpson Scale has its uses and is informative in relaying the severity of a hurricane, specifically in relation to wind speed, the actual ability of a storm to cause damage is tied to much more. The public's reliance on only this ranking system can become misleading as a Category 1 hurricane could cause just as much damage as a Category 3+ hurricane. The Impact Level Ranking System was created not only as a means to address these misconceptions but also as a general way to output a forecasted storm impact. Outputting a dollar amount for economic damage or number of deaths could have higher errors as well as be subject to greater criticism if the actual results differ. In general, this ranking system was designed as a form of thresholds, or levels, for ease of use.

The proposed system divides storm events into damage Impact Levels 0 through 5, chosen to better mirror current ranking systems for ease of understanding, i.e. the Enhanced Fujita Scale of EF-0 to EF-5 and the Saffir-Simpson scale from a Tropical Storm to Category 5 Hurricane ranking. An Impact Level of zero indicates minimal, or possibly zero, reportable damage. Minimal damage qualifies as below the $25,000,000 threshold established by the Property Claims Service. If a storm does not exceed this threshold, the damage amount is typically not reported in the TCRs. The highest Impact Level of 5 is an extremely damaging and expensive event costing more the $50 billion (2012 USD). Only two events in all the reference historical data qualify as Impact Level 5 events: Hurricane Katrina 2005 and Hurricane Sandy 2012. All the Impact Levels and thresholds are shown in Table 3-1. The Impact Levels,

following Level 0, were determined based on typically discussed threshold values that society would reference as well as "evenly" distributing the used events so that Impact Level 5 had the rarest occurring events followed by Level 4, leaving Levels 3, 2, and 1 as relatively more common rankings.

Table 3-1 Proposed Impact Level Ranking System

Impact Level	Economic Damage Amount (based on 2012 USD)	Example Event
0	< $25 million	2012 Tropical Storm Beryl
1	≥ $25 million, < $100 million	2007 Hurricane Humberto
2	≥ $100 million, < $1 billion	2008 Tropical Storm Fay
3	≥ $1 billion, < $10 billion	2008 Hurricane Gustav
4	≥ $10 billion, < $50 billion	2011 Hurricane Irene
5	≥ $50 billion	2005 Hurricane Katrina

The models were then built and designed around these levels in order to output a forecasted Impact Level for the storm characteristics provided. Based on the historical data used to train the model with a corresponding known level of damage, the model will then attempt to match the inputs as best it can with the inputs of known events, or interpolate the inputs between a range of known inputs, in order to best match a resulting Impact Level. For ease of creating the Impact Levels, it was determined that only economic damage would be used instead of both economic damage and related deaths. The targets used to train the model can only be a series of 1's and 0's, therefore only one storm resultant could be used, and in this case that resultant was decided to be economic damage. This was confirmed by ranking the historical tropical cyclone events by just resulting economic damage and comparing it to ranking economic damage and deaths combined. Using a statistical value of life of $4,000,000 (Blomquist, 2004) multiplied to the number of deaths and then added to the economic damage, the storm events were ranked by the resulting total. The events remained in the same impact levels, as without the deaths added, indicating that simply using the economic damage would be sufficient. The model will essentially output a range of economic damage in the form of these levels.

3.1.4 Model Description and Performance Evaluation

The first step in creating a neural network model is the ability to comprehend the problem, which includes the correct assimilation of data. Since neural networks are learning algorithms that can establish patterns, the programmer must ensure that the data is arranged in such a way that patterns can be significantly established. For predicting hurricane impacts in the U.S., six networks (models) were created to confirm the best way to present hurricane data to a neural network. The data presentation variances here were assigned in order to resolve the differences and factors of landfall locations. For instance, it could be possible for population to be a redundant variable if the landfall and wind radii are known since it would be a characteristic of the location and the training algorithm could hypothetically draw that conclusion. These variations will not only allude to a better way to present data, but could also help indicate which variables are more vital. The six models vary how many times meteorological parameters are entered for four possible landfall locations as well as alternate between the use of the population affected and wind radii. These variations also, in turn, result in a range of input matrix sizes to evaluate how much data is absolutely necessary. Table 3-2 shows the difference between all six models.

Table 3-2 Variations Between the Six Models used in the Simulations

Model No.	Variables	Input Matrix Size	Description
1	Population Affected At each landfall: Latitude Longitude Pressure (mbar) Wind Speed (mph) Storm Surge (feet) Precipitation (inches)	25x66	Population affect is entered first followed by the landfall locations and the relevant meteorological parameters at that location.
2	Substitute in wind radius at each landfall (LF) for population	28x66	Instead of using the population affected, use the wind radii. The wind radius will be entered at each landfall, as opposed to the max, so this will add rows (population was only the event total).
3	Population Affected Pressure (mbar) Wind Speed (mph) Storm Surge (feet) Precipitation (inches) 1st LF: Lat, Lon, 2nd LF: Lat, Lon 3rd LF: Lat, Lon 4th LF Lat, Lon	13x66	The meteorological parameters will be reported as the max between all landfalls. But the various landfalls will be noted by their location. Overall population affected will be used.
4	Pressure (mbar) Wind Speed (mph) Storm Surge (feet) Precipitation (inches) 1st LF: Lat, Lon, wind radius 2nd LF: Lat, Lon, wind radius 3rd LF: Lat, Lon, wind radius 4th LF Lat, Lon, wind radius	16x66	The meteorological parameters will be reported as the max between all landfalls. But the various landfalls will be noted by their location. The wind radius will be used here with each landfall location.
5	Pressure (mbar) Wind Speed (mph) Storm Surge (feet) Precipitation (inches) 1st LF: Lat, Lon 2nd LF: Lat, Lon 3rd LF: Lat, Lon 4th LF Lat, Lon	12x66	The meteorological parameters will be reported as the max between all landfalls. But the various landfalls will be noted by their location. No wind radii or population were used.
6	Population Affected Pressure (mbar) Wind Speed (mph) Storm Surge (feet) Precipitation (inches)	5x66	The meteorological parameters will be reported as the max between all landfalls. Total population affected will be used, but no landfall coordinates.

The training inputs for pattern recognition are in matrix form of numerical values and target (desired output) values in a matrix of 1's and 0's. The target matrix form serves to confirm or deny a certain output, in this case, Impact Levels. The trained target matrix in this research results in a 6x66 matrix. In other words each of the 66 storm events have a corresponding 6x1 matrix to indicate its Impact Level. The six rows represent Impact Levels 0 – 5. If a matrix row contains a 1, this signals a confirmation for that respective row's Impact Level. For example, if an event's target matrix contains a 1 in row 4 then the tropical cyclone is an Impact Level 3 event, if the 1 is in row 1 then the tropical cyclone is an Impact Level 0, etc. After training the network for use, the outputs for a possible event will be produced in a similar form except the numbers will not be exactly 1's or 0's, instead the decimals serve as the level of confidence the network has in placing the given event in that Impact Level. Therefore, the predicted impact level would be determined by referencing the highest value in the output matrix. Matrix Equation (3.3), from left to right, shows the impact level matrix setup, the training target matrix used for an Impact Level 3 event, and a possible output matrix for another Impact Level 3 event (once in use).

$$\underset{\text{Matrix Setup:}}{\begin{bmatrix} Impact\ Level\ 0 \\ Impact\ Level\ 1 \\ Impact\ Level\ 2 \\ Impact\ Level\ 3 \\ Impact\ Level\ 4 \\ Impact\ Level\ 5 \end{bmatrix}} = \underset{\text{Impact Level 3 Target Matrix}}{\begin{bmatrix} 0 \\ 0 \\ 0 \\ 1 \\ 0 \\ 0 \end{bmatrix}} \approx \underset{\text{Possible ANN Output Matrix}}{\begin{bmatrix} 0.0012 \\ 0.2305 \\ 0.4451 \\ 0.9872 \\ 0.4397 \\ 0.0003 \end{bmatrix}} \tag{3.3}$$

For comparison sake, each of the subsequent models has the same network structure shown in Figure 3-2. The "w" and "b" symbolize the weights and biases, respectively. The curved function line in each layer indicates a nonlinear relationship between layer/neurons. The only change is the number of inputs, here 25 for the 25x66 input matrix of Model 1 (discussed

later on). This structure may vary by the number of inputs, but the number of outputs and hidden neurons remain the same for this study. Additionally, the training data, validation data, and testing data was randomly allocated as 70%, 15%, and 15%, respectively as another means of maintaining consistency.

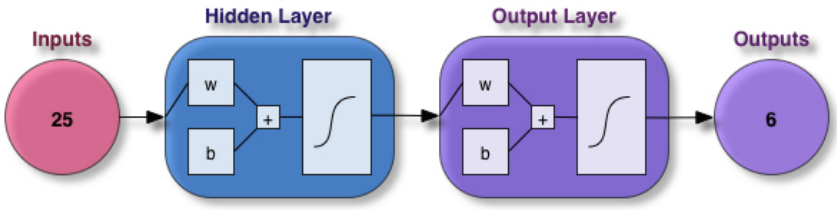

Figure 3-2 General ANN structure for all developed models

Model 1

Model 1 serves as the model basis as it contains all the originally considered elements; that is population affected, latitude, longitude, pressure, wind speed, storm surge, and precipitation at possible landfalls one through four. If there is only one landfall location the remaining landfall location inputs will default to zero. This results in an input matrix of 25x66, which could be thought of as a large input matrix possibly affecting the abilities of the neurons to make substantial connections. The data matrices for the input and output variables were simulated multiple times in order to determine the best possible resulting network. Figure 3-3 shows the training performance for the network that produced that lowest overall percent error to be used as Model 1. The performance shows when the lowest MSE was reached, resulting in terminating the training process and producing a usable ANN. The resulting network has corresponding errors for training, validation, and testing that describe how many times the pattern recognition tool correctly identified the Impact Level for the corresponding event inputs. Figure 3-4 shows the overall network error, combining that of training, validation, and testing.

For Model 1, the best performance was achieved after 48 iterations, or epochs, (number of times the data was cycled through and altered with backpropagation then checked with six additional iterations) reaching an MSE of 0.07462 and resulting in an ANN with approximately 18% error. As can be seen in Figure 3-4, Impact Levels 0 and 3 were predicted best, however Impact Level 1 had a 100% error. This turned out to be a continuing trend with each model. Each retrain within the simulations was done until the lowest overall percent error was reached and this did not always correlate with all Impact Levels having an equally low prediction error.

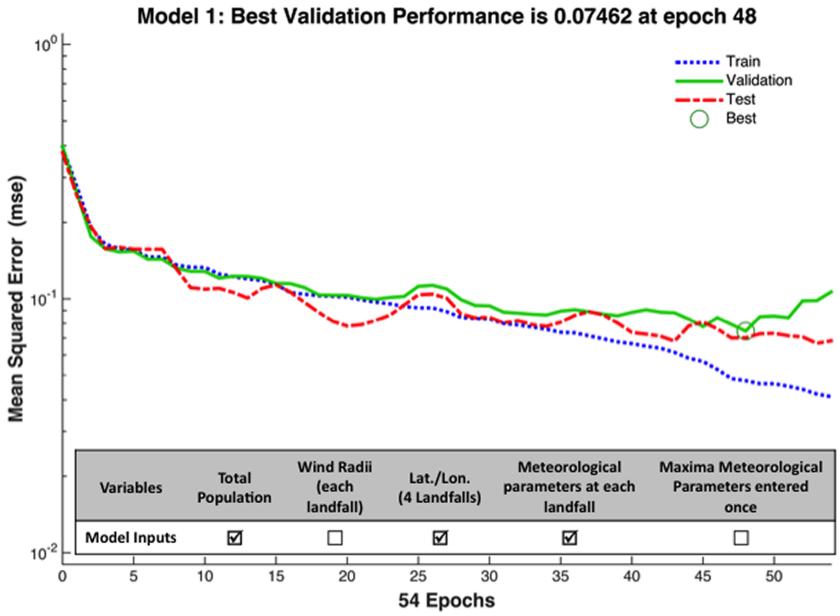

Figure 3-3 Performance for the network used as Model 1

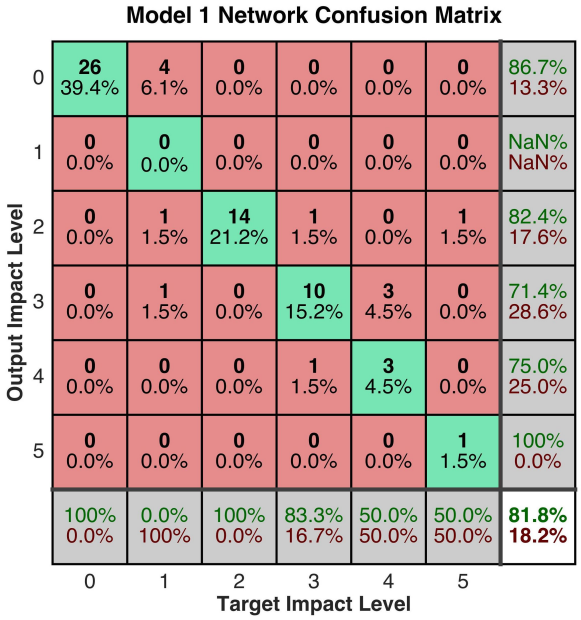

Figure 3-4 Confusion Matrix representing overall error for the network used as Model 1

Model 2

The second model built substitutes out population for the radius of tropical storm force winds upon landfall. While in Model 1 the population affected is entered once for the whole event, the wind radius can change and is therefore entered each time the storm makes landfall resulting in a larger input matrix of 28x66. The motive behind this alteration is the possibility that if the location is given and the area encompassed is also known, one could interpolate the same relevant characteristics as it would by the location and population and it might be simpler to input the wind radius directly from the tropical cyclone advisory than the extra step of extrapolating population data. Using the wind radii could potentially describe the number of people affected, infrastructure quality, and infrastructure density. Figure 3-5 shows the training performance for the network that produced that lowest overall network percent error to be used as Model 2. Figure 3-6 shows the overall network error, combining that of training, validation,

and testing. For Model 2, the best performance was achieved after 55 iterations reaching an MSE of 0.0582 and resulting in an ANN with approximately 18% error. As can be seen in Figure 3-6, all Impact Levels had less than (or equal to) 50% error, including Level 1. While the overall network percent error is similar to Model 1, Model 2 yielded better results in terms of placing each event in the correct Impact Level. The similar MSEs between Model 1 and 2 indicate that the neural network was equally able to establish a pattern between the varying inputs for the same output matrix.

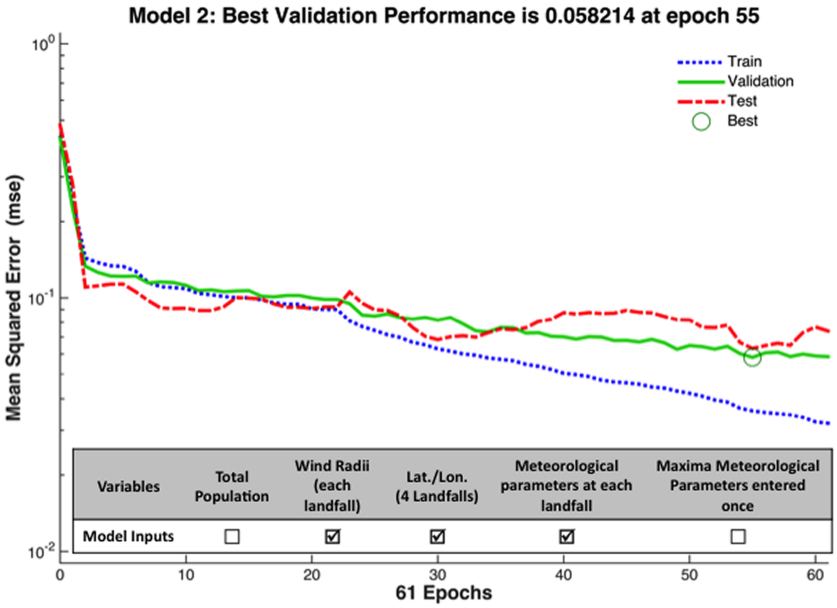

Figure 3-5 Performance for the network used as Model 2

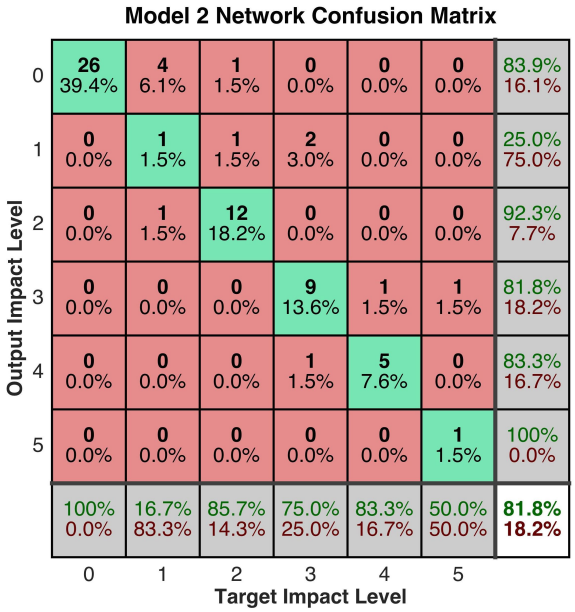

Figure 3-6 Confusion Matrix representing overall error for the network used as Model 2

Model 3

The previous two models had large input matrices and could call into question the practicality of using networks due to the large extent of the data required. In order to explore this possibility, Model 3 was created with the intention of designing a smaller input matrix. Instead of inputting the meteorology factors (wind, pressure, precipitation, storm surge) with each corresponding landfall, the overall maximum wind speed, storm surge, and precipitation along with the minimum pressure out of all the landfall locations is entered once. Along with these factors, the population affected and the latitude and longitude for four possible landfall locations were also used. This results in a smaller matrix of 13x66. Figure 3-7 and Figure 3-8 show the performance of the established Model 3 and the overall network percent error, respectively. For Model 3, the best performance was achieved after 44 iterations reaching an MSE of 0.03656 and resulting in an ANN with approximately 17% error. Compared to Models 1 and 2, the network used for Model 3 has a slightly smaller percent error. As can be seen in

Figure 3-8, Model 3 also has a large percent error for Impact Level 1 events, however Levels 0, 4, and 5 were all correctly placed when creating this network.

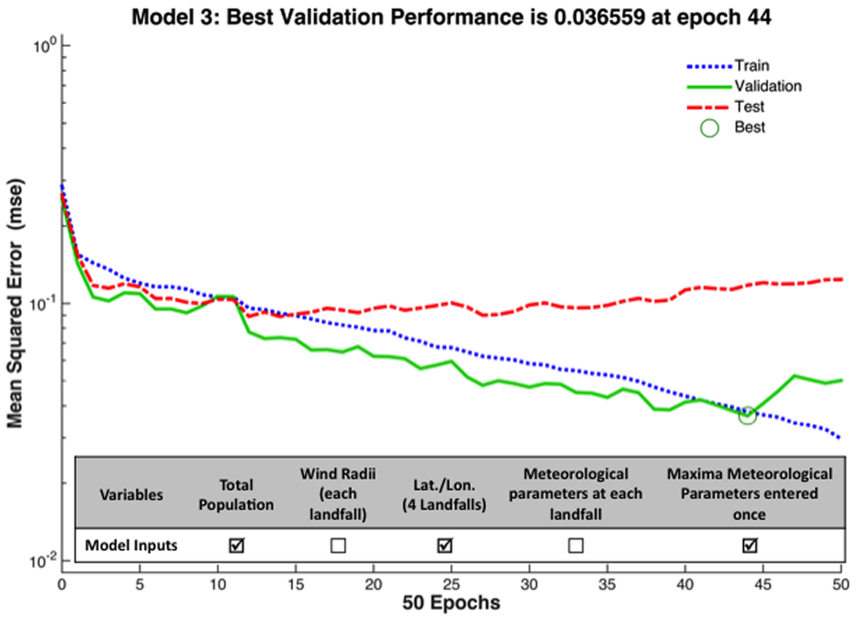

Figure 3-7 Performance for the network used as Model 3

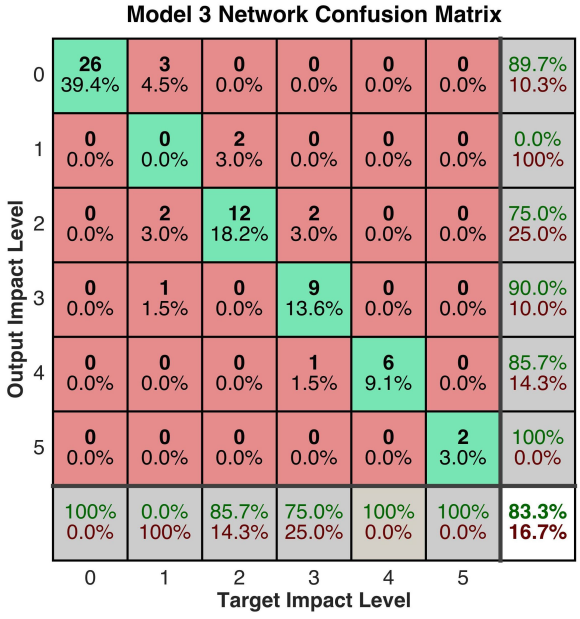

Figure 3-8 Confusion Matrix representing overall error for the network used as Model 3

Model 4

In the best interest of completeness, Model 4 is a mix of Model 2 and Model 3. The meteorological factors are inputted once as in Model 3, but instead of using the population affected, wind radii were used similarly to Model 2 by adding it in with each landfall location resulting in an input matrix of 16x66. In other words, all the pertinent meteorological factors are entered once followed by each landfall location with its associated wind radius. Figure 3-9 and Figure 3-10 show the performance of the established Model 4 and overall networks percent error, respectively. For Model 4, the best performance was achieved after 83 iterations, the most of all the models, reaching an MSE of 0.04629. Model 4 also resulted in the lowest overall network error of all six models discussed herein, with 6% error and logically corresponding to high accuracy for prediction of the training data in each Impact Level, with the least accurate being Impact Levels 3 & 4 with 17% error. The fact that the produced Model 4 network cycled through the training data the most times could attribute to the lowest resulting percent error.

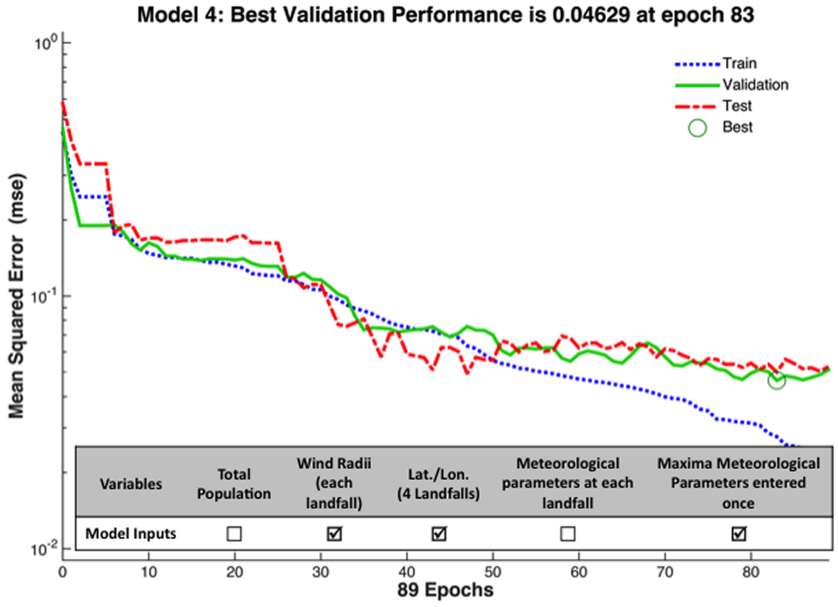

Figure 3-9 Performance for the network used as Model 4

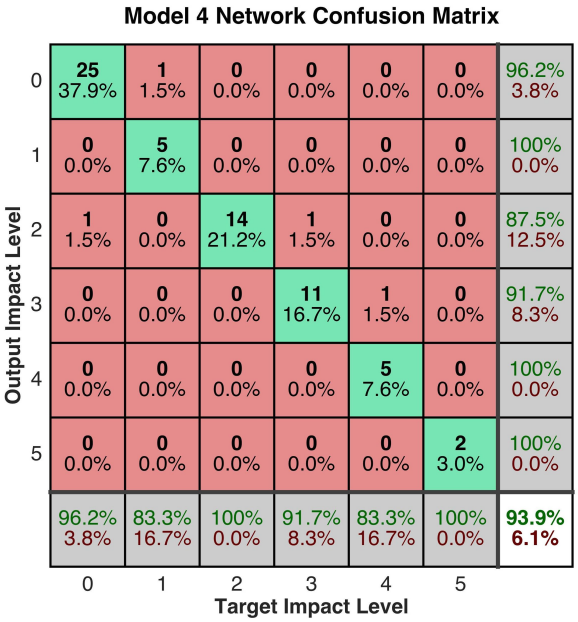

Figure 3-10 Confusion Matrix representing overall error for the network used as Model 4

Models 5 & 6

Models 5 and 6 are arguably the most unique ways to present this data. Model 5 operates under the assumption that each location maintains its population and infrastructure characteristics. This assumption led to the removal of the use of population affected or wind radii. The meteorological parameters are entered the same as in Models 3 and 4 with the four possible landfall latitudes and longitudes added leading to an input matrix of 12x66. Model 6 has the smallest input of this set of models with a 5x66 matrix. Model 6 removes the latitude and longitudes entirely by assuming that the more landfalls a storm makes, the more population there is to be affected and therefore, a likely higher amount of infrastructure. However, by leaving the landfall location out for Model 6, this theatrically negates infrastructure quality and solely focuses on quantity (density). Figure 3-11 and Figure 3-12 show the performance of the established Model 5 and overall networks percent error, respectively. Figure 3-13 and Figure

3-14 show the performance of the established Model 5 and overall networks percent error, respectively. Both of these models' networks had a resulting percent error in the teens similar to Models 1-3. Model 5 did have the second lowest percent error, however notice that both Model 5 and 6 also did not accurately place most of Impact Level 1 events used for training.

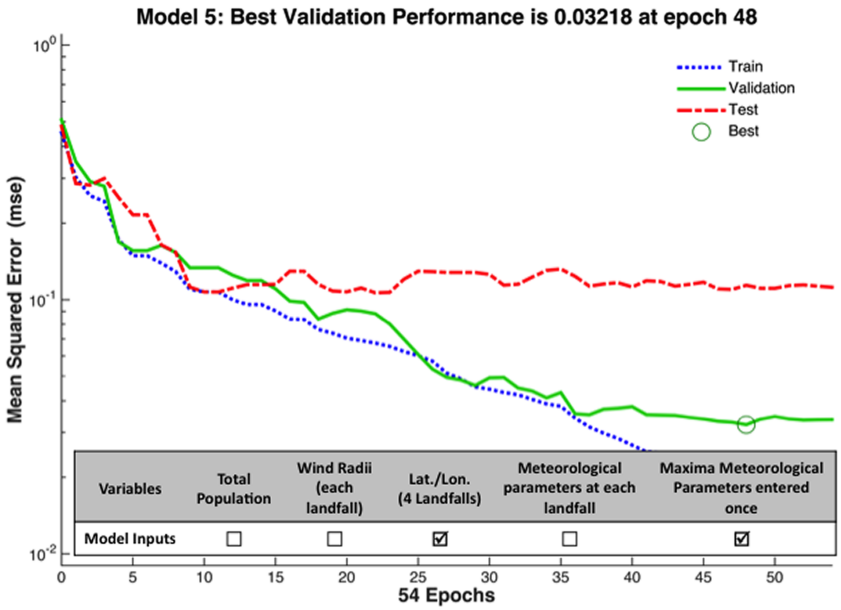

Figure 3-11 Performance for the network used as Model 5

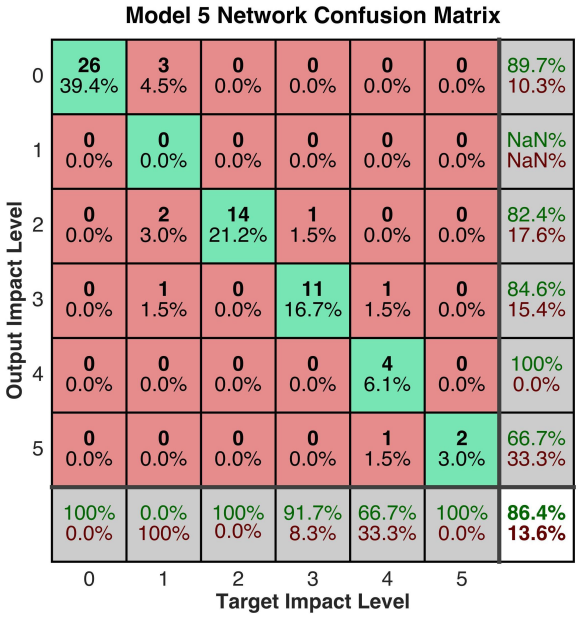

Figure 3-12 Confusion Matrix representing overall error for the network used as Model 5

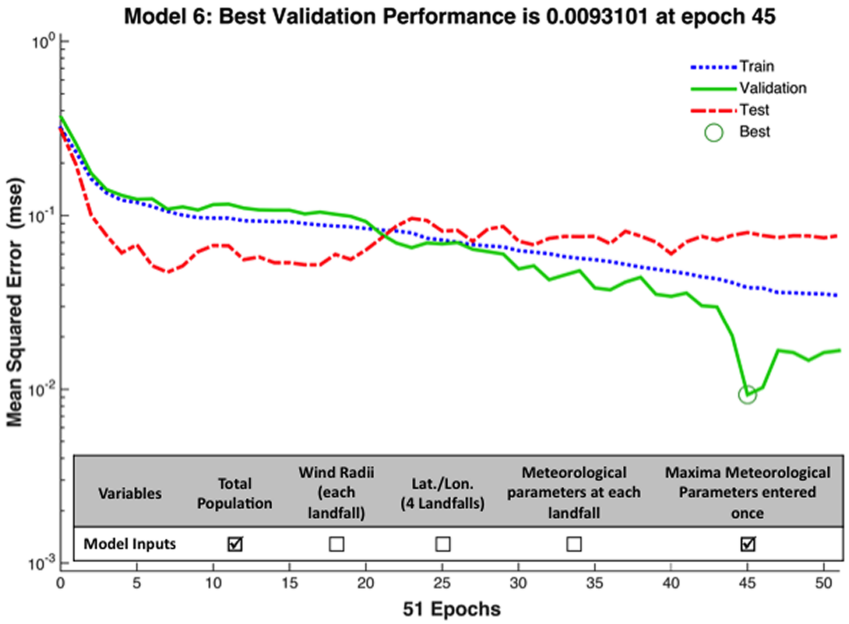

Figure 3-13 Performance for the network used as Model 6

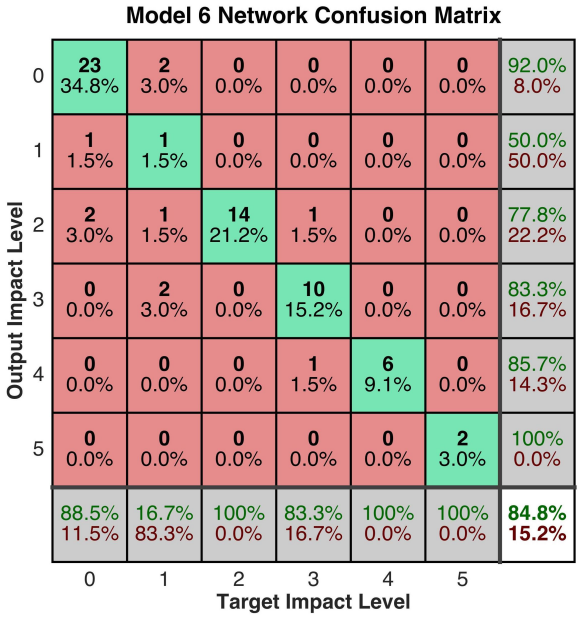

Figure 3-14 Confusion Matrix representing overall error for the network used as Model 6

Overall, these six network models preformed relatively well with MSEs below 0.1 (predictions are better when the MSEs are closer to zero) and network errors of less than 20% during this initial building/training process. The results from building each model's network translate to applicability for actual use. The performance MSE indicates how well the pattern recognition algorithm was able to establish connections between the inputs and outputs and the effectiveness of training with this data. Meanwhile, the confusion matrix demonstrates how accurately the network (corresponding to the best MSE) placed each event leading to a more accurate knowledge base for the network to reference in real-time use. In order to meet these lowest values, the networks had to be retrained multiple times until the lowest possible MSE and percent error were reached. The averages for all these simulations (count: 20) are shown in Table 3-3 and Figure 3-15. Since there were only 66 events used to build these networks the predetermined data division for each simulation resulted in only 10 data events for validation and

testing. One simulation's possible data division could have resulted in the only two Impact Level 5 events distributed to the testing stage, leaving the resulting network error to likely increase since there was no previous basis for that level in training and validation. This is why the average MSEs and errors are significantly higher than the model networks used. The corresponding standard deviations for the overall MSE and percent errors are provided in Table 3-3. Overall, Models 3 and 4 produced the best/lowest averages.

Table 3-3 Overall statistics for Model Networks 1-6 over 20 Simulations

	Model 1	Model 2	Model 3	Model 4	Model 5	Model 6
Avg. MSE	0.1068	0.1157	0.0888	0.1020	0.1005	0.0918
MSE SD	0.0364	0.0673	0.0283	0.0362	0.0425	0.0447
Avg. Percent Error	42.65%	45.45%	36.06%	41.44%	42.65%	36.36%
Percent Error SD	18.63	20.10	15.20	17.12	22.90	17.32

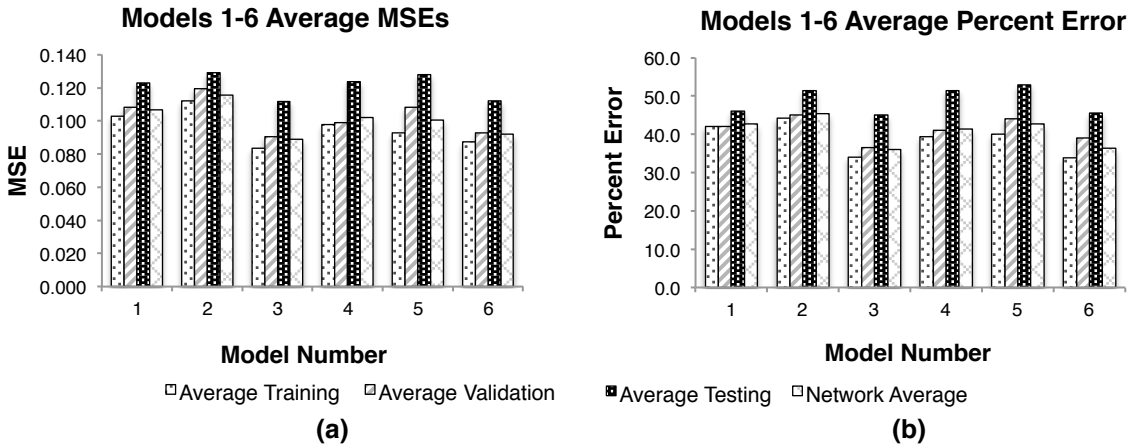

Figure 3-15 Average (a) MSEs and (b) percent errors over multiple (20) retraining simulations

3.1.5 Model Tests

The next step in determining model usability and functionality for the purposes of this study is to conduct each model using a trial event where the outcome is known. The respective inputs are entered into each model, which then provides an output in matrix form that indicates the most likely Impact Level. The events chosen for the model trials were the 2012 Hurricane

Isaac and 2013 Tropical Storm Andrea. For each trial event, all models were conducted and compared to the actual Impact Level of the storm.

Isaac was specifically chosen because it made landfall in Louisiana, which is a common landfall location among the training data, along with Texas and Florida, and its resulting damage places it in the middle ranking levels, indicating it is significant enough to evaluate without being a major event such as Katrina or Sandy. Since Isaac occurred in 2012, it is also a more recent event leading to less complications and easier evaluation. Hurricane Isaac made landfall in southeastern Louisiana in late August 2012. With a wind radius of 185 miles, it affected 5.6 million people. All possible input variables are shown in Figure 3-16. Isaac was a Category 1 Hurricane resulting in $2.35 billion (2012 USD) of economic damage, making it an Impact Level 3 storm.

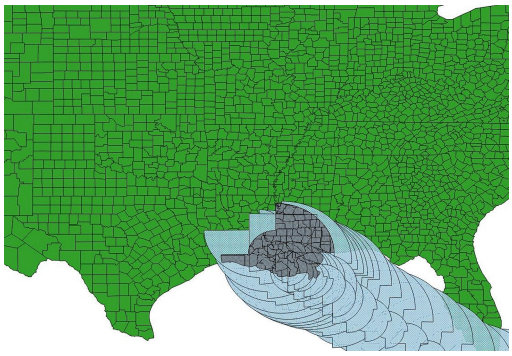

(a)

Inputs for ANN Models	
Variable	**Isaac**
No. Landfalls	1
Population	5.6 million
TS Wind Radius	185 miles
Min. Pressure	966 mbar
Wind Speed	70 knots (80.5 mph)
Storm Surge	3.4 meters (11-feet)
Precipitation	70 cm (26.71 inches)

(b)

Figure 3-16 Hurricane Isaac: (a) QGIS track, landfall location, and affected counties, and (b) corresponding possible relevant variables

The 2013 Hurricane Season was uneventful, resulting in only one storm to make landfall: Tropical Storm Andrea, which was used as another trial event. Andrea made landfall along the northwestern coast of Florida with a wind radius of 140 miles and affected 9 million people by crossing over central FL. All possible input variables are shown in Figure 3-17. Andrea was only

an Impact Level 0 tropical storm at landfall, indicating that the resulting economic damage did not cross the $25 million threshold.

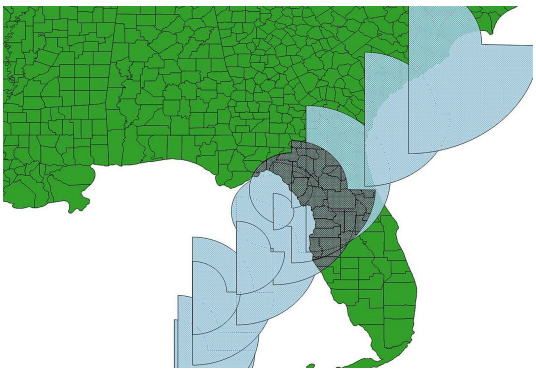

(a)

Inputs for ANN Models	
Variable	**Andrea**
No. Landfalls	1
Population	9 million
TS Wind Radius	140 miles
Min. Pressure	992 mbar
Wind Speed	50 knots (57.5 mph)
Storm Surge	1.4 meters (4.55-feet)
Precipitation	38.9 cm (15.28 inches)

(b)

Figure 3-17 Tropical Storm Andrea: (a) QGIS track, landfall location, and affected counties, and (b) corresponding possible relevant variables

After gathering all relevant data, the required variables were entered into each model for simulation. Figure 3-18 compares the output matrices for the models results of Isaac and Andrea. The value in each output matrix row is plotted as it pertains to its relevant Impact Level, such that the actual result has a value of zero for all levels except Impact Level 3 for Isaac and Impact Level 0 for Andrea. The peak value for each model represents the Impact Level it is forecasting as most likely to correspond with the input data given. A convergence of the models indicates agreement on the probability of the corresponding Impact Level being achieved.

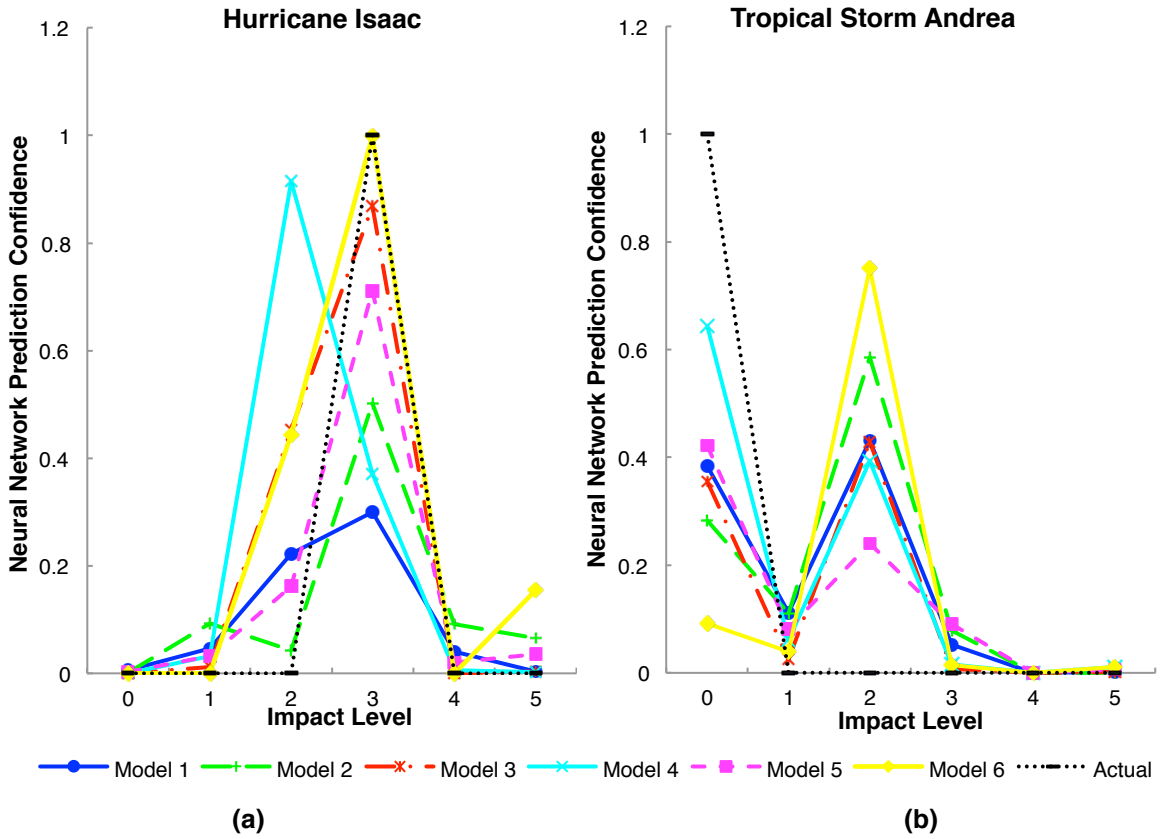

Figure 3-18 Model comparison for (a) 2012 Hurricane Isaac and (b) 2013 Tropical Storm Andrea

As can be seen, most of the models did very well with predicting the Impact Level 3 event, Hurricane Isaac, with the exception of Model 4, which predicted an Impact Level 2 event. However, the Impact Level 0 event, Andrea, has two distinct peaks at Levels 0 and 2. It is interesting to note that Model 5 (network error of 14%) was the only model to assign the highest likelihood to the correct Impact Level for both trial events, while Model 4 (lowest network error at 6%) performed the best for the Impact Level 0, where is correctly placed 96% of the training events, but was the only one to assign the highest likelihood to the incorrect Impact Level for the Impact Level 3 event, where is correctly placed 92% of the training events. Also, the models that appear to be the most confident (highest peaks) correspond to a smaller input matrix, while the two models with the largest input matrices (Models 1 & 2) are consistently less confident. What

appears to be equally true for all models is that the confidence for Impact Levels further from the actual is extremely low, i.e. the confidence for an Impact Level 5 event is nearly zero for every model result of Tropical Storm Andrea and the confidence for an Impact Level 0 event for Hurricane Isaac is also nearly zero for every model. This implies that these models are unlikely to significantly under- or over-forecast a real time hurricane event. This can also be seen in the model confusion matrices; most of the time if an event was incorrectly placed, it was one level off in either direction.

Simply based off of the training error and the trial event results, Models 3-6 are proving to be the best options for use. This signals that the use of maximum meteorological parameters (entered once) and smaller matrices produce more usable models. The use of population versus wind radii did not seem to make much of a difference, which implies that both effectively relate the amount of population and infrastructure at risk. The success of Model 5 also hints at the importance of the landfall location over population or wind radii since it does not include either of those and solely focuses on the location. Assuming this holds true, this study would support the argument for the importance of infrastructure quality/condition when determining risk and vulnerability. Of course, as time goes on and more events become available to test real time and later add to the training data set, the validity of these models and this forecasting approach will become clearer.

3.1.6 Conclusion

Hurricane impact prediction requires a multivariable approach to most accurately determine risk, vulnerability, and the resulting outcome. Researchers, engineers, and scientists who work with hurricanes intuitively understand the intricacies of each tropical cyclone event and how those intricacies will contribute to the resulting outcome. Artificial neural networks

allow for the possibility of recreating this understanding that was developed, essentially, through experience and pattern recognition. Due to the complexity of using a multivariable approach for hurricane impact prediction, the data must be presented in such a way that the network could create strong connections between the input data and eventually the resulting output data. For a multivariable hurricane problem this means defining a way to best present meteorological data (pressure, wind speed, storm surge, and precipitation) and population and infrastructure information through landfall location, population affected, and/or the radius of tropical storm force winds.

After creating six models with various ways to present this data, it was found that the neural network created the most usable and confident model networks when the maximum of each meteorological parameter (of all possible landfalls) was entered leading to smaller matrix sizes. Models that contained either population or wind radii performed equally well within this study. This indicates that the networks could draw conclusions on the amount of people and infrastructure affected simply from either population or wind radii. The location latitude and longitude designates where the storm will hit and some locations are more vulnerable than others due to old and dense infrastructure and natural features that would better protect some locations. Population also indicates how many people are affected and correspondingly how much infrastructure is potentially vulnerable. Since entering the overall maximum meteorological parameters was determined best for smaller matrices, this suggests that the location/population characteristics are more sensitive data than the meteorological factor when forecasting tropical cyclone impacts. Further investigation into neural network weights along with the eventual increase in available hurricane data, could lead to confirming these results and producing the most applicable Hurricane Impact Level Prediction Model.

3.2 Hurricane Impact Prediction: An Assessment of Variable Importance by Neural Network Weights

The economic damage resulting from a hurricane event is the product of multiple parameters including the locational characteristics, the population affected, wind speed, storm surge, pressure, and precipitation. While it is well understood how each factor may affect a building on an individual level, an evaluation over a wide area for a whole event would better illustrate how these factors each contribute to the total damage outcome. In order to address such a complex and nonlinear problem, this study will utilize the weights allotted to each factor by an artificial neural network. Since this is a more obscure approach, six models of varying ways to present these parameters will each be evaluated for the weights associated with a one hidden neuron and ten hidden neuron model. The combined results will show the significance of some factors, such as population and storm surge, and the insignificance of other factors, such as pressure and precipitation, to the total resulting economic damage communicated by the Impact Level Ranking System. This study provides a better understanding of how landfall location, population, wind speed, pressure, storm surge, and precipitation contribute to the level of economic damage that could be expected for a hurricane event.

3.2.1 Overview

Neural networks, as used in this research, utilize pattern recognition techniques and are often employed as predictive methods in various fields. A neural network establishes patterns between input matrices and target matrices, provided by the user, by treating the data as inter connecting neurons, similar to the anatomy of the human brain. Between these two matrices, or "layers", is another layer of hidden neurons. These hidden neurons serve as a method to increase

the number of connections, which are essential for nonlinear problems in which most neural network problems are. A neural network is taught by progressing through the presented data multiple times (referred to as iterations or epochs) until a lowest mean square error (MSE) is reached by using backpropagation.

The previous study reviewed the best way to present multiple variables in a hurricane impact prediction problem to a neural network. Six initial models were created that presented meteorological and locational factors differently as input matrices used to build the resulting neural network. However, each model has the same target matrix that represents the previously introduced Impact Level Ranking System. In this previous study, statistically significant results proved the existence of a pattern connection between the input and target matrices built off of historical data. These models were also conducted for two trial events, in which the models overall well-predicted Impact Level 3 event but were less certain on the Impact Level 0 event.

This study demonstrated the importance of variables such as population and location in determining and communicating risk and vulnerability. To further confirm this as well as consider the viability of each individual input factor, the study done herein assesses the individual weights between the input and hidden neurons (see neural network structure Figure 2-11). Therefore, the hidden neurons will be altered but the same defaults as in the previous study will remain, i.e. the training algorithm and the 70% training, 15% validation, and 15% testing data separation. The study discussed herein serves more as an analysis of the relevant variables when determining economic damage than a contribution to building an overall better model for hurricane impact prediction.

3.2.2 Model Variables

Models 1 through 6 vary mainly in ways to communicate the extra factor of population and infrastructure, while still containing all relevant meteorological data either at each landfall or just the maximum/minimum. This approach allows the neural network to make similar connections that an expert in the field would make by combining the severity of the meteorological factors with the vulnerability of the landfall location. For example, New York City is much more vulnerable to storm surge than the Carolina coastline due to its built out shoreline and high urbanization that does not provide any means of excess water absorption, unlike the Carolinas' with barrier islands and wetlands acting as buffers and sponges against oncoming waves and flooding. The meteorological factors used for these models are wind, pressure, storm surge, and precipitation amount. Since the neural networks only uses numerical inputs, the location was communicated by latitude and longitude while the amount of people, and therefore infrastructure, was communicated by the population falling within the tropical storm wind radius. Table 3-4 shows how these inputs are arranged for the matrix form of Model 1 and Table 3-5 outlines how the six models vary these inputs. The wind speed and storm surge used are the maximum upon landfall and the pressure is the minimum upon landfall. The precipitation is the maximum 24-hour accumulation. When these variables are only entered once, instead of each landfall, the maximum (minimum in the case of pressure) value out of all the landfalls is used.

Table 3-4 Model 1 Input Matrix

Input Parameters
Population Affected
Latitude of Landfall Location 1
Longitude of Landfall Location 1
Pressure 1 (mbar)
Wind Speed 1 (mph)
Storm Surge 1(ft)
Precipitation 1 (inches)
Latitude of Landfall Location 2
Longitude of Landfall Location 2
Pressure 2 (mbar)
Wind Speed 2 (mph)
Storm Surge 2 (ft)
Precipitation 2 (inches)
Latitude of Landfall Location 3
Longitude of Landfall Location 3
Pressure 3 (mbar)
Wind Speed 3 (mph)
Storm Surge 3 (ft)
Precipitation 3 (inches)
Latitude of Landfall Location 4
Longitude of Landfall Location 4
Pressure 4 (mbar)
Wind Speed 4 (mph)
Storm Surge 4 (ft)
Precipitation 4 (inches)

Table 3-5 Model Input Variances

Model No.	Variables	Input Matrix Size	Description
1	All	25x66	Shown in Table 3-4
2	Substitute in wind radius at each landfall (LF) for population	28x66	Instead of using the population affected, use the wind radii. The wind radius will be entered at each landfall, as opposed to the max, so this will add rows (population was only the event total).
3	Population Affected Pressure Wind Speed Storm Surge Precipitation 1st LF: Lat, Lon, 2nd LF: Lat, Lon 3rd LF: Lat, Lon 4th LF Lat, Lon	13x66	The meteorological parameters will be reported as the max between all landfalls. But the various landfalls will be noted by their location. Overall population affected will be used.
4	Pressure Wind Speed Storm Surge Precipitation 1st LF: Lat, Lon, wind radius 2nd LF: Lat, Lon, wind radius 3rd LF: Lat, Lon, wind radius 4th LF Lat, Lon, wind radius	16x66	The meteorological parameters will be reported as the max between all landfalls. But the various landfalls will be noted by their location. The wind radius will be used with each landfall location.
5	Pressure Wind speed Storm Surge Precipitation 1st LF: Lat, Lon 2nd LF: Lat, Lon 3rd LF: Lat, Lon 4th LF Lat, Lon	12x66	The meteorological parameters will be reported as the max between all landfalls. But the various landfalls will be noted by their location. No wind radii or population were used.
6	Population Affected Pressure Wind Speed Storm Surge Precipitation	5x66	The meteorological parameters will be reported as the max between all landfalls. Total population affected will be used, but no landfall coordinates.

3.2.3 Methodology

The purpose of using backpropagation for neural network training is to propagate the error back, after each iteration, through the function in order to adjust the weights and biases on the neurons for each layer. The weights are placed on the neuron connections between layers, i.e. from an input neuron to each hidden neuron and from a hidden neuron to each output neuron. If the weight is positive then the connection is an excitatory one, whereas a negative weight correlates to an inhibitory connection. This means that a negative weight actually imposes a restraint on the connection, and therefore the result at the next connection. These weights can roughly show the importance of each input, however with more hidden neurons and more connections, it becomes harder to determine how these weights dictate the importance of each variable. The biases act directly on the hidden and output neurons and serve more so as a way to move a function over so that it is bound by the outputs 0 and 1 and do not directly impact the importance of any specific neuron.

As a starting point, weights are typically adjusted until the lowest mean square error is reached resulting in the creation of the best possible network. It is possible, when creating the network, to also produce the resulting weights an biases using the MATLAB command [b, IW, LW] = seperatewb(net,wb). The “b” represents the biases on the hidden neurons and the output layer neurons. The “IW” is termed the “inner weights” and represents the weights on the connections between the inputs and the hidden neurons, while the “LW” is termed the “layer weights” and represents the weights between the hidden neurons and the outputs. These inner weights are in a matrix with the size of number of hidden neurons by number of inputs and the layer weights, for these models, are in a matrix with the size of the number of outputs by number of hidden neurons.

In order to draw a rough sense of how the variables for each of the six models contributed to the overall outcome, these weights and biases were extracted for a one hidden neuron model, as demonstrated in Figure 3-19. This does over-simplify the networks and could lead to higher network percent errors, but it is the best way to approximate the inputs' individual contribution. This structure results in a smaller web of interconnecting neurons, which can be easier to trace reactions through the network. For this approach, each model was simulated ten times and an average for each weight was taken along with the percent error and MSE for reference. The averages are assessed herein as they would account for times the network resulted in excitatory (positive) and inhibitory (negative) weight connections. There is, however, still significant speculation over whether or not these weights can correctly communicate how exactly the inputs contribute to the outputs since there are also weights between the hidden neuron and the outputs (Impact Levels 0 – 5). This is because the weights from the input neurons mostly describe how those variables connect to that one hidden neuron, from here the information travels in six different possible directions for the Impact Levels. Even more specifically, these weights cannot directly say which input variable is most important for each Impact Level, or amount of damage.

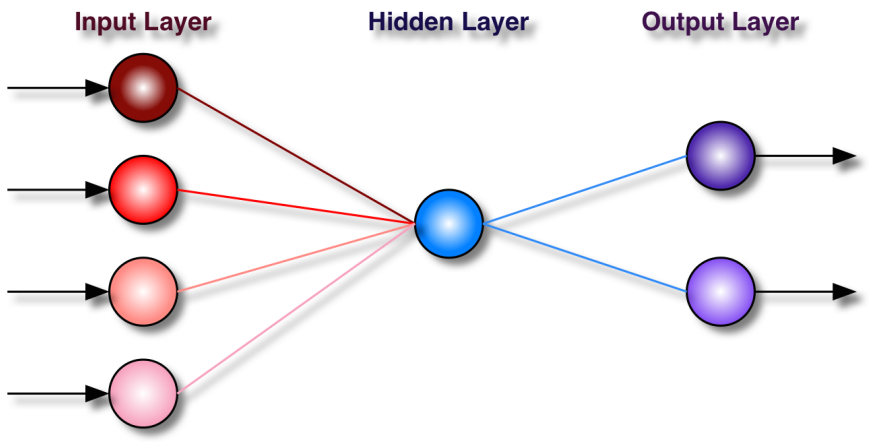

Figure 3-19 Basic neural network structure with one hidden neuron

However, for comparison sake, the models were also built and simulated with ten hidden neurons until a resulting overall percent error of under 20% was achieved. The weights and biases were also taken from this lowest percent error network. This lowest percent error for ten hidden neurons was incorporated for the overall analysis when it was realized that the results for one hidden neuron had significantly larger percent errors that always exceeded 20%. Again, since this many neurons indicate a more complex web of data transference, the importance of each variable is hard to track. Therefore, the average weight of each input variable to each hidden neuron was taken, i.e. each variable has ten weights, one to each hidden neuron. In this case, only the weights between the input neurons and the hidden neurons will be shown as a means of comparison.

Overall, this approach would give an idea of which variables are more important and those that could possibly be reconsidered. It will also provide another way to assess the accuracy of each model in how it makes connections from the given variables. The weights on the connections between the hidden neuron and the output Impact Levels could also help assess the likelihood of an event being placed in each level.

3.2.4 Model Analysis

Model 1

In originally building and testing Model 1, it was found that the large amount of input variables, due to entering the meteorological factors at each landfall, actually exacerbates the overall resulting error and performance in comparison with the other models. The original simulations from the first study (Section 3.1), with the default of ten hidden neurons, produced a lowest and average percent error of approximately 18% and 46%, respectively. When this model data was evaluated with one hidden neuron it produced a lowest and average percent error over

10 simulations of approximately 44% and 69%, respectively. Table 3-6 summarizes the average overall weight connections and average biases for the one hidden neuron versions of Model 1, the maximum and minimum average weights are shown in bold for reference.

Table 3-6 Model 1 Average Weights and Biases over 10 Simulations for 1 Hidden Neuron Structure

Input Variable	Input Weights	Hidden Neuron	Layer Weights	Output Layer
Population	0.1829	1 (Bias = -0.1269)	-1.7585	Impact Level 0 (Bias = 1.5958)
Landfall 1				
Latitude	-0.0354			
Longitude	-0.0152			
Pressure	**-0.3404**			
Wind Speed	0.1310			
Storm Surge	0.1470			
Precipitation	-0.0943		3.3258	Impact Level 1 (Bias = -2.0703)
Landfall 2				
Latitude	**0.2179**			
Longitude	0.2137			
Pressure	0.0520			
Wind Speed	0.1344		-1.6832	Impact Level 2 (Bias = 0.3209)
Storm Surge	0.1162			
Precipitation	0.0932			
Landfall 3				
Latitude	0.0478			
Longitude	-0.0140		3.3703	Impact Level 3 (Bias = 0.6071)
Pressure	-0.0483			
Wind Speed	0.0551			
Storm Surge	0.0709			
Precipitation	0.0750		3.3971	Impact Level 4 (Bias = 1.9526)
Landfall 4				
Latitude	-0.1256			
Longitude	-0.0120			
Pressure	0.0466			
Wind Speed	-0.0158		-1.4491	Impact Level 5 (Bias = -1.9080)
Storm Surge	N/A			
Precipitation	-0.0090			

One of the first things to note for the Model 1 results is that there were no weights between the fourth landfall storm surge and the hidden neuron. This is because there was only

one training event that actually had four landfall locations and there wasn't a corresponding storm surge for the fourth location. This resulted in zeros for this whole row of the input matrix and it was therefore disregarded. On the landfalls where storm surge did occur, it can be seen that it positively contributes to the resulting outcome. If this holds throughout the connections, then this supports what would be expected, since it has been widely noted that storm surge is likely the most significant factor in resulting economic damage from a hurricane, as was covered in Section 2.2.2. Population is also positive as would be expected, while pressure is typically negative. Pressure was originally included due to its meteorological correlation to wind speed, however, it does not directly interact with infrastructure to cause damage. Precipitation and wind speed seem to vary more among landfalls in concerns to their positive or negative contribution, this could signal that these are more neutral factors overall. The tricky factors, that will be a common complication in each model, are the landfall locations. There are instances when both the latitude and longitude are negative and instances where both are positive, however, there are also situations where one is negative and one is positive. For further comparison, Figure 3-20 below shows the averaged input weights between ten hidden neurons for a model network resulting in 15% error.

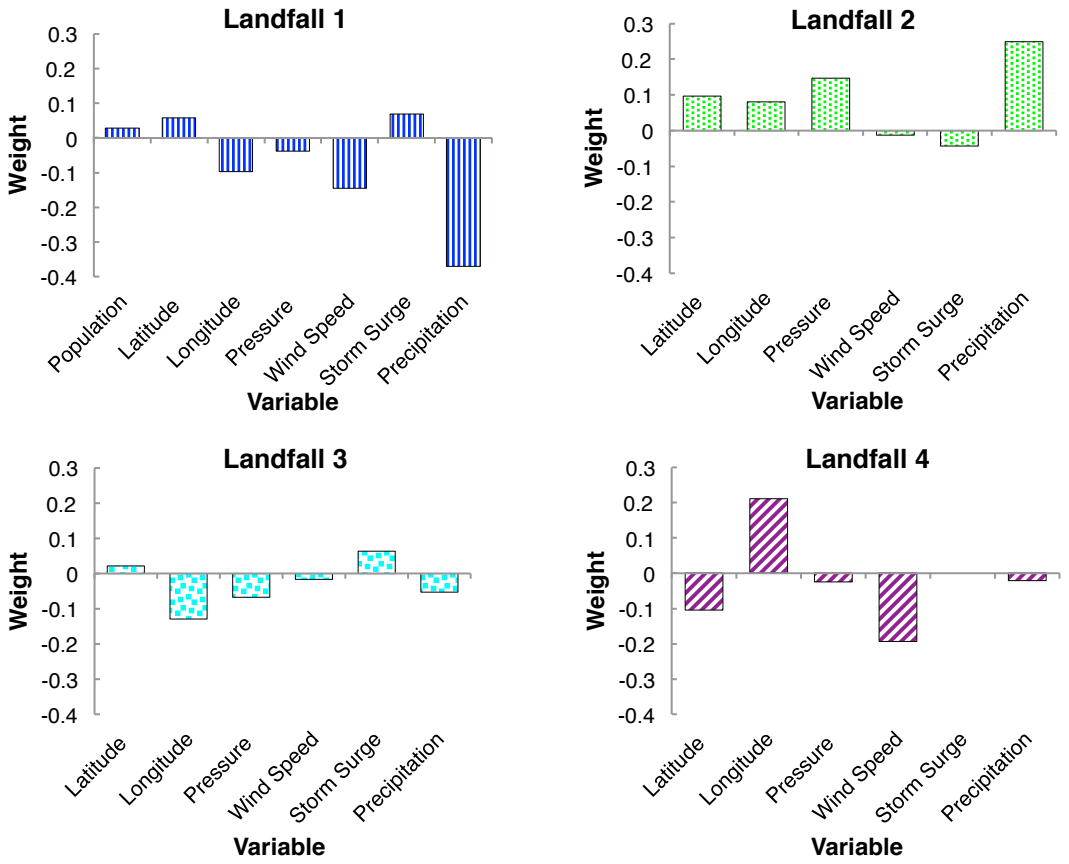

Figure 3-20 Model 1 average weights between 10 hidden neurons for different landfalls.

The results of the ten hidden neuron simulations roughly correlate to the results achieved with one hidden neuron except that now storm surge seems to become an inhibitory connection for some landfalls. Precipitation, specifically, becomes more complex in that for the first landfall it is the most inhibitory, yet the most excitatory of all 25 inputs for the next landfall. The overall results for Model 1 show that the values of all the input weights are each relatively closer to zero and correlates to the issue of having excessive number of inputs resulting in weaker established connections between neurons.

Model 2

As with Model 1, Model 2 also has a large number of inputs that increased the overall resulting error and lowered the performance in comparison with the other models. The original

simulations from the first study (Section 3.1),, with the default of ten hidden neurons, produced a lowest and average percent error of approximately 18% and 45%, respectively. When this model data was evaluated with one hidden neuron it produced a lowest and average percent error over ten simulations of approximately 61% and 79%, respectively. Table 3-7 summarizes the average overall weight connections and average biases for the one hidden neuron versions of Model 2, the maximum and minimum average weights are shown in bold for reference.

Model 2 serves to replace the population used in Model 1 with the wind radius at each location based on the theory that since the tropical storm strength wind radii were used to extrapolate the population, the neural network could make that same deduction if it also had the landfall location (storm center). As with the population from Model 1, the wind radii have a positive correlation between neurons and at a generally higher value than the other variables. The wind speed and precipitation also have a similar relation as in Model 1, along with latitude and longitude varying in sign. However, the pressure and storm surge seemed to have switched signs from the Model 1 results. Also, the pressure at landfall two seems to be the most contributing factor while the storm surge for the first landfall inhibits the network function the most, which is essentially the opposite of what would be expected throughout the network connections. Similarly to Model 1, due to the large number of inputs, the weight values for Model 2 are rather close to zero. For further comparison, Figure 3-21 below shows the averaged input weights between ten hidden neurons for a model network resulting in 18% error.

Table 3-7 Model 2 Average Weights and Biases over 10 Simulations for 1 Hidden Neuron Structure

Input Layer	Input Weights	Hidden Neuron	Layer Weights	Output Layer
Landfall 1				
Latitude	-0.0417			
Longitude	-0.0762			
Pressure	0.1810		2.9656	Impact Level 0 (Bias = -3.7642)
Wind Speed	0.0064			
Wind Radius	0.1086			
Storm Surge	**-0.2476**			
Precipitation	-0.1367			
Landfall 2				
Latitude	0.2379		1.6407	Impact Level 1 (Bias = -1.0652)
Longitude	0.1041			
Pressure	**0.3639**			
Wind Speed	0.2381			
Wind Radius	0.2842			
Storm Surge	0.3222		3.3459	Impact Level 2 (Bias = -0.7395)
Precipitation	0.0359			
Landfall 3		1 (Bias = -0.2235)		
Latitude	0.2188			
Longitude	0.2105			
Pressure	0.3136			
Wind Speed	0.0825		-1.64711	Impact Level 3 (Bias = -0.4576)
Wind Radius	0.0953			
Storm Surge	-0.0413			
Precipitation	0.2399			
Landfall 4				
Latitude	0.1480		-1.15642	Impact Level 4 (Bias = -1.5953)
Longitude	0.1723			
Pressure	0.2547			
Wind Speed	0.2468			
Wind Radius	0.2929		2.47846	Impact Level 5 (Bias = 0.88242)
Storm Surge	N/A			
Precipitation	0.3006			

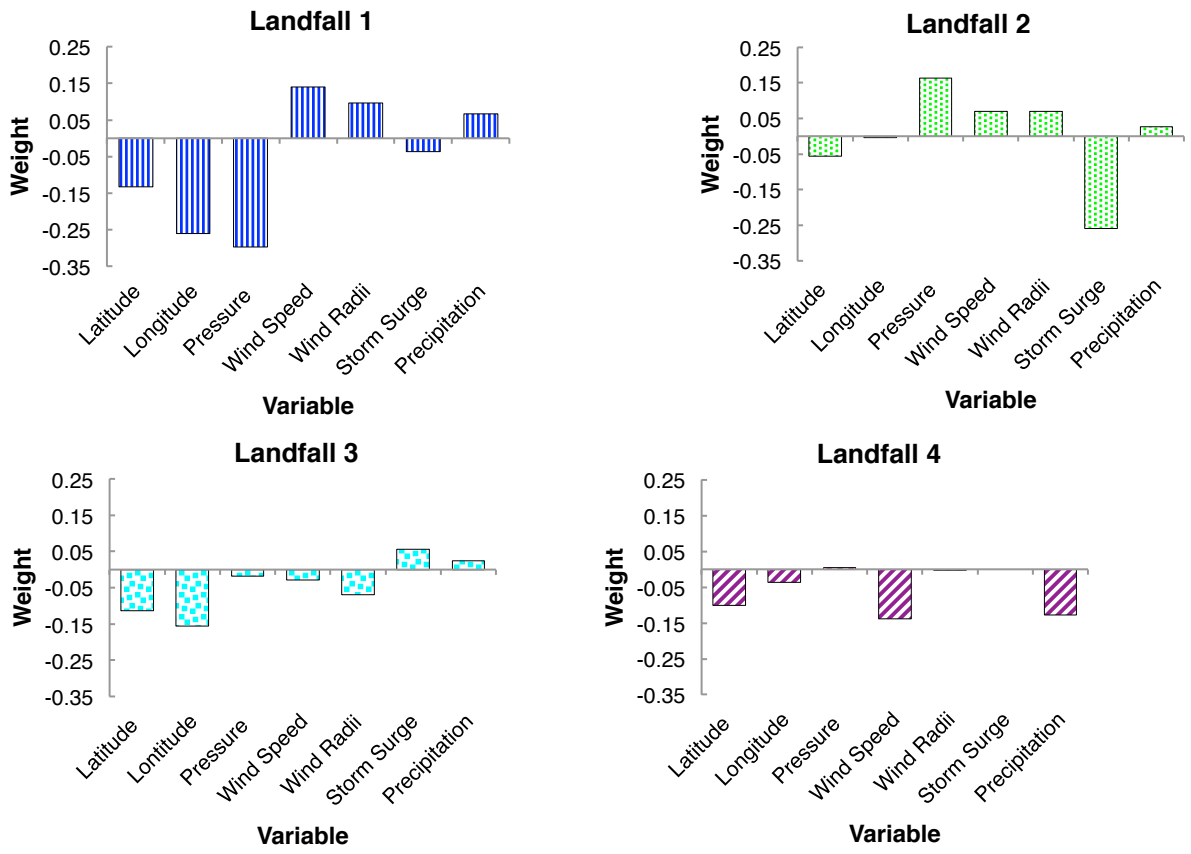

Figure 3-21 Model 2 average weights between 10 hidden neurons

If these averaged weights for the ten hidden neurons were absolute in the contribution of each variable, there would be more issues with this model as the pressure not only contributes most positively, and negatively, to the network function, but the storm surge is mostly inhibitory throughout the landfalls. The landfall locations are also all inhibitory, while the wind radii seem to vary with landfall. While these weight values, for both the single hidden neuron and ten hidden neurons, do not demonstrate the expected importance of each variable, this does correspond with the previously determination of Model 2 being the least accurate, or reliable, of the built model networks.

Model 3

Model 3 is the first model to reduce the number of inputs by nearly half of the first model. The original simulations from the first study (Section 3.1), with the default of ten hidden neurons, produced a lowest and average percent error of approximately 17% and 36%, respectively. When this model data was simulated with one hidden neuron it produced a lowest and average percent error over ten simulations of approximately 59% and 76%, respectively. Table 3-8 lines up the average overall weight connections and average biases for the one hidden neuron versions of Model 3, the maximum and minimum average weights are shown in bold for reference.

Table 3-8 Model 3 Average Weights and Biases over 10 Simulations for 1 Hidden Neuron Structure

Input Layer	Input Weights	Hidden Neuron	Layer Weights	Output Layer
Population	0.2033	1 (Bias = -0.2999)	1.4645	Impact Level 0 (Bias = -1.9011)
Pressure	-0.1863			
Wind Speed	0.1486			
Storm Surge	0.6270		1.1427	Impact Level 1 (Bias = -1.7324)
Precipitation	-0.1022			
Latitude 1	0.1422		-0.0315	Impact Level 2 (Bias = -0.1126)
Longitude 1	**-0.5038**			
Latitude 2	0.5301		0.0115	Impact Level 3 (Bias = -0.0749)
Longitude 2	**0.6942**			
Latitude 3	0.2052		3.2306	Impact Level 4 (Bias = 2.0995)
Longitude 3	0.3997			
Latitude 4	0.2662		-0.9601	Impact Level 5 (Bias = -2.4218)
Longitude 4	0.1296			

By reducing the number of neurons, it can be seen that the range of weight values has increased and exceeded an absolute value of 0.5 (from zero), unlike the previous two models. The meteorological parameters have also reverted back to the positive/negative values that would be expected. Storm surge and population are two large exhibitory connections, while pressure is still an inhibitory connection. Precipitation, however, still seems to be a week inhibitor within the network functions, bringing into question its actual relevance to damage. The landfall

locations still exhibit unusual behavior in alternating signs, however, only one longitude has a negative sign, while the rest remain positive. Figure 3-22 below shows the averaged input weights between ten hidden neurons for a model network resulting in 19% error.

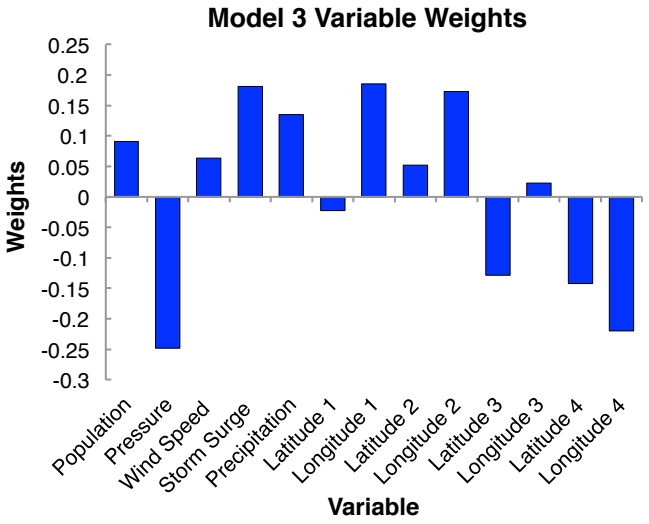

Input Variable	Average Weight
Population	0.09078
Pressure	**-0.24847**
Wind Speed	0.06392
Storm Surge	0.18131
Precipitation	0.13502
Latitude 1	-0.02246
Longitude 1	**0.1856**
Latitude 2	0.05192
Longitude 2	0.17279
Latitude 3	-0.12875
Longitude 3	0.02223
Latitude 4	-0.14188
Longitude 4	-0.21954

Figure 3-22 Model 3 average weights between 10 hidden neurons

The ten hidden neuron simulation of Model 3 kept the same overall level of importance among the inputs. Population and flooding contributors maintained an average excitatory connection. Latitude and longitude still go back and forth between inhibitory and excitatory, however a negative weight on the fourth landfall would make sense given that only one event had four landfall locations. Overall, the factors considered for Model 3 are weighted as expected, if these weights were considered directly linked to the outputs.

Model 4

Model 4 is similar to Model 3, but brings wind radii back in and disregards the determined population. The original simulations from the first study (Section 3.1), with the default of ten hidden neurons, produced a lowest and average percent error of approximately 6% (the lowest of all models) and 41%, respectively. When this model data was simulated with one

hidden neuron it produced a lowest and average percent error over ten simulations of approximately 58% and 74%, respectively. Table 3-9 lines up the average overall weight connections and average biases for the one hidden neuron versions of Model 4, the maximum and minimum weights are shown in bold for reference.

Table 3-9 Model 4 Average Weights and Biases over 10 Simulations for 1 Hidden Neuron Structure

Input Layer	Input Weights	Hidden Neuron	Layer Weights	Output Layer
Pressure	0.0180	1 (Bias = 0.1184)	-8.4901	Impact Level 0 (Bias = 8.2982)
Wind Speed	-0.0647			
Storm Surge	-0.1472			
Precipitation	0.0487		0.0008	Impact Level 1 (Bias = -0.0064)
Latitude 1	0.1461			
Longitude 1	-0.0398			
Wind Radius 1	**0.1719**		3.3617	Impact Level 2 (Bias = -0.6636)
Latitude 2	-0.2172			
Longitude 2	-0.1822			
Wind Radius 2	-0.1549		3.3665	Impact Level 3 (Bias = 0.6372)
Latitude 3	-0.2873			
Longitude 3	-0.2568			
Wind Radius 3	**-0.1373**		-1.6731	Impact Level 4 (Bias = -1.0358)
Latitude 4	-0.3137			
Longitude 4	0.0005			
Wind Radius 4	-0.2606		-2.7339	Impact Level 5 (Bias = -3.9934)

Model 4 produced the lowest percent error of all the models; however, it was the only model to not correctly forecast the impact of Hurricane Isaac for the trial simulations. The results for this model produce unusual results where the majority of the inputs inhibit the network connection to the hidden neurons and those that are positive are not ones that would be expected,

such as pressure. Figure 3-23 below shows the averaged input weights between ten hidden neurons for a model network resulting in 19% error.

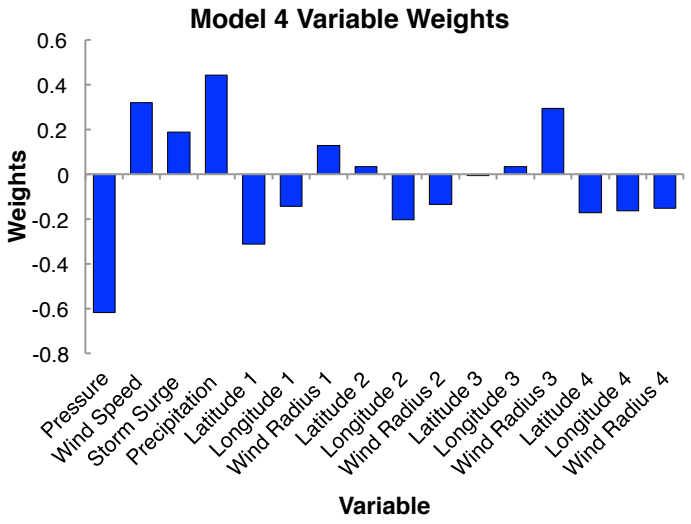

Input Variable	Average Weight
Pressure	**-0.6164**
Wind Speed	0.3206
Storm Surge	0.1873
Precipitation	**0.4424**
Latitude 1	-0.3110
Longitude 1	-0.1428
Wind Radius 1	0.1285
Latitude 2	0.0329
Longitude 2	-0.2029
Wind Radius 2	-0.1334
Latitude 3	-0.0051
Longitude 3	0.0328
Wind Radius 3	0.2951
Latitude 4	-0.1719
Longitude 4	-0.1641
Wind Radius 4	-0.1519

Figure 3-23 Model 4 average weights between 10 hidden neurons

Even in the ten hidden neuron simulation, there are still many variables that correspond to an average inhibitory connection to the hidden neuron layer. However, the meteorological parameters seem to correlate more to the weights that would be expected for direct relation to the resulting impacts; storm surge and precipitation are excitatory while pressure is inhibitory. Generally, though, this model proves to be the most difficult in tracing the importance of variables since most seem to hinder the network.

Model 5

Model 5 assumes population density can be extrapolated simply from the location of landfall. The original simulations from the first study (Section 3.1), with the default of ten hidden neurons, produced a lowest and average percent error of approximately 14% and 43%, respectively. When this model data was simulated with one hidden neuron it produced a lowest

and average percent error over ten simulations of approximately 58% and 79%, respectively. Table 3-10. lines up the average overall weight connections and average biases for the one hidden neuron versions of Model 5, the maximum and minimum weights are shown in bold for reference.

Table 3-10 Model 5 Average Weights and Biases over 10 Simulation for 1 Hidden Neuron Structure

Input Layer	Input Weights	Hidden Neuron	Layer Weights	Output Layer
Pressure	**-0.2803**	1 (Bias = -0.1476)	1.6367	Impact Level 0 (Bias = -1.7163)
Wind Speed	0.0591			
Storm Surge	-0.2127		1.4156	Impact Level 1 (Bias = -1.4099)
Precipitation	-0.2397			
Latitude 1	0.3795		-1.7482	Impact Level 2 (Bias = 0.1670)
Longitude 1	-0.1139			
Latitude 2	0.3164		1.4839	Impact Level 3 (Bias = -1.7539)
Longitude 2	**0.5310**			
Latitude 3	-0.1016		1.3759	Impact Level 4 (Bias = -1.9008)
Longitude 3	-0.1401			
Latitude 4	-0.0375		0.9755	Impact Level 5 (Bias = -0.9434)
Longitude 4	0.2135			

Unfortunately, in using one hidden neuron, Model 5 produced input weights similar to that of Model 4. The Model 5 weights between the inputs and the single hidden neuron are mainly inhibitory, with flooding hazards being mostly inhibitory, while it seems to focus the positive correlations to the second landfall location. Figure 3-24 below shows the averaged input weights between ten hidden neurons for a model network resulting in 18% error.

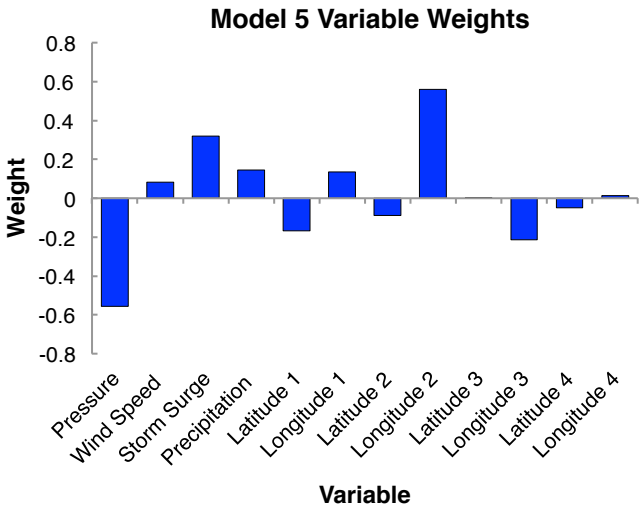

Input Variable	Average Weight
Pressure	**-0.5579**
Wind Speed	0.0842
Storm Surge	0.3211
Precipitation	0.1446
Latitude 1	-0.1667
Longitude 1	0.1366
Latitude 2	-0.0874
Longitude 2	**0.5605**
Latitude 3	0.0043
Longitude 3	-0.2142
Latitude 4	-0.0495
Longitude 4	0.0134

Figure 3-24 Model 5 average weights between 10 hidden neurons

The ten hidden neuron simulation produced slightly different results, in that there are slightly less inhibitory reactions occurring. As with Model 4, the meteorological parameters' weights correlate more to what is expected to contribute more to resulting economic damage with a high positive weight on storm surge and high negative weight on pressure. For Model 5 though, the most excitatory and inhibitory factors remained as the longitude for landfall two and the pressure, respectively. In addition, the landfall locations seem to have kept their relative level of contribution to the overall network while still seeming to vary randomly.

Model 6

Model 6 consists of the least amount of inputs and utilizes the assumption that the population will correlate to the amount of infrastructure in harms way, but likely not communicate the quality to the network. The original simulations, with the default of ten hidden neurons, produced a lowest and average percent error of approximately 15% and 36%, respectively. When this model data was simulated with one hidden neuron it produced a lowest and average percent error of approximately 58% and 73%, respectively. Table 3-11 lines up the

average overall weight connections and biases for the one hidden neuron versions of Model 6, the maximum and minimum weights are shown in bold for reference. Figure 3-25 shows this same data but in a more visualized way.

Table 3-11 Model 6 Average Weights and Biases over 10 Simulations for 1 Hidden Neuron Structure

Input Layer	Input Weights	Hidden Neuron	Layer Weights	Output Layer
Population	0.7153	1 (Bias = -0.7521)	-0.2954	Impact Level 0 (Bias = -0.3565)
Pressure	**-1.0585**		1.3034	Impact Level 1 (Bias = -1.5020)
Wind	0.0034		1.6799	Impact Level 2 (Bias = -0.6923)
Storm Surge	**1.0416**		0.5254	Impact Level 3 (Bias = -0.8408)
Precipitation	-0.3739		0.5637	Impact Level 4 (Bias = -0.8332)
			4.3868	Impact Level 5 (Bias = 2.0988)

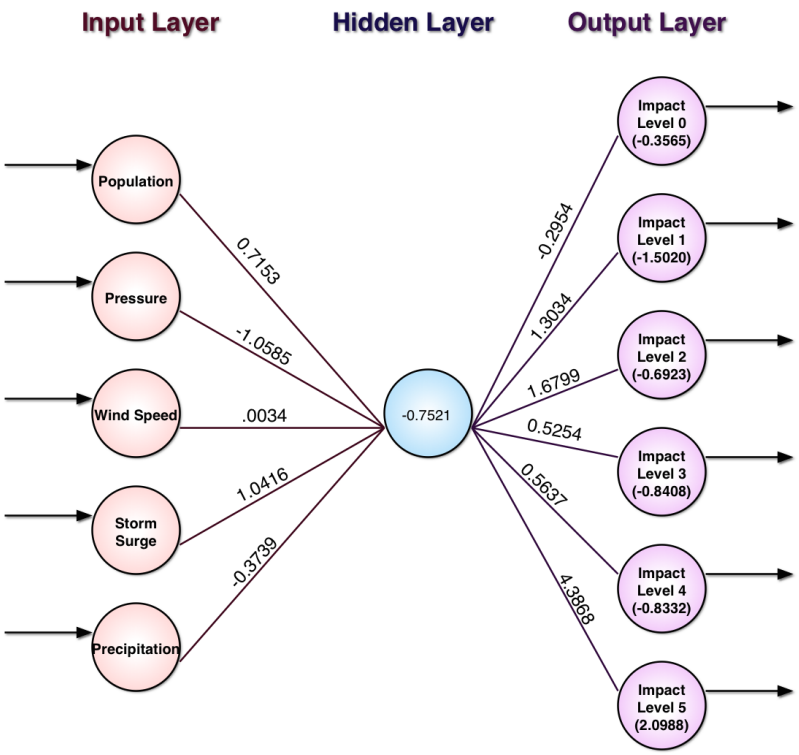

Figure 3-25 Model 6 average weights and biases for 1 hidden neuron

Model 6 produced network weights that were expected, with pressure being the most inhibitory neuron connection and storm surge being the most excitatory followed by population. Precipitation, as with the other models is still coming up as inhibitory. Figure 3-26 below shows the averaged input weights between ten hidden neurons for a model network resulting in 17% error.

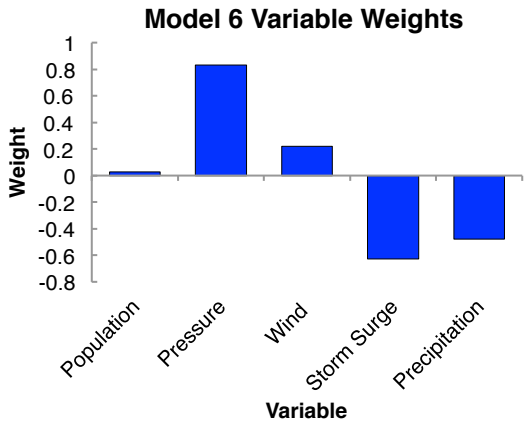

Input Variable	Average Weight
Population	0.0266
Pressure	**0.8310**
Wind	0.2218
Storm Surge	**-0.6268**
Precipitation	-0.4806

Figure 3-26 Model 6 average weights between 10 hidden neurons

The Model 6 with ten hidden neurons is the only example resulting in less optimal input weights than those from the one hidden neuron network. This can specifically be seen in pressure and storm surge switching positions between most excitatory and most inhibitory. Following that, wind and population, while both still positive, switch which contributes a more excitatory connection to the hidden neurons. If the neurons definitively connected to the resulting outputs, the one hidden neuron case for Model 6 would actually show a preferable weight allocation to that of the ten hidden neuron case.

3.2.5 Discussion

These six models were designed in various ways to present the basic same variables to the neural network. It was previously determined that, when creating a neural network, it is a

balance between making sure all the relevant data is there without creating too big of an input matrix. Herein, these six models are used to assess the importance of the various hurricane factors that would theoretically contribute to the resulting economic damage (Impact Levels).

The weights between neurons represent an excitatory or inhibitory connection. Within a feedforward network with a hidden neuron layer, the input related weights represent the connection between the inputs (hurricane related factors) and hidden neurons. Due to the complex web created with a hidden layer of multiple neurons, the best way to extrapolate an idea of the importance hurricane impact prediction factors is to analyze all the model data from the above section together, as seen in Table 3-12.

Table 3-12 Overall Input Variable Weights

	1 Hidden Neuron						Average over 10 Hidden Neurons						Overall	
	Model 1	Model 2	Model 3	Model 4	Model 5	Model 6	Model 1	Model 2	Model 3	Model 4	Model 5	Model 6		
Population	↑		↑			↑	↑		↑			↑	↑	Population
Latitude 1	↓	↓	↑	↑	↑		↑	↓	↓	↓	↓		↓	Latitude 1
Longitude 1	↓	↓	↓	↓	↓		↓	↓	↑	↓	↑		↓	Longitude 1
Pressure 1	↓	↑	↓	↑	↓	↓	↓	↓	↓	↓	↓	↑	↓	Pressure 1
Wind Speed 1	↑	↑	↑	↓	↑	↑	↓	↑	↑	↑	↑	↑	↑	Wind Speed 1
Wind Radius 1		↑		↑				↑		↑			↑	Wind Radius 1
Storm Surge 1	↑	↓	↑	↓	↓	↑	↑	↓	↑	↑	↑	↓	↑	Storm Surge 1
Precipitation 1	↓	↓	↓	↑	↓	↓	↓	↑	↑	↑	↑	↓	↓	Precipitation 1
Latitude 2	↑	↑	↑	↓	↑		↑	↓	↑	↑	↓		↑	Latitude 2
Longitude 2	↑	↑	↑	↓	↑		↑	↓	↑	↓	↑		↑	Longitude 2
Pressure 2	↑	↑					↑	↑					↑	Pressure 2
Wind Speed 2	↑	↑					↓	↑					↑	Wind Speed 2
Wind Radius2		↑		↓				↑		↓			–	Wind Radius2
Storm Surge 2	↑	↑					↓	↓					–	Storm Surge 2
Precipitation 2	↑	↑					↑	↑					↑	Precipitation 2
Latitude 3	↑	↑	↑	↓	↓		↑	↓	↓	↓	↑		↑	Latitude 3
Longitude 3	↓	↑	↑	↓	↓		↓	↓	↑	↑	↓		↓	Longitude 3
Pressure 3	↓	↑					↓	↓					↓	Pressure 3
Wind Speed 3	↑	↑					↓	↓					–	Wind Speed 3
Wind Radius 3		↑		↓				↓		↑			–	Wind Radius 3
Storm Surge 3	↑	↓					↑	↑					↑	Storm Surge 3
Precipitation 3	↑	↑					↓	↑					↑	Precipitation 3
Latitude 4	↓	↑	↑	↓	↓		↓	↓	↓	↓	↓		↑	Latitude 4
Longitude 4	↓	↑	↑	↑	↑		↑	↓	↓	↓	↑		↑	Longitude 4
Pressure 4	↑	↑					↓	↑					↑	Pressure 4
Wind Speed 4	↓	↑					↓	↓					↓	Wind Speed 4
Wind Radius 4		↑		↓				↓		↓			↓	Wind Radius 4
Storm Surge 4														Storm Surge 4
Precipitation 4	↓	↑					↓	↓					↓	Precipitation 4

The overall analysis looks at each variable and the number of times it plays a excitatory (positive) or inhibitory (negative) role. Since only two of the models distribute the

meteorological factors to each landfall, these factors for the remaining models were lined up with the first landfall set. Population comes up consistently as an excitatory factor, followed by the tropical storm wind radius at three of the four landfalls. Storm surge is also largely excitatory along with wind speed. Therefore, these factors have a strong connection to the subsequent economic damage. For the reverse, pressure is mostly inhibitory across the board, followed by precipitation. Pressure doesn't directly interact with the built environment, so the fact that this variable inhibits the pattern building process indicates it would likely not contribute to any damage. However, the precipitation is more varied. When more hidden neurons are used, precipitation is more excitatory overall. Also, among multiple landfalls the total contribution is mostly a wash. Therefore, precipitation is more of a neutral factor in predicting hurricane impacts.

Landfall locations are trickier, as the latitude and longitude weights are not consistent throughout the models and the overall summation. In considering all the models, landfall location one is mainly inhibitory but following that the second and fourth landfalls are excitatory with the third latitude excitatory as well. The only model that does not use multiple landfalls, Model 6, has population as an excitatory connection. Overall, this indicates a stronger importance of multiple landfalls, over a single landfall location, relevant to the resulting total damage. It is worth noting that most storms to hit north of the Mason-Dixon line have to make more than one landfall due to the geography of the coastline. This might be the neural network's way of assessing infrastructure quality, since infrastructure further north is generally older and in poorer condition.

3.2.6 Conclusion

The resulting impacts of hurricanes on society are due to more than wind speed (the category ranking by the Saffir-Simpson Scale). Within this study, the importance of many possible factors are examine for their contribution to the overall resulting economic damage (Impact Level) of a tropical cyclone, or hurricane, event along the U.S. coastline. Six models are used as a way to present the relative data, including wind speed, storm surge, precipitation, population, and location latitude and longitude, to the neural network in order to establish a general level of importance for each factor. A consistently excitatory factor was the population, with storm surge and wind speed being other contributing factors. Landfall location would sometimes contribute positively to outcome. While the numbers of connections in a neural network make it difficult to interoperate with high confidence how each factor contributed to the determination of economic damage, these results are mostly consistent with the current research and expert knowledge in this area.

3.3 Hurricane Impact Prediction: Evaluation of Neural Network Training Algorithms as a Means of Problem Identification

Forecasting the resulting damage from a tropical cyclone (hurricane) is a complex multifaceted problem that has proven difficult to establish concrete connections for. Accurately forecasting resulting economic damage from a hurricane event can provide an improved way of communicating storm severity. However, to reach this point, the connections between multiple variables, such as landfall location, wind speed, storm surge, and precipitation, and the economic damage must first be accurately established. Neural networks provide a way to build complex connections based off of various learning algorithms that attempt to replicate how the human brain learns from similar data. These algorithms vary in strategy and may provide different results for varying problem type. Within this study, variations in training algorithms, which assess patterns based on optimization or probability, will be explored. Most training algorithms utilize optimization, however, some current models suggest that forecasting hurricane damage is more probabilistic. This study will use these multiple input variables along with the Impact Level Ranking System in order to establish the type of problem at hand and further reduce the error for predicting the range of economic damage expected from a hurricane event.

3.3.1 Overview

The research studies covered so far have analyzed six possible models for the best way to present historical hurricane data to a neural network and for evaluating the importance of each data variable. These models utilize meteorological parameters (wind speed, pressure, storm surge, and precipitation) along with societal factors, which include population and landfall location, in order to build the best possible model to communicate the risk and potential damage from a

landfalling tropical cyclone (or hurricane, to use the term loosely) by the Impact Level Ranking System previously discussed.

These six models were built using the MATLAB neural network pattern recognition toolbox. The data used for this study consists of 66 hurricane events and their respective meteorological parameters, landfall locations, and QGIS extrapolated population affected by tropical storm force wind radii. The six models varied these parameters in their respective input matrix, while the corresponding target matrices were the same for each model and served to indicate each event's Impact Level (zero through five) by using binary methods. For evaluation of these six models, the program defaults were used for consistency and produced low percent errors for the resulting networks. These defaults include the maximum number of epochs (1000), the performance goal (as close as possible to 0 for MSE), and the time to train (infinite). Some of these algorithms may have additional defaults that are specific to the variables used, such as the starting designation for lambda ($5e^{-7}$) for scaled conjugate gradient (discussed in further detail below). These neural network models have been shown to successfully determine a correlation between the various input factors (meteorological and societal) and the respective Impact Levels.

Neural networks are structures of neurons and the connections between those neurons, which are strengthened by using backpropagation in order to reach the lowest possible error. There are several variations of backpropagation available, some of which are explored herein to further lower the percent error of this model and evaluate the resulting implications for the hurricane impact prediction problem using the Impact Level Ranking System.

3.3.2 Base Model Description

Based on the past two studies, Model 3 was chosen as the best model for neural network programming alterations. Per the study of the performance of each of the six models, Model 3

was determined to be one of the best performing models since it had a lower overall percent error and did relatively well during the trial phase. During the performance assessment of all six models, Model 3 had the lowest averaged percent error of 36% with a lowest reached error of 17% and standard deviation of 15. Model 3 also correctly predicted the Impact Level of Hurricane Isaac and did comparatively well with Tropical Storm Andrea by predicting either an Impact Level 0 (actual level) or 2. This study also indicated that smaller input matrices are best for producing lower percent errors. Requiring less input variables also allows for a better ease of use for future and real time applications.

In the evaluation of model weights in relation of the input variables, Model 3 produced excitatory, or positive, weights on the connections to population and storm surge, which would be expected for estimating economic damage. It also produced an inhibitory, or negative, weight on pressure, which is also expected since pressure doesn't directly interact with the built environment to cause damage. Wind speed, which was excitatory, covers pressure's secondary relation to economic damage.

Model 3, herein referred to as "the model", is set up to include population, pressure, wind speed, storm surge, precipitation, and four possible landfall locations as its input variables as shown in the matrix Equation (3.4) below. Therefore, the model still accounts for all the originally determined variables with an input layer of 13 neurons. The original network structure for this model involved ten neurons within the hidden layer and a data separation of 70/15/15 percentages for training, validation, and testing, respectively. The simulation utilizes training, validation, and testing phases in order to achieve the best possible network by using iterations to proceed through the provided data through these phases until it establishes a significant pattern that results in the lowest possible error checked by six subsequent iterations. Additionally, for the

previous studies, the default backpropagation algorithm used by the pattern recognition toolbox was kept, but will be altered herein.

$$\begin{bmatrix} Population \\ Pressure\ (mbar) \\ Wind\ Speed\ (mph) \\ Storm\ Surge\ (feet) \\ Precipitation\ (inches) \\ Landfall\ 1\ Latitude \\ Landfall\ 1\ Longitude \\ Landfall\ 2\ Latitude \\ Landfall\ 2\ Longitude \\ Landfall\ 3\ Latitude \\ Landfall\ 3\ Longitude \\ Landfall\ 4\ Latitude \\ Landfall\ 4\ Longitude \end{bmatrix} \rightarrow \begin{bmatrix} Impact\ Level\ 0 \\ Impact\ Level\ 1 \\ Impact\ Level\ 2 \\ Impact\ Level\ 3 \\ Impact\ Level\ 4 \\ Impact\ Level\ 5 \end{bmatrix} \tag{3.4}$$

3.3.3 Methods

Backpropagation is the more general term for how the mean square error is minimized in a neural network, but there are multiple methods, and subsequent algorithms, to accomplish this. In backpropagation the data is trained and validated by the neural network, which produces a predicted value. This predicted value is compared to the provided target value and the difference, or error, between the two is propagated backward to adjust the neuron weights and biases. The network retrains, revalidates, and retests the data and this continues until the error between the approximated output and the provided target output in minimized.

The two methods that are the basis for multiple training algorithms are gradient descent and Gauss-Newton. Most training algorithms either directly use these methods while slightly altering one aspect or they utilize both methods together. The exploration of the use of these algorithms in relation to historical hurricane data will aid in determining the best way to utilize neural network predictive methods for future hurricane events.

Gradient descent reaches the minimum square errors by taking a step back from an initial guessed value proportional to the negative gradient of the fitting function to update the variable values (Constantinescu, Lazarescu, & Tahboub, 2008; Gavin, 2013). This continues until the minimum error between the approximated output value, y_j, and the target value, Y_j, is reached. The gradient of a two variable problem would be equivalent to the Laplace of that function. For a multivariable problem, such as the one discussed herein, this is represented with the Jacobian matrix, J, of size outputs, *n*, by variables, *m*, for a connection from the *i*th to the *j*th neuron. The gradient of the error function, E_{ij}, Equation (2.6), with respect to each variables, s, becomes:

$$\frac{\partial}{\partial s_i} E_{ij} = -\left(Y_j - y_j\right) W_{ij} J_{ij} \tag{3.5}$$

where Wij is the weight between the *i*th and *j*th neuron, which is adjusted. Generally this is done in equal steps, γ, and moves in the direction of the steepest decent. The resulting propagation, g, between each *i*th and *j*th neuron directs the variables into the steepest descent pattern, is represented by

$$g_{ij} = \gamma J_{ji} W_{ij} \left(Y_j - y_j\right) \tag{3.6}$$

The gradient descent method is typically used for a large number of variables, but for moderate problems, the Gauss-Newton method performs faster and is therefore more likely used (Gavin, 2013). The Gauss-Newton method instead assumes that the error function is quadratic and the guesses are near the optimal solutions. The iterations start with an initial guess of the minimum and continue until the difference between the guess and actual reaches the minimum of the quadratic function. The steps taken to minimize this difference introduces the Hessian matrix, $J_{ji}W_{ij}J_{ij}$, instead of just the gradient of the function such that the propagation is now

$$g_{ij} = \left(J_{ji} W_{ij} J_{ij}\right)^{-1} J_{ij} W_{ij} \left(Y_j - y_j\right) \tag{3.7}$$

where g_{ij} is still the propagation between neurons, W_{ij} is the weight, and Y_j and y_j are still the target and approximated output value, respectively. The Levenberg-Marquardt algorithm is a combination of the gradient method and the Gauss-Newton method for non-linear problems. When the parameters of the approximate function, **Y**, are close to their optimal value, the Levenberg-Marquardt algorithms acts like the Gauss-Newton function, but when they are far off, it acts more like the gradient descent method (Gavin, 2013). It does this by inserting a parameter, λ, associated with the identity matrix, I, within the propagation equation from the Gauss-Newton method to give the relationship

$$\left(J_{ji}W_{ij}J_{ij} + \lambda I_{ij}\right)g_{ij} = J_{ij}W_{ij}\left(Y_j - y_j\right) \tag{3.8}$$

This algorithm is the standard within MATLAB and is referred to as the fastest. However, the pattern recognition toolbox uses the scaled conjugate gradient (SCG) training algorithm. SCG mainly uses the gradient descent method to determine the direction of descent then determines the size of the steps the algorithm takes in that direction in order to reach the desired minimum by using the line-search technique instead of having to compute the Hessian matrix. This approach is combined with the Levenberg-Marquardt approach to account for possible situations where the Hessian matrix is not positive and definite (Møller, 1993). The SCG method is one of the more complicated and detailed algorithms but can save time by reducing the number of calculations done per iteration.

Another alteration of the gradient descent method is to account for an adaptive learning rate. The learning rate for a neural network refers to the scale (or amount) by which the weights and biases are adjusted. The gradient descent algorithm uses a default rate that remains constant through all iterations and can end up negatively affecting the outcome. By setting the learning rate to a default number and then allowing it to oscillate with the iterations in the training process,

it can improve the performance. This adjusts the weights and biases as well as the errors, but if the error is more than the previous error by a predefined ratio (default is 1.04), then those weights and biases are discarded while decreasing the learning rate in an attempt to produce better results during the next iteration (MathWorks, 2015).

The One-Step-Secant (OSS) algorithm is one that intertwines conjugate gradient method and Quasi-Newton (secant) method. The Quasi-Newton method, which is partially the Gauss-Newton method, is used for optimization when there is not enough space, time, or resources to store the Hessian or Jacobian matrix for each iteration. It instead aims to find a point when the gradient is zero. For the OSS algorithm, during each iteration, it assumes the previous Hessian matrix is the identity matrix. Therefore, an approximate Hessian matrix is updated after each iteration. This makes the OSS algorithm better for moderate or simpler networks. (Constantinescu et al., 2008)

A feedforward network using backpropagation can also utilize a training algorithm that is more based on statistical methods, such as the Bayesian Regulation algorithm. This indicates that Bayesian problems are less of optimization problems than the previously discussed algorithms. Instead, the Bayesian approach determines the maximum probability for the weights during training to then be utilized for testing (Neal, 1992). The framework for this approach consists of a utility, network "likelihood" model, and priors components. The utilities component consists of the learning goal, in this case the lowest mean-square error. The "likelihood" model gives an idea of how the data should be produced, in this study the Levenberg-Marquardt algorithm is used. The priors consist of prior distribution and probability that can change with each iteration (Buntine & Weigend, Andreas, 1991). After multiple iterations, the Bayesian algorithm applies

probabilities to each variable based on learning from the Levenberg-Marquart results and the corresponding prior distribution.

These five training algorithms were chosen for this study as part of a whole exercise to build the most accurate hurricane impact prediction model using the Impact Level Ranking System by establishing the type of problem at-hand. All of these algorithms use the lowest mean square error as the stopping mechanism, i.e. the mechanism being minimized by the above equations and methods. Ten hidden neurons and a data split of 70% training, 15% validation, and 15% testing were used for each version as a means of reliable and comparable consistency. As with previous studies for this research, each variation was simulated twenty times, collecting the average and lowest percent error reached. Since these methods distinctly vary, another item tracked was the number of iterations for each training algorithm.

3.3.4 Analysis

The goal of training algorithms is generally to reach a minimum error, however not all algorithms reach a minimum in the same way or pattern. Figure 3-27 demonstrates how these minimums were reached for the best-produced networks (lowest percent error) of this model problem. All of these algorithms have been designated to stop at the lowest reached MSE, which is determined by evaluating whether or not the MSE continues to decrease or starts to increase again (over train) within six iterations (or epochs). If the MSE begins to increase, the network then stops and produces a usable network associated with the respective lowest MSE. Most algorithms determine this lowest value during the validation phase. However, due to the fact that the Bayesian algorithm is a probabilistic model, not optimization, it does not have a validation phase. The Bayesian algorithm splits the data that was originally allocated to the validation section to the training phase, which is the phase used to determine the lowest error.

Most of the algorithms have the same descent pattern to the minimum MSE. The gradient descent with adaptive learning has a steeper descent drop-off than most of the others and shows the oscillation in learning rates towards the end. Bayesian Regulation has a very steep drop off in training to reach the lowest MSE of all the algorithms used herein. These lowest MSEs are reached when the most accurate weights and biases (probabilities for the Bayesian algorithm) for the model network are achieved, hence a low error between the desired output and the actual output.

While simulating each of these model variations, it was observed that the number of iterations changed drastically between some of the training algorithms. Figure 3-28 shows the average number of iterations to reach the lowest MSE for each training algorithm in comparison with the number of iterations each respective algorithm took to reach the best resulting network with the lowest percent error. Bayesian Regulation uses the most iterations in order to best determine the correct probabilities and the lowest MSE. This algorithm took the longest time to terminate and produce the resulting network and would sometimes reach the max number of iterations allowable at 1000. If this occurred, it usually produced a higher MSE and overall percent error, indicating an inability to establish the best pattern and probabilities. The better simulations using this algorithm had a lower number of iterations, which was contrary to the other algorithms. The Levenberg-Marquardt (LM) had the lowest number of iterations and took about the same amount of time as the other remaining algorithms. With the exception of the Bayesian network, a higher number of iterations was indicative of a more accurate resulting network model.

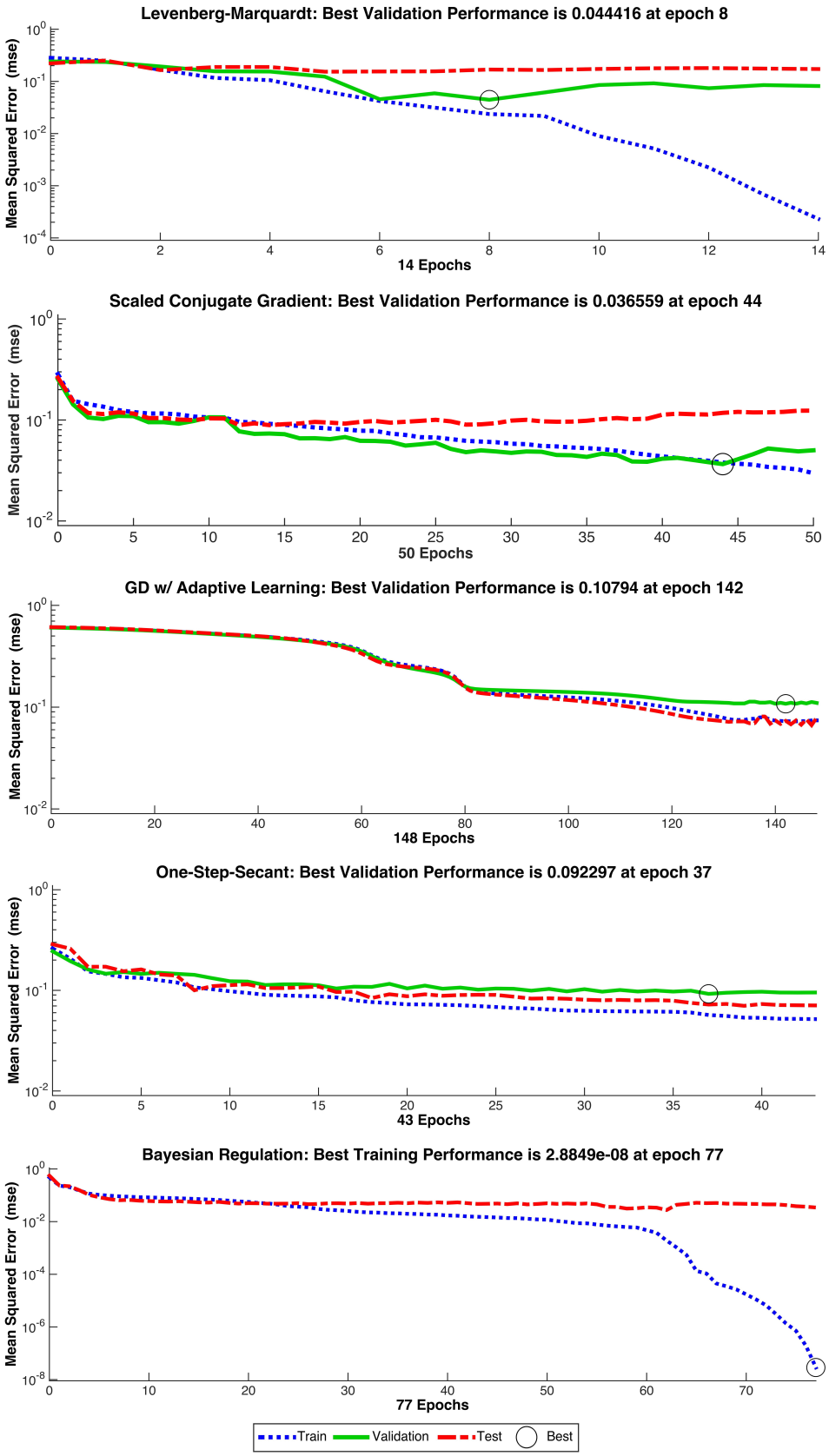

Figure 3-27 Model network performances for varying training algorithms

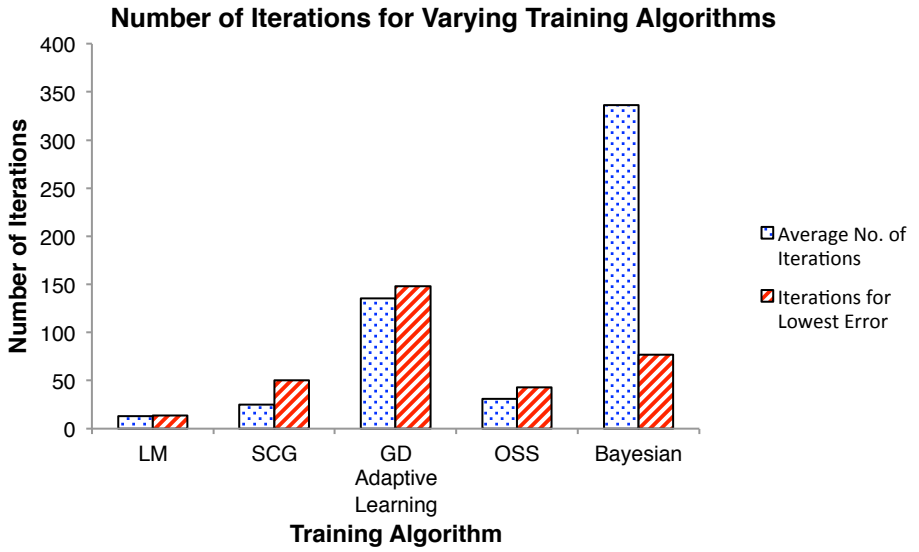

Figure 3-28 Average number of iterations to reach the lowest mean square error for varying training algorithms

The more accurate models, as with the previous studies for this research, were determined based on the lowest overall percent error achieved for each alteration. Figure 3-29 represents the comparison of the percent errors for the best possible model network achieved with each training algorithm. It is common for a lower MSE to be indicative of a low network percent error. The Bayesian Regulation algorithm, therefore, produced a correspondingly low percent error, which turned out to be the lowest error ever reached with this data. This algorithm also appears to have resolved the issue from previous studies where Impact Level 1 events were typically incorrectly forecasted. As can be seen with the other four algorithms, the percent error for Impact Level 1 events is still typically either 100% or 83%.

These confusion matrices aid in showing how the network predicts certain events once it has reached the lowest MSE as discussed above and can imply how the model used will perform when used real time. While the Levenberg-Marquardt algorithm performs quickly and is capable of producing a low percent error, it also demonstrates a tendency for the model to predict an

event far off from its actual Impact Level. For example, one Impact Level 5 events (Hurricane Sandy or Katrina) was forecasted (output) as an Impact Level 2 event. Also, over-forecasting can be equally dangerous and one Impact Level 1 event, which is a seemingly mundane event, was forecasted as an Impact Level 4 event, which is the same level as 2011 Hurricane Irene.

Corresponding to these confusion matrices, Figure 3-30 provides an overall picture of how the training algorithms performed on average as well as the best results reached. Not only did Bayesian Regulation produce the lowest percent error, the average was also significantly lower than even any pervious attempts made to lower the percent error for this research problem with a corresponding standard deviation of 3.1. In addition to showing Bayesian Regulations as the best performing network, the gradient descent with adaptive learning and one-step-secant emerged as the least applicable algorithms for this problem with the highest percent errors and standard deviations of approximately 17 and 19, respectively.

Four of these five algorithms involve either gradient descent or Gauss-Newton methods for optimization. The Levenberg-Marquardt and SCG performance both utilize the option of alternating between gradient descent and Gauss-Newton, which resulted in under 20% error, as opposed to the other two methods focused on optimization. Bayesian Regulation is the only probabilistic method used in this study and its exemplary performance in building a neural network suggests that hurricane impact prediction is more of a probabilistic and statistical problem.

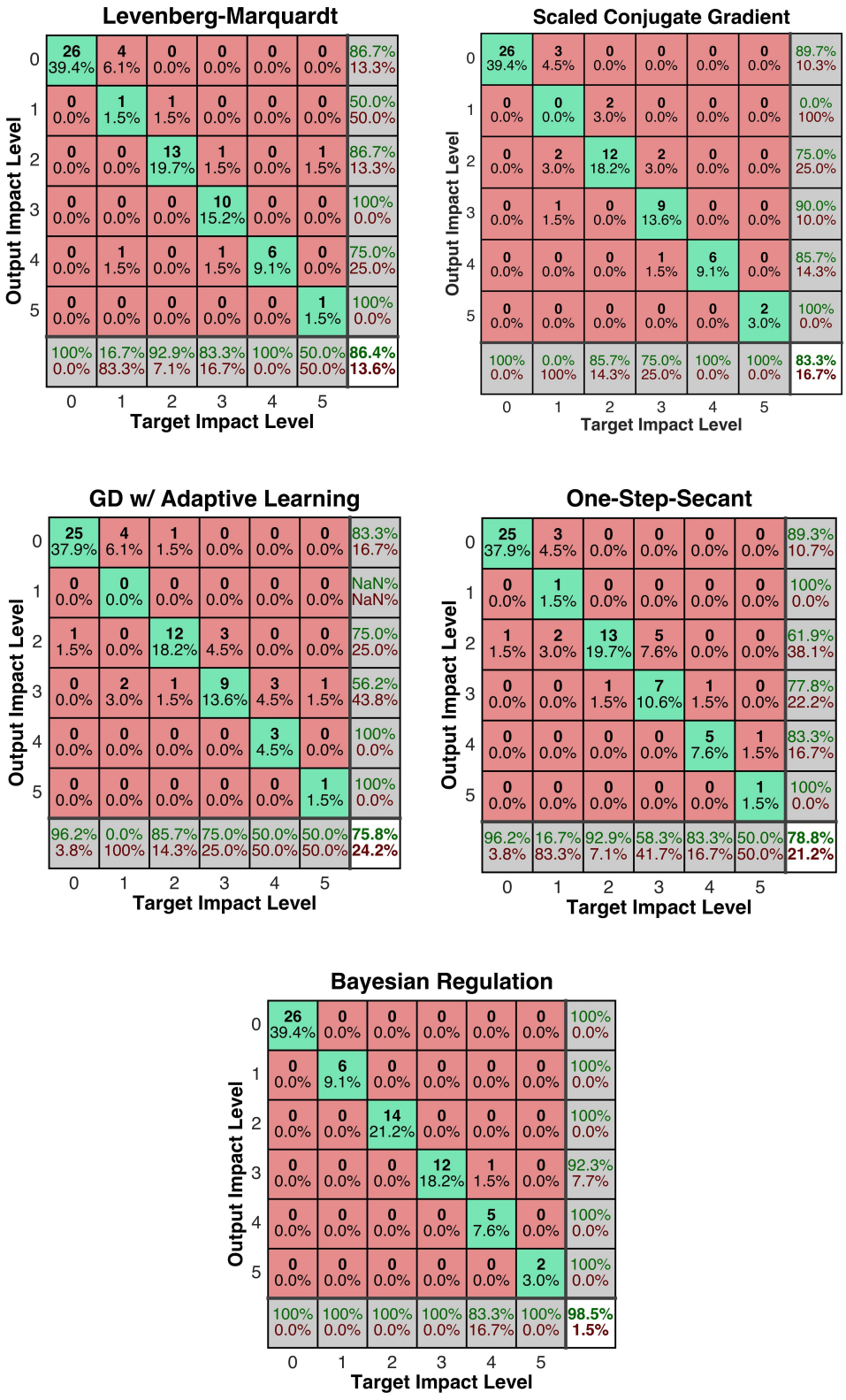

Figure 3-29 Confusion matrices representing lowest resulting network percent error for varying training algorithms

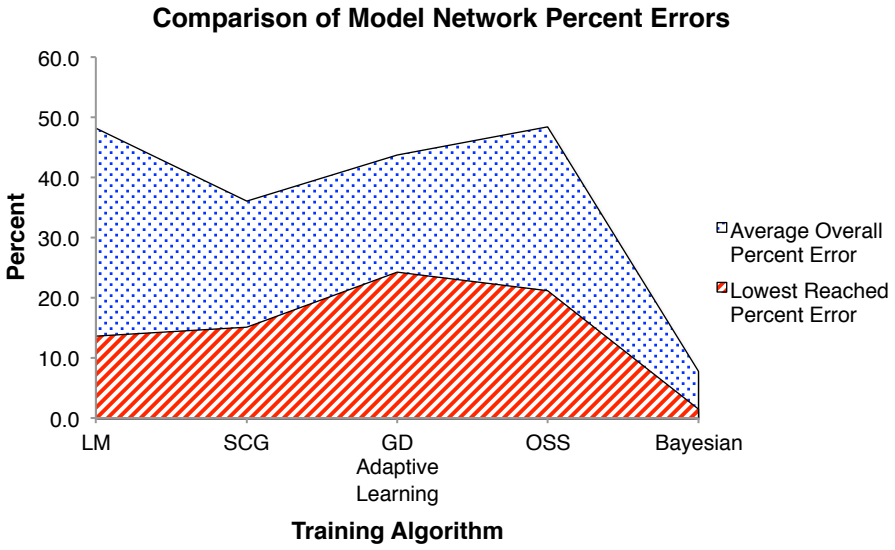

Figure 3-30 Comparison of model network percent errors for varying training algorithms

3.3.5 Conclusion

This study examined how varying training algorithms, while all other neural network parameters were held constant, affected the network performance for a hurricane impact prediction model using the Hurricane Impact Level Ranking System. As this model only has 66 historical events available to use for training, validation, and testing, determining the alternate approaches is vital in finding the best way to make use of the limited data available. Backpropagation is the general approach for pattern recognition by neural networks, but the algorithms used to achieve this can vary. Of the algorithms used herein: Levenberg-Marquardt, scaled conjugate gradient, gradient descent with adaptive learning, one-step-secant, and Bayesian Regulation, the Bayesian algorithm produced the best performing neural network for hurricane impact prediction using probabilistic, instead of optimization, methods.

CHAPTER 4

DISCUSSION: PROPOSED HURRICANE IMPACT LEVEL RANKING SYSTEM MODEL

4.1 Synopsis

The research conducted herein was initiated with the intent to create a more comprehensive predictive ranking system for tropical cyclones making landfall in the U.S. The Saffir-Simpson Scale is the current system in use to describe the severity of a tropical cyclone based solely on wind speed. However, when these storms make landfall, the wind speed is not enough to communicate the associated risk and resulting impact. Since the impact, i.e. economic damage, is also associated with storm surge, precipitation, population affected, and the infrastructure characteristics of the affected location, these factors should also be incorporated.

Wind, the main parameter used to categorize hurricanes, can change with infrastructure type and density. Urban areas have the potential to reduce the wind speed overall due to friction, however, wind tunnel effects could also take place. Additionally, once the wind speed picks up enough to cause damage a domino effect can begin to occur as debris move downwind, enhancing damage in that direction. Similarly, urban areas have a negative effect on the impacts of storm surge and precipitation as areas with impervious surfaces cannot adequately absorb or channel the excess water, causing the water level to rise. Conversely, locations with barrier islands and wetlands can absorb some of the brunt of storm surge. These meteorological factors become more imperative when more of society is affected indicating an increased number of residential structures as well as utilities and businesses within harms way. The high volume and quality of infrastructure affects the resulting damage arguably as much as the meteorological factors do.

The Impact Level Ranking System, as reshown in Table 4-1, is based off of the economic damage (2012 USD) of a tropical cyclone, which is mainly what the general public associates with a severe event. In order to predict the economic damage, or Impact Level, a model was created utilizing all of the relevant factors mentioned. This is an artificial neural network model that establishes patterns between these factors and the range of economic damage communicated through the created Impact Level Ranking System. These patterns, or connections, are established off of 66 historical hurricane events tracing back to the 1998 hurricane season.

Table 4-1 The Impact Level Ranking System

Impact Level	Economic Damage Amount (based on 2012 USD)	Example Event
0	< $25 million	2012 Tropical Storm Beryl
1	≥ $25 million, < $100 million	2007 Hurricane Humberto
2	≥ $100 million, < $1 billion	2008 Tropical Storm Fay
3	≥ $1 billion, < $10 billion	2008 Hurricane Gustav
4	≥ $10 billion, < $50 billion	2011 Hurricane Irene
5	≥ $50 billion	2005 Hurricane Katrina

Initially, six different models were assessed for the best way to communicate the data, specifically location and infrastructure, to the neural network. The use of latitude and longitude for four different locations, population, and wind radii were specifically altered. Along with the performance of these models, the neural network weights on the inputs were also evaluated in order to determine a best usable network model. A single model was then selected and evaluated for varying training algorithms.

Of the six initial models, Model 3 was chosen for its low percent error, accuracy and confidence with the trial events (Hurricane Isaac and Tropical Storm Andrea), and weights that resembled what would typically be expected with excitatory connections from population and storm surge and inhibitory connection on storm center pressure. Model 3 also had a lower number of inputs, allowing the network to establish stronger connections and ease of use for the

operator. During the initial performance assessment of all six models, Model 3 had the lowest averaged percent error of 36% with a lowest reached error of 17% and standard deviation of approximately 15. Once the training algorithm was altered in the third study, Model 3's average percent error dropped to 8% with a lowest reached error of 1.5% and standard deviation of 3 for the Bayesian Regulation algorithm.

The propose of all these studies was to not only explore how a neural network would establish a pattern specifically for hurricane impact prediction, but also to build a model with the lowest possible percent error for real time use based on what was learned from these studies. These two goals tie together in that the methods that produce the lowest percent errors also say something about the hurricane impact prediction problem. The studies previously discussed indicate that while multiple variables are best for determining the level of impact for a single storm event, these variables need to be kept as concise as possible. Some variables are also more vital than others, which is why certain existing models only utilize particular parameters, such as storm surge and infrastructure type/quality, and might negate other parameters such as pressure or precipitation. The connections between these variables and the resulting economic damage was shown to be a statistical problem based on the success of the Bayesian Regulation training algorithm. Neural networks are highly capable of adjusting for all of these parameters and serve as a reliable predictive model.

4.2 Decision for Proposed Final ANN Model

The results of mainly the first study led to the selection of Model 3 for further evaluation using programming alterations. Prior to the assessment of training algorithms, this model was adjusted for 1, 5, 10, 20, 50, 100, 500, and 1000 hidden neurons as well as for various data

separations between the training, validation, and testing phases. Of the total 66 storm events, 70% are allotted to training while 15% goes to validation and testing, each. In determining the best way to divide this data, the amount allocated to each phase was altered slightly and to the point where the data was split almost evenly (35/35/30 percent separation). The data was also manually split so that the programmer determined what events went to each phase. This is done by rearranging the input events so that they are split up sequentially (instead of randomly) such that the first 70% to training and the following 15% to validation and 15% to testing. Rearranging the events allows the programmer to dictate what they would consider the best way to experience or learn these events and the associated patterns to establish for forecasting. Figure 4-1 and Figure 4-2 show how these changes affected the model's percent error (averaged of twenty data simulations).

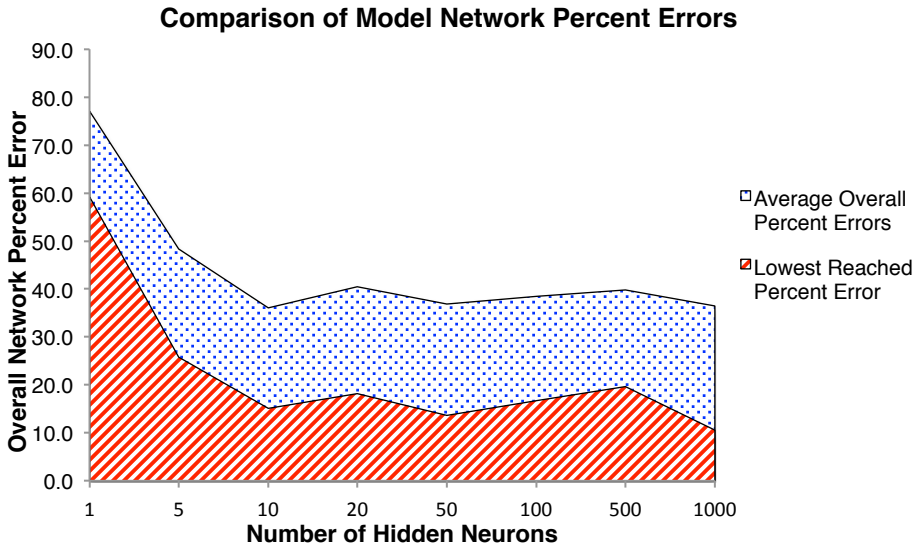

Figure 4-1 Comparison of Model 3 network percent errors with varying number of hidden neurons

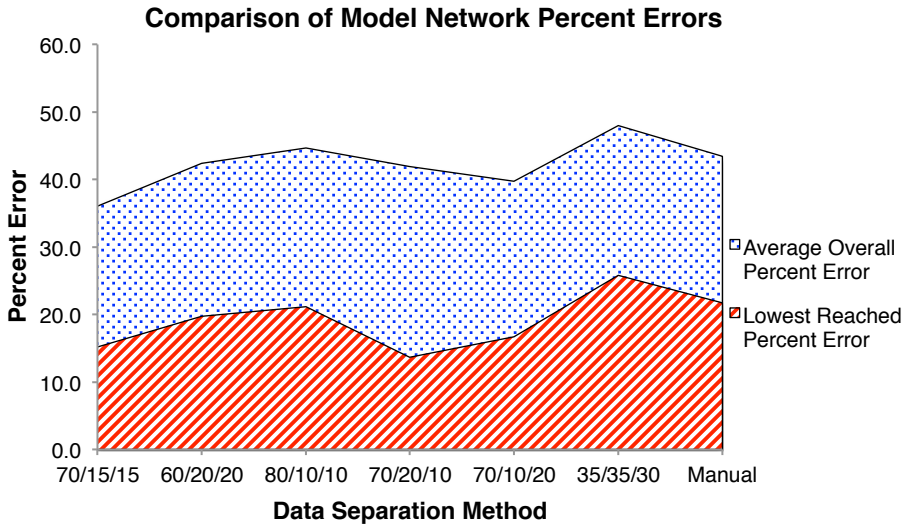

Figure 4-2 Comparison of Model 3 network percent errors with varying data separation methods

After attempting to alter these select aspects of the network, it was found that at least 10 hidden neurons were needed for best connections and that the Bayesian Regulation training algorithm, with a 85% (57 events) training and 15% (9 events) testing data separation, would produce the lowest percent error. While 1000 hidden neurons would theoretically produce enhanced results, Bayesian Regulation also has the longest performance time, indicating that simulating this algorithm with that many hidden neurons would become problematic for practical use. The small changes in data allocation did not significantly affect the resulting percent error unless the amount used during the training phase was significantly lowered. Therefore, Model 3 with 10 hidden neurons, a data allocation of 85% (57 event) used for training and 15% (9 events) for testing, and the Bayesian Regulation training algorithms is now the structure of the proposed final Hurricane Impact Level Prediction Model.

The final model network was built with these alterations and performed exceptionally well during the process. Figure 4-3 shows the model's performance as determined by the training data. Successful simulations using the Bayesian algorithm consistently produced exceptionally

low MSEs once the probabilities were correctly determined. The low MSE for the final network corresponds to a low percent error of 1.5% as shown by the confusion matrices in Figure 4-4. The training error was reduced to 0% with only a single misplaced event during testing. This misplaced event was determined to be 2006 Hurricane Ernesto, which was an Impact Level 2 event with approximately $466,000,000 (2012 USD) in damage. Incorrectly forecasted as an Impact Level 3 event (threshold to cross $1 billion), Ernesto was one of the top three costliest storms of its level. Considering the 66 possible events, incorrectly placing one event during the whole process in considered a successful model network. The placement accuracy is also show by Figure 4-5 in the form of an error histogram. The error histogram serves to show how each component of an events output matrix compared to the corresponding target matrix, i.e. how far off the network outputs were from 1 or 0. The vast majority of the output instances varied from the target by nearly zero, with the exception of the incorrectly places Hurricane Ernesto and 2004 Hurricane Gaston, which was correctly placed but not as confidently. Gaston was an Impact Level 2 event with approximately $137,000,000 (2012 USD) in economic damage. The network placed it as an Impact Level 2 with the highest value of 0.90 in the Impact Level 2 row, however, it also had a high confidence level of 0.71 for the Impact Level 1 output row; both of these values are shown in the histogram as differing by 0.09 and -0.71, respectively. Given these overall results, this final model is considered both accurate and usable.

One of the most popular uses for a pattern recognition neural network is for making medical diagnoses, for example breast cancer. MATLAB has a pre-established breast cancer data set for determining benign or malignant masses from biopsy results. For comparison of accuracy, this example was executed through the MATLAB pattern recognition toolbox (with 10 hidden neurons, 70/15/15 data separation, and scaled conjugate gradient training algorithm). The cancer

example has percent errors consistently less than 5% and MSEs in the hundredths place. By these defaults, the original six models had over double the percent errors, but the MSEs were similar. This is likely due to the fact that the cancer example has greater than 600 data scenarios. The output/target matrix also only has 2 rows: benign and malignant. Once the algorithm was changed to Bayesian Regulation for Model 3, the percent errors dropped to a similar range (standard deviation of 2.8 for the percent error of the final model) to that of the cancer example, while the MSE dropped drastically lower. Given that the cancer data set serves as a successful training example and the final adjusted model for hurricane impact prediction reached similarly low percent errors, considering the difference in available data, it is fair to conclude that the final hurricane impact prediction model has successfully established patterns between the multiple variables and a resulting economic damage level.

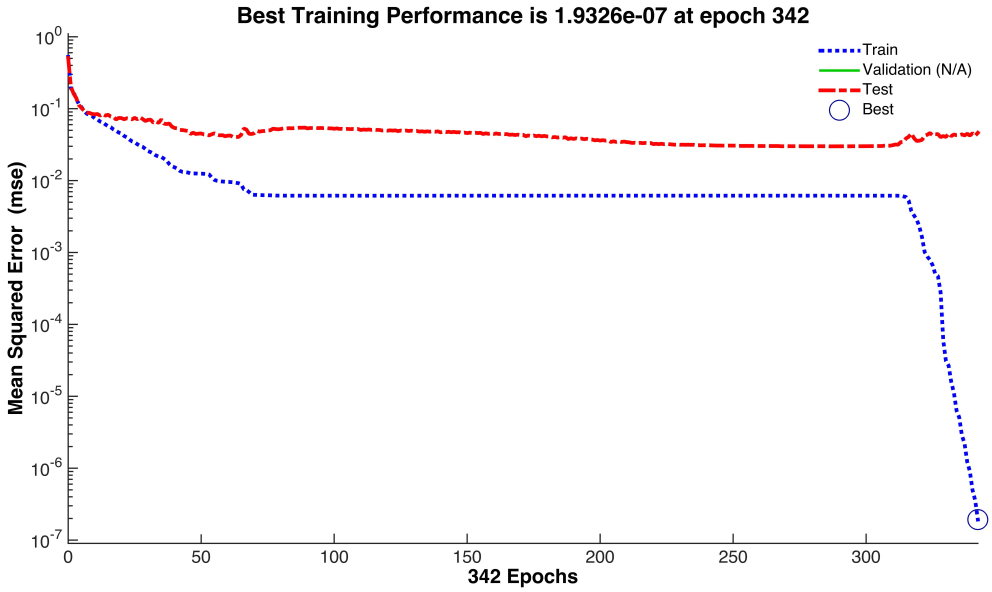

Figure 4-3 Performance of the final Hurricane Impact Level Ranking System Model

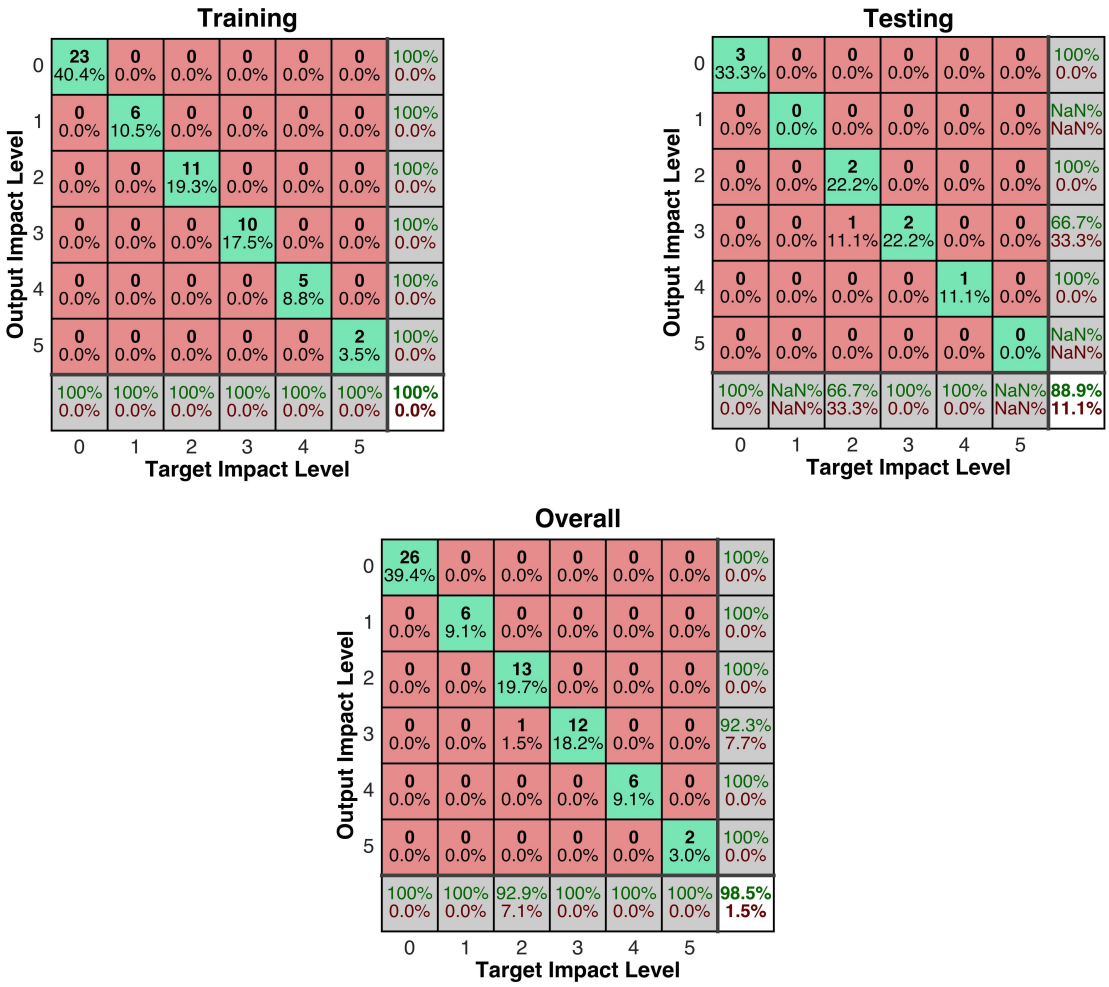

Figure 4-4 Confusion matrices for the final Hurricane Impact Level Ranking System Model

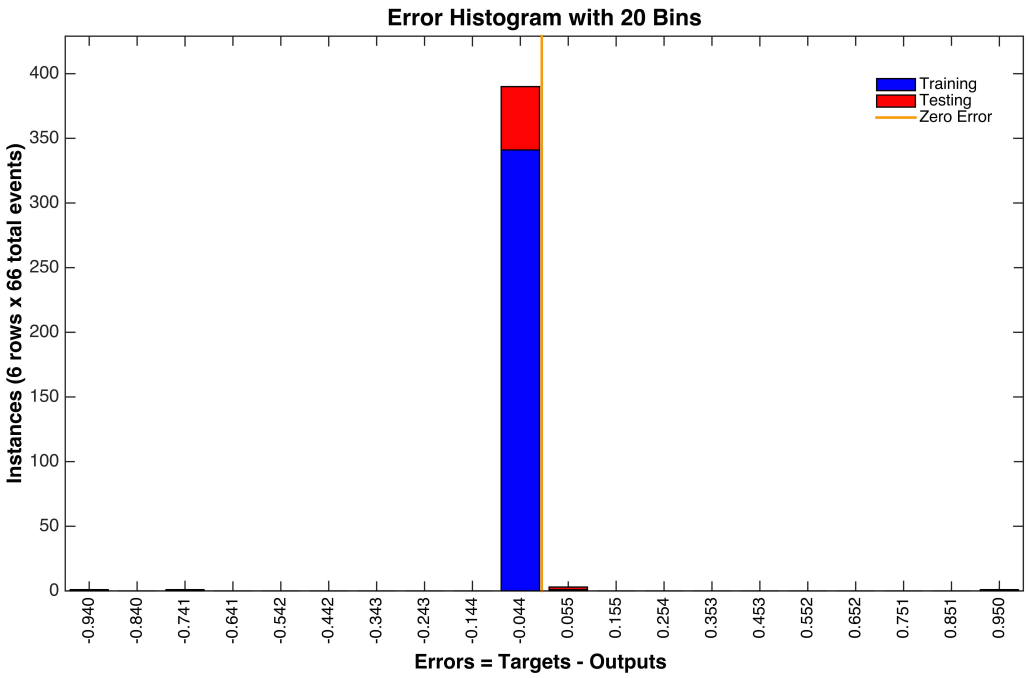

Figure 4-5 Error histogram for the final Hurricane Impact Level Ranking System Model

Once a viable network was established, the final model was conducted for 2012 Hurricane Isaac and 2013 Tropical Storm Andrea. Hurricane Isaac was an Impact Level 3 event and Tropical Storm Andrea was an Impact Level 0 event. Originally, Model 3 did produce definitive results for Hurricane Isaac (Impact Level 3 event), but borderline results for Tropical Storm Andrea (Impact Level 0 event). Once adjusted, the final model not only produced accurate results for both events but with more confidence as well. Figure 4-6 shows the initial Model 3 results in comparison with the final model results and the actual Impact Level as reference for Hurricane Isaac and Tropical Storm Andrea. Coupling these results with the network performance, the model is now considered both precise and accurate.

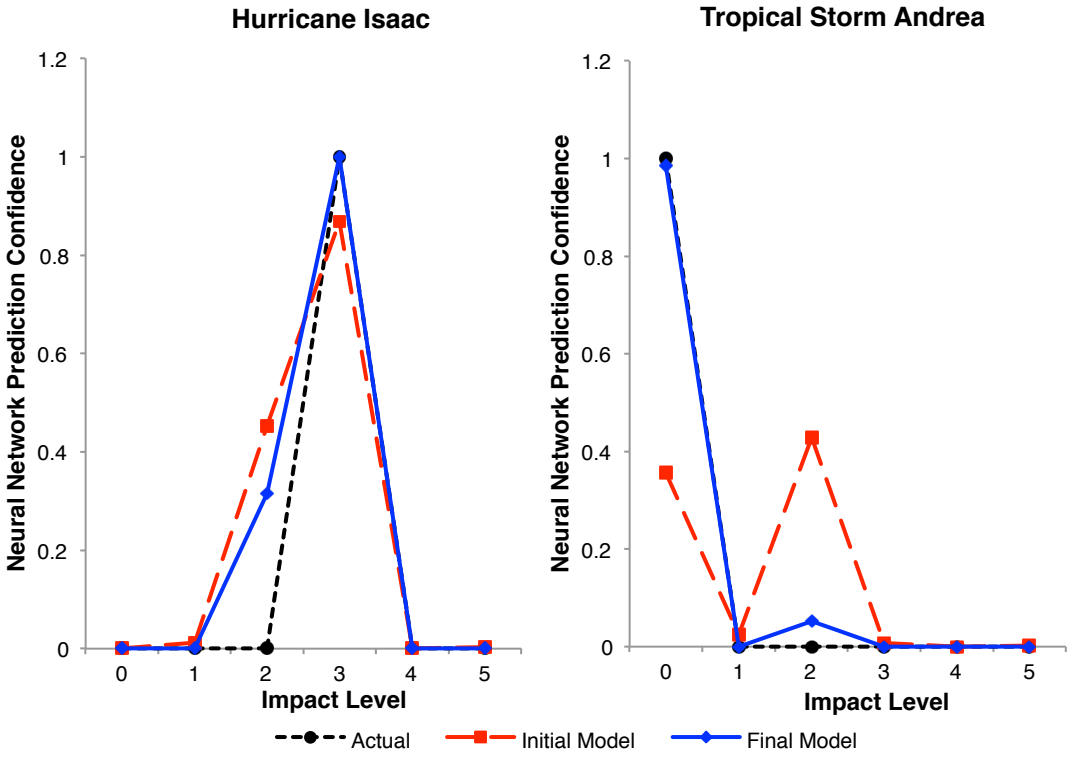

Figure 4-6 Evaluation of the final model from the initial Model 3 for Hurricane Isaac and Tropical Storm Andrea

This use of this network model would require the user to input the population affected, minimum pressure, maximum wind speed, storm surge, 24-hour precipitation, and four possible landfall locations. Given that this model focuses on tropical cyclones only making landfalls along the U.S. coastline, the landfall locations not used will default to zero within the input matrix to the network. From here, the model network will attempt to extrapolate the resulting outcome based off of its base of historical data. The network will produce an output matrix of size 6x1, which the model will interoperate to provide the user with a forecasted Impact Level.

4.3 Sources of Uncertainty

As with most research, there are limitations and possible error associated with this model. The main concern stems from the lack of data available. Most neural networks are built with hundreds of cases/events, but this network was trained with only 66 events. Once rebuilt for real time use, after this research, to include Hurricane Isaac and Tropical Storm Andrea, this model network would be based off of 68 events with the possibility to increase each season. Also, since the historical data used to train the network is only for the continental United States (CONUS), the model will only be suitable for CONUS events. Storms to hit the Caribbean or Hawaii would not be applicable in this case. The Caribbean Islands have a very different infrastructure than the U.S. and it is also very rare for a tropical cyclone to actually make landfall on the Hawaiian Islands. The amount and type of data used when building the network essentially dictates prediction capability.

Additionally, the sources of possible error within this research are mostly linked to human error. The historical and extrapolated population data were all gathered by hand. Some of this data, such as the economic damage and population, were also altered and used in the form of an estimate. The population that was extracted from makeshift tropical storm force wind radii due to lack of shapefile data at that time is also subject to additional possible human error during the process. Following the data collection, there is smaller possibility for error due to misuse/misinterpretation of the MATLAB neural network pattern recognition toolbox. This is all standard error that has a chance of occurring in any research. Due to the results produced by building and conducting trials of the final model, these errors had minimal impact on the accuracy of the final model.

CHAPTER 5

CONCLUSION AND FUTURE APPLICATIONS

5.1 Prospective Applications

The final Hurricane Impact Level Prediction Model demonstrated statistically significant results for both network performance and trial use. Given these results, this model now has the possibility to be applied for real time use. The main focus, and prospective application for this work, is to create a viable model to simulate with real time tropical cyclone events approaching the U.S. coastline. Tropical cyclones are typically well forecasted by the NWS days in advance, making them an excellent extreme weather event for this research. Tropical storm and hurricane watches are typically issued 48 hours before the onset of the anticipated conditions, while warnings are subsequently issued 36 hours in advance. However, the advisories, with the relevant data, are usually updated every six hours in the form of Public Advisories issued by the National Hurricane Center (NHC). These public advisories standardly contain the wind speed, pressure, whether or not the storm system is anticipated to strengthen, the forecasted rainfall accumulation, and forecasted storm surge in select locations. The storm surge, generated by the Sea, Lake, and Overland Surges from Hurricanes (SLOSH) model, is typically the last factor to be added to these advisories. The NHC also has a corresponding map for the storm's anticipated track and strength.

For real time use, these public advisories with the data provided by the NHC are the main source of data to enter into this model. Most of these numbers can be directly read from the advisories and applied to the model. However, for population, the given radius of tropical storm winds (also provided in the advisories and watches/warnings) and an extrapolated landfall

location from the forecast track will have to be used within a GIS system, as was previously done to gather the historical data, in order to determine an estimate for the number of people within the path. For extreme events, this step may be circumvented if the media has already advertised an estimated number of people affected. Once all this data is acquired for the forecasted landfall location, the model can be simulated almost immediately following a watch or warning, producing a corresponding forecasted Impact Level. This Impact Level can also be updated as the forecast updates.

Another possible application of the model could be analyzing worse case scenario events and possibly budgeting for an upcoming season. The model created does not need to necessarily use for an actual event, instead it could be fed parameters to illustrate the result of a hypothetical storm making landfall in New York versus Florida. While the Impact Levels consist of ranges of economic damage, this could still give an idea of the magnitude of an event. Additionally, by comparing certain hypothetical events (changing storm surge or location), emergency managers could better understand the risks at hand and establish thresholds prior to an actual event. SLOSH is already a well and rightfully used model to help emergency managers determine evacuation zones. However, with the addition of this model, managers could build upon that for the addition of parameters, such as high precipitation, not only for evacuation purposes but also for anticipated recovery efforts to include, but not limited to, supplies and response workers. Society works off of what they know, and having a comparative system using previous events could assist in understanding and communicating the anticipated overall risks.

5.2 Societal Uses and Benefits

This model and ranking system is proposed as a solution to the societal perception problems surrounding natural hazards. The Impact Level Ranking System, specifically, was simply designed to allocate storms in terms the everyday individual would understand quickly and easily. Ideally, this system would be used with the Saffir-Simpson scale in communicating a tropical cyclone event to the public. For example, 2012 Hurricane Sandy could have been designated a Category 1 Hurricane, Impact Level 5.

The use of this system in such a way could help get the message across in extremely severe events, while potentially reducing crying wolf scenarios produced by over dramatization. Impact Level 0 – 2 events are relatively minor and barely register as anything significant in society's mind. However, most storms people remember fall into the Impact Level 3 – 5 range due to their cost of damage exceeding $1 billion. These associations are how people personally weigh risks and make decisions. The one thing that would need to be kept in mind, however, is location. This system is for the event as a whole. While Hurricane Irene in 2011 caused immense damage in New England, Virginia and Maryland, which were also in its path, mainly only had down tree limbs causing some power outages. This is also why this model is best used along with the Saffir-Simpson Scale and other models used by emergency managers, such as SLOSH. In this application, the Impact Level Ranking System can provide an overall picture of the resulting outcome of a storm, while other tools can show where the focus of that impact will be, further providing society with a clear picture of the developing situation.

5.3 Future Research

The work done in this thesis is the first step in assuring the viability of this model. Before actual exposure to the public further work should be conducted as a safety precaution to cover all bases and ensure that this model is capable of accomplishing the proposed applications. Real time use, hypothetical scenarios, and a sociological study are just some possible ways to further this project.

The use of hypothetical scenarios would actually serve more as a study to assess the vulnerability of certain locations. For example, a possible hypothetical storm with the same meteorological parameters could be simulated for a landfall in the northeast versus a landfall in Florida. A scenario similar to this would help determine area vulnerability and assess the differences between two distinct locations. Additionally, a highly urbanized location could be kept constant as certain meteorological parameters are altered in order to investigate the thresholds for each Impact Level at the specified location. This same work would then be done for another location with possibly less people and some protective geographical features, such as wetlands, for evaluation of how these thresholds may change with location. There are assuredly other possible scenarios for evaluation in this sense, and the combination of these multiple assessments would aid in describing location vulnerability specifically for tropical cyclones.

It would seem most logical to simulate real time event with oncoming storms privately before using the model for communicating such events to the public. For a few hurricane seasons, this model could be simulated alongside public advisories as issued. The change in the possible outcome (Impact Level) with each advisory would be tracked for assessment of accuracy over time and in relation to the forecast accuracy. In order to accomplish this, the results will be verified with the produced TCRs published by the NHC at the end of each season, likely in

January of the following year. This work will not only help determine the viability of using this model, but how its accuracy changes with each updated forecast.

The usability of this model is mostly dependent on its accuracy in forecasting, however it also has to be determined interpretable by the general populace. The concept of a general sociological assessment, or poll, of how people within hurricane prone areas understand and react to hurricanes could imply a realistic applicability of the model. This study could introduce the model in order to gauge how the public would interpret and react to such a system. Overall, this may not be entirely necessary for use but more so for further evaluating the public's perception of such events. With the proper formatting and marketing, the Impact Level Ranking System has the potential for countrywide understanding and use.

The communication of the scientific and engineering aspects of a natural hazard event to the general public has consistently been problematic. During such events, complex interactions occur simultaneously making it difficult to communicate the overall impact to society. Using neural networks to mimic how scientists and engineers assess these interactions, the final Hurricane Impact Level Ranking System Prediction Model is capable of bridging this gap in communication by using comparative techniques to communicate the risk of an oncoming event. The potential future use of this model could affect how the weather community approaches public outreach and risk and vulnerability, leading to a more robust and inclusive categorization system.

REFERENCES

Ahrens, D. C. (2008). Essentials of Meteorology - Hurricanes. In P. Adams, A. Brady, H. Humphrey, B. Broyer, Janet Bollow Associates, & S. Kenter (Eds.), *Essentials of Meteorology: And Invitation to the Atmosphere* (Fifth Edit., pp. 299–325). Thompson Brooks/Cole.

Baker, E. J. (1991). Hurricane evacuation behavior. *International Journal of Mass Emergency Disasters*, *9*, 287–310.

Baxt, W. G. (1995). Application of artificial neural networks to clinical medicine. *The Lancet*, *346*, 1135–1138.

Blake, S., Walker, R., & Walker, R. (2011). Potable Water Issues during Disaster Response and Recovery: Lessons Learned from Recent Coastal Disasters. In *Solutions to Coastal Disasters* (pp. 779–794). Anchorage, AK: ASCE.

Blomquist, G. C. (2004). Self-protection and averting behavior, values of statistical lives, and benefit cost analysis of environmental policy. *Review of Economics of the Household*, *2*(1), 89–110.

Booth, D. B. (1991). Urbanization and the Natural Drainage System - Impacts, Solutions, and Prognoses. *The Northwest Environmental Journal*, *7*(1), 92–118.

Borden, K. A., & Cutter, S. L. (2008). Spatial patterns of natural hazards mortality in the United States. Retrieved from http://www.ij-healthgeographics.com/content/7/1/64

Bryant, E. (2005). *Natural Hazards* (Second.). Cambridge, United Kingdom: Cambridge University Press.

Buntine, W. L., & Weigend, Andreas, S. (1991). Bayesian Back-Propagation. *Complex Systems*, *5*, 603–643.

Burton, C. G. (2010). Social Vulnerability and Hurricane Impact Modeling. *Natural Hazards Review*, *11*(2), 58–68. doi:10.1061/(ASCE)1527-6988(2010)11:2(58)

Chan, S., & Revkin, A. C. (2005). Water Returned to Lake Contains Toxic Material. *The New York Times*. New York, NY.

Chen, Q., Wang, L., & Tawes, R. (2008). Hydrodynamic response of northeastern Gulf of Mexico to hurricanes. *Estuaries and Coasts*, *31*, 1098–1116.

Chisolm, E. I., & Matthews, J. C. (2012). Impact of Hurricanes and Flooding on Buried Infrastructure. *Leadership and Management in Engineering*, *12*(3), 151–156. doi:10.1061/(ASCE)LM.1943-5630.0000182

Constantinescu, R., Lazarescu, V., & Tahboub, R. (2008). Geometrical Form Recognition Using "One-Step-Secant" Algorithm in Case of Neural Network. *U.P.B. Sci. Bull., Series C*, *70*(2), 15–28.

Copeland, C. (2005). *Hurricane-Damaged Drinking Water and Wastewater Facilities: Impacts, Needs, and Response*.

Crossett, K. M., Culliton, T. J., Wiley, P. C., & Goodspeed, T. R. (2004). Population trends along the coastal United States: 1980-2008. Retrieved from http://www.oceanservice.noaa.gov/programs/mb/supp_cstl_population.html

Cutter, S. L. (1996). Vulnerability of Environmental Hazards. *Progress in Human Geography*, *20*(4), 529–539.

Cutter, S. L., Boruff, B. J., & Shirley, W. L. (2003). Social Vulnerability to Environmental Hazards. *Social Science Quarterly*, *84*(2), 242–261.

Cutter, S. L., & Emrich, C. T. (2006). Moral Hazard, Social Catastrophe: The Changing Face of Vulnerability along the Hurricane Coasts. *The ANNALS of the American Academy of Political and Social Science*, *604*(1), 102–112. doi:10.1177/0002716205285515

Dao, T., Li, Y., van de Lindt, J. W., & Bjarnadottir, S. (2013). Combined Loss due to Hurricanes and Storm Surge. In *Structures Congress* (Vol. 4, pp. 2020–2031). Pittsburgh, PA: ASCE.

Dash, N., & Gladwin, H. (2007). Evacuation Decision Making and Behavioral Responses: Individual and Household. *Natural Hazards Review*, *8*(3), 69–77.

Dawson, C. W., & Wilby, R. L. (2001). Hydrological modelling using artificial neural networks. *Progress in Physical Geography*, *25*(1), 80–108. doi:10.1177/030913330102500104

Dow, K., & Cutter, S. L. (1998). Crying Wolf: Repeat Responses to Hurricane Evacuation Orders. *Coastal Management*, *26*(4), 237–252.

Dow, K., & Cutter, S. L. (2000). Public orders and personal opinions: Household strategies for hurricane risk assessment. *Environmental Hazards*, *2*(4), 143–155.

Farber, S. (1987). The Value of Coastal Wetlands for Protection of Property against Hurricane Wind Damage. *Journal of Environmental Economics and Management*, *14*, 143–151.

FEMA. (n.d.). Disaster Declarations. Retrieved from http://www.fema.gov/disasters

Ferreira, C. (2011). Sensitivity of Hurricane Storm Surge Numerical Simulations to Wetland Parameters in Corpus Christi, TX. In *World Environmental and Water Resources Congress* (pp. 3149–3157). Palm Springs, California: ASCE.

Gavin, H. P. (2013). *The Levenberg-Marquardt method for nonlinear least squares curve-fitting problems*. Durham, NC.

Google Map Data. (2015). Google Maps. Retrieved February 23, 2015, from https://www.google.com/maps/@30.9733766,-91.4299096,8z

Hall, S. G., & Ashley, W. S. (2008). Effects of Urban Sprawl on the Vulnerability to a Significant Tornado Impact in Northeastern Illinois. *Natural Hazards Review*, *9*(November), 209–219.

Hamid, S. S., Pinelli, J., Chen, S., & Gurley, K. (2011). Catastrophe Model-Based Assessment of Hurricane Risk and Estimates of Potential Insured Losses for the State of Florida. *Natural Hazards Review*, *12*(4), 171–176. doi:10.1061/(ASCE)NH.1527-6996.0000050.

Hecht-Nielsen, R. (1988). Neurocomputing: picking the human brain. *IEEE Spectrum*, (March), 36 –41.

Henk, R. H., Ballard, A. J., Robideau, R. L., Peacock, W. G., Maghelal, P., Lindell, M. K., … Boxil, S. (2007). Disaster Preparedness in Texas. College Station, TX: Texas Transportation Institute.

Herseth, A., & Ashley, E. (2013). *FEMA Mitigation Assessment Team Program: Observations and Recommendations Since Hurricane Andrew*. Retrieved from http://www.digitalhurricane.org/

Holmes, J. D., & Syme, M. J. (1994). Wind Loads on steel-framed low-rise buildings. *Steel Construction (Australian Institute of Steel Construction)*, *28*, 2–12.

Kaufman, S., Qing, C., Levenson, N., & Hanson, M. (2012). *Transportation During and After Hurricane Sandy*. New York, NY.

Kwasinski, A., Weaver, W. W., Chapman, P. L., & Krein, P. T. (2009). Telecommunications Power Plant Damage Assessment for Hurricane Katrina – Site Survey and Follow-Up Results. *IEEE Systems Journal*, *3*(3), 277–287.

Li, Y., van de Lindt, J. W., Dao, T., Bjarnadottir, S., & Ahuja, A. (2012). Loss Analysis for Combined Wind and Surge in Hurricanes. *Natural Hazards Review*, *13*(1), 1–10. doi:10.1061/(ASCE)NH.1527-6996.0000058.

Lu Dang Khoa, N., Sakakibara, K., & Nishikawa, I. (2006). Stock Price Forecasting using Back Propagation Neural Networks with Time and Profit Based Adjusted Weight Factors. In *SICE-ICASE International Joint Conference* (pp. 5484–5488). Bexco, Busan, Korea.

Lwin, M. M., Yen, W. P., & Shen, J. J. (2014). Effects of Hurricane Katrina on the Performance of U.S. Highway Bridges. *Journal of Performance of Constructed Facilities*, *28*(1), 40–48. doi:10.1061/(ASCE)CF.1943-5509.0000507

MathWorks. (2015). Gradient descent with adaptive learning rate backpropagation. Retrieved February 1, 2015, from http://www.mathworks.com/help/nnet/ref/traingda.html

Mileti, D., & Beck, E. M. (1975). Communication in crisis: Explaining evacuation symbolically. *Communication Res.*, *2*(1), 24–49.

Møller, M. F. (1993). A Scaled Conjugate Gradient Algorithm for Fast Supervised Learning. *Neural Networks*, *6*, 525–533. doi:10.1016/S0893-6080(05)80056-5

Morton, R. A. (2007). *HISTORICAL CHANGES IN THE MISSISSIPPI-ALABAMA BARRIER ISLANDS AND THE ROLES OF EXTREME STORMS, SEA LEVEL, AND HUMAN ACTIVITIES*. St. Petersburg, FL.

National Hurricane Center. (2012). Hurricanes in History. Retrieved from http://www.nhc.noaa.gov/outreach/history/

National Hurricane Center (NHC). (2014). Glossary of NHC Terms. Retrieved from http://www.nhc.noaa.gov/aboutgloss.shtml#r

National Oceanic and Atmospheric Administration. (2009). Historical hurricane data. Retrieved from http://www.noaa.gov

National Oceanic and Atmospheric Administration (NOAA). (2005). Hurricane Katrina. Retrieved from http://www.britannica.com/EBchecked/topic/1087226/Hurricane-Katrina

National Oceanic and Atmospheric Administration (NOAA), & National Hurricane Center (NHC). (2012). 2012 Tropical Cyclone Advisory Archive. Retrieved from http://www.nhc.noaa.gov/archive/2012/

National Oceanic and Atmospheric Administration (NOAA), & National Hurricane Center (NHC). (2014a). NHC Data Archive: Tropical Cyclone Reports. Retrieved from http://www.nhc.noaa.gov/data/#tcr

National Oceanic and Atmospheric Administration (NOAA), & National Hurricane Center (NHC). (2014b). NHC GIS Archive - Tropical Cyclone Best Track. Retrieved from http://www.nhc.noaa.gov/gis/archive_besttrack.php

National Resources Defense Council (NRDC). (2005). After Katrina: New Solutions for Safe Communities and a Secure Energy Future.

Neal, R. M. (1992). *Bayesian Training of Backpropagation Networks by the Hybrid Monte Carlo Method*. *Tech. Rep. CRG-TR-92-1*. Toronto, Ontario, Canada.

Nicholls, R. J., & Small, C. (2002). Improved Estimates of Coastal Population and Exposure to Hazards Released. *Eos*, *83*(28), 301–305.

Nirupama, N. (2013). Is it possible to rank hurricanes in a unique manner? *Natural Hazards*, *67*(2), 963–968. doi:10.1007/s11069-013-0560-y

Peters, G., DiGioia, A M, J., Hendrickson, C., & Apt, J. (2007). Transmission Line Reliability: Climate Change and Extreme Weather. *Electrical Transmission Line and Substation Structures*, 12–26.

Pielke Jr., R. A., Gratz, J., Landsea, C. W., Collins, D., Saunders, M. A., & Musulin, R. (2008). Normalized Hurricane Damage in the United States: 1900-2005. *Natural Hazards Review*, *9*(1), 29–42.

Pinelli, J., Pita, G., Gurley, K., Torkian, B., Hamid, S., & Subramanian, C. (2011). Damage Characterization : Application to Florida Public Hurricane Loss Model. *Natural Hazards Review*, *12*(4), 190–195. doi:10.1061/(ASCE)NH.1527-6996.0000051.

Rauber, R. M., Walsh, J. E., & Charlevoix, D. J. (2008). Severe & Hazardous Weather - Hurricanes. In G. Botsford, L. Rogers, C. McMurray, & R. Hortsman (Eds.), *Severe & Hazardous Weather: An Introdution to Meteorology* (Third Edit., pp. 463–498). Kendal/Hunt Publishing Company.

Renn, O., Burns, W. J., Kasperson, J. X., Kasperson, R. E., & Slovic, P. (1992). The social amplification or risk: Theoretical foundations and empirical applications. *Journal of Social Issues*, *48*(4), 137–160.

Sarle, W. S. (1994). Neural Networks and Statistical Models. In *Ninteenth Annual SAS Users Group Conference* (pp. 1–13). Cary, NC.

Schneider, P. J., & Schauer, B. a. (2006). HAZUS—Its Development and Its Future. *Natural Hazards Review*, *7*(2), 40–44. doi:10.1061/(ASCE)1527-6988(2006)7:2(40)

Shamseldin, A. Y. (1997). Application of a neural network technique to rainfall-runoff modelling. *Journal of Hydrology*, *199*, 272–294. doi:10.1016/S0022-1694(96)03330-6

Simmons, K. M., & Sutter, D. (2005). Protection from nature's fury: Analysis of fatalities and injuries from F5 tornadoes. *Natural Hazards Review*, *6*(2), 82–87.

Smith, A. B., & Katz, R. W. (2013). U. S. Billion-dollar Weather and Climate Disasters: Data Sources, Trends, Accuracy and Biases. *Natural Hazards*, *67*(2), 387–410.

Sorensen, J. H. (2000). Hazard Warning Systems: Review of 20 Years of Progress. *Natural Hazards Review*, *1*(2), 119–125.

Stearns, M., & Padgett, J. E. (2012). Impact of 2008 Hurricane Ike on Bridge Infrastructure in the Houston/Galveston Region. *Journal of Performance of Constructed Facilities*, *26*(August), 441–452. doi:10.1061/(ASCE)CF.1943-5509.0000213.

Stein, R. M., Dueñas-Osorio, L., & Subramanian, D. (2010). Who evacuates when hurricanes approach? The role of risk, information, and location. *Social Science Quarterly*, *91*(3), 816–34. Retrieved from http://www.ncbi.nlm.nih.gov/pubmed/20645467

Stenabaugh, S. E., & Kopp, G. A. (2012). Failure vs . Flight : An experimental study of wind speeds associated with roof failures of houses. *Forensic Engineering*, *9*, 851–860.

Svozil, D., Kvasnieka, V., & Pospichal, J. (1997). Introduction to multi-layer feed-forward neural networks. *Chemometrics and Intelligent Laboratory Systems*, *39*, 43–62.

Syvitski, J. P. M., Kettner, A. J., Overeem, I., Hutton, E. W. H., Hannon, M. T., Brakenridge, G. R., … Nicholls, R. J. (2009). Sinking deltas due to human activities. *Nature Geoscience*, *2*(10), 681–686. doi:10.1038/ngeo629

Tansel, B., & Sizirici, B. (2011). Significance of Historical Hurricane Activity on Structural Damage Profile and Posthurricane Population Fluctuation in South Florida Urban Areas. *Natural Hazards Review*, *12*(4), 196–201. doi:10.1061/(ASCE)NH.1527-6996.0000045.

U.S. Census Bureau. (2010). Construction Price Indexes. Retrieved from https://www.census.gov/construction/cpi/

U.S. Census Bureau. (2014). Geography - TIGER Products. Retrieved from https://www.census.gov/geo/maps-data/data/tiger.html

U.S. Department of Commerce. (2013). U.S. Census Bureau State & County QuickFacts. Retrieved from http://quickfacts.census.gov/qfd/index.html#

Unanwa, C. O., & McDonald, J. R. (2000). Building Wind Damage Prediction and Mitigation Using Damage Bands. *Natural Hazards Review*, *1*(November), 197–203.

Vickery, P. J., Lin, J., Skerlj, P. F., Twisdale, Lawrence A, J., & Huang, K. (2006). HAZUS-MH Hurricane Model Methodology. I : Hurricane Hazard, Terrain, and Wind Load Modeling. *Natural Hazards Review*, *7*(2), 82–93.

Vickery, P. J., Skerlj, P. F., Lin, J., Twisdale, Lawrence A, J., Young, M. A., & Lavelle, F. M. (2006). HAZUS-MH Hurricane Model Methodology. II : Damage and Loss Estimation. *Natural Hazards Review*, *7*(2), 94–103.

Wamsley, T. V., Cialone, M. a., Smith, J. M., Atkinson, J. H., & Rosati, J. D. (2010). The potential of wetlands in reducing storm surge. *Ocean Engineering*, *37*(1), 59–68. doi:10.1016/j.oceaneng.2009.07.018

Werbos, P. J. (1990). Backpropagation Through Time : What It Does and How to Do It. *Proceedings of the IEEE*, *78*(October), 1550–1560.

White, H. (1989). Learning in Artificial Neural Networks : A Statistical Perspective. *Neural Computation Massachusetts Institute of Technology*, *1*, 425–464.

Widrow, B., Rumelhart, D. E., & Lehr, M. A. (1994). Neural Networls: Applications in Industry, Business and Science. *Communications of the ACM*, *37*(3), 93–105.

Willoughby, H. E., Rappaport, E. N., & Marks, F. D. (2007). Hurricane Forecasting: The State of the Art. *Natural Hazards Review*, *8*(3), 45–49.

Yao, J. T., & Tan, C. L. (2000). Time dependent directional profit model for financial time series forecasting. In *Proceeding of the IJCNN* (pp. 291–296). Como, Italy.

Yau, S. C., Lin, N., & Vanmarcke, E. (2011). Hurricane Damage and Loss Estimation Using an Integrated Vulnerability Model. *Natural Hazards Review*, *12*(November), 184–189. doi:10.1061/(ASCE)NH.1527-6996.0000035.

Zhong, L., Li, M., & Zhang, D.-L. (2010). How do uncertainties in hurricane model forecasts affect storm surge predictions in a semi-enclosed bay? *Estuarine, Coastal and Shelf Science*, *90*(2), 61–72. doi:10.1016/j.ecss.2010.07.001

APPENDIX A

TABLE OF HISTORICAL HURRICANE DATA

		2013	2012			
		TS. Andrea	H. Sandy	H. Issac	TS. Debby	TS. Beryl
	Population Affected	9,000,000	17,000,000	5,600,000	9,000,000	5,200,000
First Landfall Location	Latitude (deg. North)	29.5	39.4	29.2	29.3	30.2
	Longitude (deg. West)	83.4	74.4	90.2	83.2	81.4
	Pressure (mbar)	992	945	966	995	994
	Wind Speed (mph)	57.5	80.5	80.5	40.25	63.25
	TS Force Wind Radius (miles)	140	485	185	175	115
	Storm Surge (feet)	4.55	12.65	11.03	4.5	2.93
	Precipitation (inches)	15.28	12.83	26.71	28.78	15
Second Landfall Location	Latitude (deg. North)					
	Longitude (deg. West)					
	Pressure (mbar)					
	Wind Speed (mph)					
	TS Force Wind Radius (miles)					
	Storm Surge (feet)					
	Precipitation (inches)					
Third Landfall Location	Latitude (deg. North)					
	Longitude (deg. West)					
	Pressure (mbar)					
	Wind Speed (mph)					
	TS Force Wind Radius (miles)					
	Storm Surge (feet)					
	Precipitation (inches)					
Fourth Landfall Location	Latitude (deg. North)					
	Longitude (deg. West)					
	Pressure (mbar)					
	Wind Speed (mph)					
	TS Force Wind Radius (miles)					
	Storm Surge (feet)					
	Precipitation (inches)					
	Economic Damage (2012 USD)		$50,000,000,000.00	$2,350,000,000.00	$250,000,000.00	$25,000,000.00
	Impact Level	**0**	**5**	**3**	**2**	**0**

TS = Tropical Storm

H = Hurricane

Blank = Not Reported (default to 0)

		2011			2010	
		TS. Lee	H. Irene	TS. Don	TS. Bonnie	TS. Hermine
	Population Affected	7,000,000	60,000,000	24,000	5,600,000	1,600,000
First Landfall Location	Latitude (deg. North)	29.6	34.7	27.3	25.4	25.3
	Longitude (deg. West)	92.1	76.6	97.4	80.2	97.4
	Pressure (mbar)	986	952	1007	1007	989
	Wind Speed (mph)	46	86.25	34.5	40.25	69
	TS Force Wind Radius (miles)	275	260	105	85	105
	Storm Surge (feet)	4.67	7.09	1.89	0.92	3.4
	Precipitation (inches)	15.48	15.74	2.56	3.25	16.37
Second Landfall Location	Latitude (deg. North)		39.4			
	Longitude (deg. West)		74.4			
	Pressure (mbar)		959			
	Wind Speed (mph)		69			
	TS Force Wind Radius (miles)		320			
	Storm Surge (feet)		4.63			
	Precipitation (inches)		11.68			
Third Landfall Location	Latitude (deg. North)		40.6			
	Longitude (deg. West)		74			
	Pressure (mbar)		965			
	Wind Speed (mph)		63.25			
	TS Force Wind Radius (miles)		320			
	Storm Surge (feet)		4.65			
	Precipitation (inches)		11.48			
Fourth Landfall Location	Latitude (deg. North)					
	Longitude (deg. West)					
	Pressure (mbar)					
	Wind Speed (mph)					
	TS Force Wind Radius (miles)					
	Storm Surge (feet)					
	Precipitation (inches)					
	Economic Damage (2012 USD)	$326,023,329.80	$16,352,916,224.81	0		$246,568,421.05
	Impact Level	**2**	**4**	**0**	**0**	**2**

TS = Tropical Storm

H = Hurricane

Blank = Not Reported (default to 0)

		2009		2008		
		TS. Claudette	H. Ida	H. Dolly	TS. Edouard	TS. Fay
	Population Affected	521,000	3,400,000	2,000,000	5,000,000	15,000,000
First Landfall Location	Latitude (deg. North)	30.4	30.3	26.4	29.6	24.5
	Longitude (deg. West)	86.5	88	97.2	94.2	81.8
	Pressure (mbar)	1005	999	967	996	998
	Wind Speed (mph)	46	40.25	86.25	63.25	57.5
	TS Force Wind Radius (miles)	70	175	140	70	115
	Storm Surge (feet)	3	6.53	4	3.92	1.13
	Precipitation (inches)	4.66		15	6.48	7.02
Second Landfall Location	Latitude (deg. North)					25.9
	Longitude (deg. West)					81.6
	Pressure (mbar)					991
	Wind Speed (mph)					63.25
	TS Force Wind Radius (miles)					125
	Storm Surge (feet)					1.29
	Precipitation (inches)					13.82
Third Landfall Location	Latitude (deg. North)					29.3
	Longitude (deg. West)					81.1
	Pressure (mbar)					993
	Wind Speed (mph)					63.25
	TS Force Wind Radius (miles)					150
	Storm Surge (feet)					3.96
	Precipitation (inches)					27.65
Fourth Landfall Location	Latitude (deg. North)					29.8
	Longitude (deg. West)					84.7
	Pressure (mbar)					997
	Wind Speed (mph)					51.75
	TS Force Wind Radius (miles)					90
	Storm Surge (feet)					
	Precipitation (inches)					27.5
	Economic Damage (2012 USD)			$1,029,949,748.74		$549,306,532.66
	Impact Level	**0**	**0**	**3**	**0**	**2**

TS = Tropical Storm

H = Hurricane

Blank = Not Reported (default to 0)

		2008			2007	
		H. Gustav	H. Hanna	H. Ike	TS. Barry	TS. Erin
	Population Affected	5,400,000	7,600,000	11,200,000	4,000,000	743,000
First Landfall Location	Latitude (deg. North)	29.2	33.8	29.3	27.5	28
	Longitude (deg. West)	90.7	78.7	94.7	82.7	96.9
	Pressure (mbar)	954	981	950	1000	1006
	Wind Speed (mph)	103.5	69	109.25	34.5	34.5
	TS Force Wind Radius (miles)	200	260	275	90	85
	Storm Surge (feet)	12.5	5	12.79		3.1
	Precipitation (inches)	21	9.65	14.46	8	12.81
Second Landfall Location	Latitude (deg. North)					
	Longitude (deg. West)					
	Pressure (mbar)					
	Wind Speed (mph)					
	TS Force Wind Radius (miles)					
	Storm Surge (feet)					
	Precipitation (inches)					
Third Landfall Location	Latitude (deg. North)					
	Longitude (deg. West)					
	Pressure (mbar)					
	Wind Speed (mph)					
	TS Force Wind Radius (miles)					
	Storm Surge (feet)					
	Precipitation (inches)					
Fourth Landfall Location	Latitude (deg. North)					
	Longitude (deg. West)					
	Pressure (mbar)					
	Wind Speed (mph)					
	TS Force Wind Radius (miles)					
	Storm Surge (feet)					
	Precipitation (inches)					
	Economic Damage (2012 USD)	$4,217,889,447.24	$156,944,723.62	$28,956,301,507.54		
	Impact Level	**3**	**2**	**4**	**0**	**0**

TS = Tropical Storm

H = Hurricane

Blank = Not Reported (default to 0)

		2007		2006		
		TS. Gabrielle	H. Humberto	TS. Alberto	TS. Beryl	H. Ernesto
	Population Affected	6,000	982,000	3,400,000	1,300,000	8,600,000
First Landfall Location	Latitude (deg. North)	34.8	29.6	29.9	41.3	24.9
	Longitude (deg. West)	76.4	94.3	83.7	70.1	80.6
	Pressure (mbar)	1005	985	998	1000	1003
	Wind Speed (mph)	57.5	92	46	51.75	46
	TS Force Wind Radius (miles)	45	60	115	105	105
	Storm Surge (feet)		2.82	4.09	0.9	
	Precipitation (inches)	9.03	14.13	7.08	0.33	8.72
Second Landfall Location	Latitude (deg. North)					33.9
	Longitude (deg. West)					78.1
	Pressure (mbar)					985
	Wind Speed (mph)					69
	TS Force Wind Radius (miles)					105
	Storm Surge (feet)					3
	Precipitation (inches)					14.61
Third Landfall Location	Latitude (deg. North)					
	Longitude (deg. West)					
	Pressure (mbar)					
	Wind Speed (mph)					
	TS Force Wind Radius (miles)					145
	Storm Surge (feet)					
	Precipitation (inches)					
Fourth Landfall Location	Latitude (deg. North)					
	Longitude (deg. West)					
	Pressure (mbar)					
	Wind Speed (mph)					
	TS Force Wind Radius (miles)					
	Storm Surge (feet)					
	Precipitation (inches)					
	Economic Damage (2012 USD)		$46,520,495.71			$466,093,600.76
	Impact Level	**0**	**1**	**0**	**0**	**2**

TS = Tropical Storm

H = Hurricane

Blank = Not Reported (default to 0)

		2005				
		TS. Arlene	H. Cindy	H. Dennis	H. Katrina	H. Rita
	Population Affected	3,000,000	2,200,000	7,400,000	15,000,000	9,600,000
First Landfall Location	Latitude (deg. North)	30.3	29.2	30.4	26	29.7
	Longitude (deg. West)	87.5	90.1	87.1	80.1	93.7
	Pressure (mbar)	991	991	946	984	937
	Wind Speed (mph)	57.5	74.75	120.75	80.5	115
	TS Force Wind Radius (miles)	150	105	230	80	205
	Storm Surge (feet)	5	5.5	6.94	5	11.95
	Precipitation (inches)	6.77	7.56	7.67	14.04	16
Second Landfall Location	Latitude (deg. North)		30.2		30.2	
	Longitude (deg. West)		89.5		89.6	
	Pressure (mbar)		995		920	
	Wind Speed (mph)		51.75		126.5	
	TS Force Wind Radius (miles)		105		230	
	Storm Surge (feet)		6.2		27.8	
	Precipitation (inches)		9.06		14.92	
Third Landfall Location	Latitude (deg. North)					
	Longitude (deg. West)					
	Pressure (mbar)					
	Wind Speed (mph)					
	TS Force Wind Radius (miles)				230	
	Storm Surge (feet)					
	Precipitation (inches)					
Fourth Landfall Location	Latitude (deg. North)					
	Longitude (deg. West)					
	Pressure (mbar)					
	Wind Speed (mph)					
	TS Force Wind Radius (miles)					
	Storm Surge (feet)					
	Precipitation (inches)					
	Economic Damage (2012 USD)		$312,320,000.00	$2,176,480,000.00	$105,408,000,000.00	$11,748,112,000.00
	Impact Level	**0**	**2**	**3**	**5**	**4**

TS = Tropical Storm

H = Hurricane

Blank = Not Reported (default to 0)

		2005		2004		
		TS. Tammy	H. Wilma	TS. Bonnie	H. Charley	H. Frances
	Population Affected	9,600,000	14,200,000	529,000	12,400,000	15,800,000
First Landfall Location	Latitude (deg. North)	30.4	25.9	29.6	26.6	27.2
	Longitude (deg. West)	81.4	81.7	85.1	82.2	80.2
	Pressure (mbar)	1002	950	1001	941	960
	Wind Speed (mph)	51.75	120.75	63.25	149.5	103.5
	TS Force Wind Radius (miles)	260	230	70	105	200
	Storm Surge (feet)	4.2	7	1.9	1.61	5.89
	Precipitation (inches)	9.93	10.78	3.22	5.2	15.84
Second Landfall Location	Latitude (deg. North)				33	30.1
	Longitude (deg. West)				79.4	84
	Pressure (mbar)				992	982
	Wind Speed (mph)				80.5	57.5
	TS Force Wind Radius (miles)				115	85
	Storm Surge (feet)				0.68	2.06
	Precipitation (inches)				5.05	18.07
Third Landfall Location	Latitude (deg. North)					
	Longitude (deg. West)					
	Pressure (mbar)					
	Wind Speed (mph)					
	TS Force Wind Radius (miles)				115	
	Storm Surge (feet)					
	Precipitation (inches)					
Fourth Landfall Location	Latitude (deg. North)					
	Longitude (deg. West)					
	Pressure (mbar)					
	Wind Speed (mph)					
	TS Force Wind Radius (miles)					
	Storm Surge (feet)					
	Precipitation (inches)					
	Economic Damage (2012 USD)		$20,105,600,000.00		$15,894,706,896.55	$9,465,517,241.38
	Impact Level	**0**	**4**	**0**	**4**	**3**

TS = Tropical Storm

H = Hurricane

Blank = Not Reported (default to 0)

		2004				
		H. Gaston	TS. Hermine	H. Ivan	H. Jeanne	TS. Matthew
	Population Affected	1,100,000	773,000	11,300,000	14,800,000	2,900,000
First Landfall Location	Latitude (deg. North)	33	41.5	30.2	27.2	29.2
	Longitude (deg. West)	79.6	70.9	87.9	80.2	91
	Pressure (mbar)	985	1011	946	950	999
	Wind Speed (mph)	74.75	40.25	120.75	120.75	40.25
	TS Force Wind Radius (miles)	60	45	290	205	115
	Storm Surge (feet)	4.5		12.5	3.8	5.85
	Precipitation (inches)	12.6	0.5	15.79	11.97	16.23
Second Landfall Location	Latitude (deg. North)			29.8		
	Longitude (deg. West)			93.6		
	Pressure (mbar)			1004		
	Wind Speed (mph)			34.5		
	TS Force Wind Radius (miles)			60		
	Storm Surge (feet)			3.4		
	Precipitation (inches)			17		
Third Landfall Location	Latitude (deg. North)					
	Longitude (deg. West)					
	Pressure (mbar)					
	Wind Speed (mph)					
	TS Force Wind Radius (miles)					
	Storm Surge (feet)					
	Precipitation (inches)					
Fourth Landfall Location	Latitude (deg. North)					
	Longitude (deg. West)					
	Pressure (mbar)					
	Wind Speed (mph)					
	TS Force Wind Radius (miles)					
	Storm Surge (feet)					
	Precipitation (inches)					
	Economic Damage (2012 USD)	$136,724,137.93		$14,934,482,758.62	$7,256,896,551.72	
	Impact Level	**2**	**0**	**4**	**3**	**0**

TS = Tropical Storm

H = Hurricane

Blank = Not Reported (default to 0)

		2003				2002
		TS. Bill	H. Claudette	TS. Grace	H. Isabel	TS. Bertha
	Population Affected	2,900,000	5,000,000	7,100,000	21,300,000	58,000
First Landfall Location	Latitude (deg. North)	29.3	28.3	29	34.9	29.4
	Longitude (deg. West)	91	96.2	95.1	76.2	89.3
	Pressure (mbar)	997	979	1007	957	1008
	Wind Speed (mph)	57.5	92	40.25	103.5	40.25
	TS Force Wind Radius (miles)	145	140	205	345	60
	Storm Surge (feet)	5.54	5.28		10.6	
	Precipitation (inches)	6.26	4.67	7.94	20.2	2.12
Second Landfall Location	Latitude (deg. North)					
	Longitude (deg. West)					
	Pressure (mbar)					
	Wind Speed (mph)					
	TS Force Wind Radius (miles)					N/A
	Storm Surge (feet)					
	Precipitation (inches)					
Third Landfall Location	Latitude (deg. North)					
	Longitude (deg. West)					
	Pressure (mbar)					
	Wind Speed (mph)					
	TS Force Wind Radius (miles)					
	Storm Surge (feet)					
	Precipitation (inches)					
Fourth Landfall Location	Latitude (deg. North)					
	Longitude (deg. West)					
	Pressure (mbar)					
	Wind Speed (mph)					
	TS Force Wind Radius (miles)					
	Storm Surge (feet)					
	Precipitation (inches)					
	Economic Damage (2012 USD)	$56,744,186.05	$204,279,069.77		$3,824,558,139.53	
	Impact Level	**1**	**2**	**0**	**3**	**0**

TS = Tropical Storm
H = Hurricane
Blank = Not Reported (default to 0)

		2002				
		TS. Edouard	TS. Fay	TS. Hanna	H. Isidore	H. Kyle
	Population Affected	4,800,000	8,900,000	2,400,000	10,300,000	1,300,000
First Landfall Location	Latitude (deg. North)	29.4	28.5	29.1	29.1	33
	Longitude (deg. West)	81.1	96.3	89.1	90.3	79.5
	Pressure (mbar)	1009	999	1003	984	1011
	Wind Speed (mph)	40.25	57.5	57.5	63.25	40.25
	TS Force Wind Radius (miles)	85	140	145	345	45
	Storm Surge (feet)				8.3	2.1
	Precipitation (inches)	5	17.29	15.56	11.9	6.35
Second Landfall Location	Latitude (deg. North)					33.9
	Longitude (deg. West)					78.4
	Pressure (mbar)					1011
	Wind Speed (mph)					40.25
	TS Force Wind Radius (miles)					45
	Storm Surge (feet)					0.5
	Precipitation (inches)					5.6
Third Landfall Location	Latitude (deg. North)					
	Longitude (deg. West)					
	Pressure (mbar)					
	Wind Speed (mph)					
	TS Force Wind Radius (miles)					
	Storm Surge (feet)					
	Precipitation (inches)					
Fourth Landfall Location	Latitude (deg. North)					
	Longitude (deg. West)					
	Pressure (mbar)					
	Wind Speed (mph)					
	TS Force Wind Radius (miles)					
	Storm Surge (feet)					
	Precipitation (inches)					
	Economic Damage (2012 USD)			$23,980,343.98	$395,675,675.68	$5,995,086.00
	Impact Level	**0**	**0**	**0**	**2**	**0**

TS = Tropical Storm

H = Hurricane

Blank = Not Reported (default to 0)

		2002	2001			2000
		H. Lili	TS. Allison	TS. Barry	H. Gabrielle	H. Gordon
	Population Affected	4,300,000	8,700,000	2,300,000	9,300,000	4,200,000
First Landfall Location	Latitude (deg. North)	29.5	28.9	30.4	27.1	29.3
	Longitude (deg. West)	92.2	95.3	86.3	82.6	83.2
	Pressure (mbar)	963	1003	990	983	991
	Wind Speed (mph)	92	51.75	69	69	63.25
	TS Force Wind Radius (miles)	195	200	140	145	105
	Storm Surge (feet)		2.5		5.1	
	Precipitation (inches)	8.57	36.99	8.91	13.6	4.83
Second Landfall Location	Latitude (deg. North)		29.6			
	Longitude (deg. West)		91.6			
	Pressure (mbar)		1004			
	Wind Speed (mph)		34.5			
	TS Force Wind Radius (miles)		N/A			
	Storm Surge (feet)		2.5			
	Precipitation (inches)		29.86			
Third Landfall Location	Latitude (deg. North)					
	Longitude (deg. West)					
	Pressure (mbar)					
	Wind Speed (mph)					
	TS Force Wind Radius (miles)					
	Storm Surge (feet)					
	Precipitation (inches)					
Fourth Landfall Location	Latitude (deg. North)					
	Longitude (deg. West)					
	Pressure (mbar)					
	Wind Speed (mph)					
	TS Force Wind Radius (miles)					
	Storm Surge (feet)					
	Precipitation (inches)					
	Economic Damage (2012 USD)	$1,031,154,791.15	$6,264,441,591.78	$37,586,649.55	$288,164,313.22	$13,942,857.14
	Impact Level	**3**	**3**	**1**	**2**	**0**

TS = Tropical Storm

H = Hurricane

Blank = Not Reported (default to 0)

		2000	1999			
		TS. Helene	H. Bret	H. Dennis	H. Floyd	TS. Harvey
	Population Affected	1,400,000	1,500,000	2,300,000	6,000,000	6,800,000
First Landfall Location	Latitude (deg. North)	30.5	26.9	34.8	33.8	25.9
	Longitude (deg. West)	86.6	97.4	76.5	78	81.7
	Pressure (mbar)	1006	951	984	956	999
	Wind Speed (mph)	40.25	115	69	103.5	57.5
	TS Force Wind Radius (miles)	105	125	140	200	115
	Storm Surge (feet)	1	1.1		4.2	1
	Precipitation (inches)	7.86	13.18	19.13	19.06	10.03
Second Landfall Location	Latitude (deg. North)					
	Longitude (deg. West)					
	Pressure (mbar)					
	Wind Speed (mph)					
	TS Force Wind Radius (miles)					
	Storm Surge (feet)					
	Precipitation (inches)					
Third Landfall Location	Latitude (deg. North)					
	Longitude (deg. West)					
	Pressure (mbar)					
	Wind Speed (mph)					
	TS Force Wind Radius (miles)					
	Storm Surge (feet)					
	Precipitation (inches)					
Fourth Landfall Location	Latitude (deg. North)					
	Longitude (deg. West)					
	Pressure (mbar)					
	Wind Speed (mph)					
	TS Force Wind Radius (miles)					
	Storm Surge (feet)					
	Precipitation (inches)					
	Economic Damage (2012 USD)		$80,439,560.44	$210,483,516.48	$8,043,956,043.96	$20,109,890.11
	Impact Level	**0**	**1**	**2**	**3**	**0**

TS = Tropical Storm

H = Hurricane

Blank = Not Reported (default to 0)

		1999	1998			
		H. Irene	H. Bonnie	TS. Charley	H. Earl	TS. Frances
	Population Affected	5,900,000	11,100,000	10,400,000	1,600,000	17,000,000
First Landfall Location	Latitude (deg. North)	24.6	34.4	27.8	30.1	28.2
	Longitude (deg. West)	81.6	77.7	97.1	85.7	96.9
	Pressure (mbar)	987	964	1000	987	990
	Wind Speed (mph)	80.5	109.25	46	80.5	51.75
	TS Force Wind Radius (miles)	140	230	200	200	345
	Storm Surge (feet)	2.9	6		5.3	5.1
	Precipitation (inches)	15.43	11	7.230678	16.38	11.38
Second Landfall Location	Latitude (deg. North)					
	Longitude (deg. West)					
	Pressure (mbar)					
	Wind Speed (mph)					
	TS Force Wind Radius (miles)					
	Storm Surge (feet)					
	Precipitation (inches)					
Third Landfall Location	Latitude (deg. North)					
	Longitude (deg. West)					
	Pressure (mbar)					
	Wind Speed (mph)					
	TS Force Wind Radius (miles)					
	Storm Surge (feet)					
	Precipitation (inches)					
Fourth Landfall Location	Latitude (deg. North)					
	Longitude (deg. West)					
	Pressure (mbar)					
	Wind Speed (mph)					
	TS Force Wind Radius (miles)					
	Storm Surge (feet)					
	Precipitation (inches)					
	Economic Damage (2012 USD)	$1,072,527,472.53	$1,015,491,329.48	$70,520,231.21	$111,421,965.32	$705,202,312.14
	Impact Level	**3**	**3**	**1**	**2**	**2**

TS = Tropical Storm

H = Hurricane

Blank = Not Reported (default to 0)

		1998		
		H. Georges	TS. Hermine	H. Mitch
	Population Affected	11,200,000	2,200,000	7,400,000
First Landfall Location	Latitude (deg. North)	24.5	29.1	26.2
	Longitude (deg. West)	81.8	90.9	81.9
	Pressure (mbar)	981	1000	989
	Wind Speed (mph)	103.5	40.25	63.25
	TS Force Wind Radius (miles)	175	85	200
	Storm Surge (feet)	6		3
	Precipitation (inches)	28.36	1	7
Second Landfall Location	Latitude (deg. North)	30.4		
	Longitude (deg. West)	88.9		
	Pressure (mbar)	964		
	Wind Speed (mph)	103.5		
	TS Force Wind Radius (miles)	175		
	Storm Surge (feet)	9		
	Precipitation (inches)	38.46		
Third Landfall Location	Latitude (deg. North)			
	Longitude (deg. West)			
	Pressure (mbar)			
	Wind Speed (mph)			
	TS Force Wind Radius (miles)			
	Storm Surge (feet)			
	Precipitation (inches)			
Fourth Landfall Location	Latitude (deg. North)			
	Longitude (deg. West)			
	Pressure (mbar)			
	Wind Speed (mph)			
	TS Force Wind Radius (miles)			
	Storm Surge (feet)			
	Precipitation (inches)			
	Economic Damage (2012 USD)	$8,321,387,283.24	0	$56,416,184.97
	Impact Level	**3**	**0**	**1**

TS = Tropical Storm

H = Hurricane

Blank = Not Reported (default to 0)